

**Materials for the Photoluminescent Sensing of Rare Earth Elements: Challenges and Opportunities**

| | |
|-------------------------------|--|
| Journal: | <i>Journal of Materials Chemistry C</i> |
| Manuscript ID | TC-REV-04-2020-001939.R1 |
| Article Type: | Review Article |
| Date Submitted by the Author: | 21-May-2020 |
| Complete List of Authors: | Crawford, Scott; National Energy Technology Laboratory, Functional Materials Baltrus, John; National Energy Technology Laboratory, Ohodnicki, Paul; National Energy Technology Laboratory, |
| | |

ARTICLE

Materials for the Photoluminescent Sensing of Rare Earth Elements: Challenges and Opportunities

Scott E. Crawford,^{*a} Paul R. Ohodnicki, Jr.^a and John P. Baltrus^aReceived 00th January 20xx,
Accepted 00th January 20xx

DOI: 10.1039/x0xx00000x

Rare earth elements (REEs) are widely used in high-performance technologies including wind turbine magnets, electronic vehicle batteries, lighting displays, circuitry, and national defense systems. A combination of projected increasing demand for REEs, monopolistic economic conditions, and environmental hazards associated with the mining and separation of REEs has led to significant interest in recovering REEs from alternative sources such as coal waste streams. However, rapidly locating high-value waste streams in the field remains a significant challenge primarily because of slow analytical methods, and existing techniques with low limits of detection such as inductively-coupled plasma mass spectrometry suffer from high equipment and operating costs and a lack of portability. Alternatively, luminescence-based sensors for REEs present a potential path for sensitive, portable, low-cost detection. The development and design of materials suitable for the luminescence-based detection of REEs are crucial to realizing this potential. Here, we review a broad range of materials used (or that have the potential to be used) for REE luminescence-based detection, including organic compounds, biomolecules, polymers, metal complexes, nanoparticles, and metal-organic frameworks. A general overview of REE optoelectronic properties and luminescent sensing protocols is first presented, followed by analyses of material-specific sensing mechanisms, emphasizing sensing figures of merit including sensitivity, selectivity, reusability and portability. The review concludes with a discussion of remaining barriers to luminescent REE sensing, how each sensor class may be best deployed, and directions for future material and spectrometer design. Taken together, this review provides a broad overview of sensing materials and methods that should be foundational for the continued development of high-performance sensors.

1. Introduction

Rare earth elements (REEs) are broadly defined as the 14 lanthanides (Ce-Lu, characterized by a partially filled 4f subshell), along with lanthanum, scandium and yttrium.^{1,2} REEs are essential to advanced technologies, including electronics, high-performance magnets and turbines, optical displays, and national defense systems.^{1,3-8} Despite their relatively high abundance within the earth's crust, REE production is hindered by economic and environmental challenges:^{5,9-11} extracting and isolating individual REEs is tedious and expensive, requiring multiple extraction steps using harsh solvents.^{5,6,11,12} Mitigating the environmental effects of REE mining has rendered REE production unprofitable in many nations, contributing to monopolistic conditions in the global market.^{9,11,12}

Diversification of REE sources is one potential path for circumventing the economic and environmental challenges associated with REE mining. In particular, strategies involving REE recycling and recovery from natural water sources,^{13,14} waste streams such as coal refuse,^{3,15,16} fly ash,^{1,16} acid mine drainage,^{10,17,18} and industrial wastewaters,¹⁹ and REE-rich end-

of-life products (such as magnets, electronics, etc.) are being explored.²⁰⁻²³ A key step in enhancing the economic feasibility of REE extraction from waste streams is the ability to locate high value streams prior to engaging in tedious extraction processing, and to characterize downstream production and refining steps.²⁴⁻²⁶ There is thus a critical need to develop sensors capable of rapid REE detection and quantification within waste and recycling streams.^{24,27}

Atomic emission techniques, such as inductively-coupled plasma mass spectrometry (ICP-MS) or optical emission spectroscopy (ICP-OES), are the most commonly-used techniques for analyzing REE content in waste streams due to their high sensitivity (down to part-per-billion or part-per-trillion concentration levels) and ability to distinguish individual elements. Despite these advantages, significant drawbacks to ICP techniques include high instrumentation (~\$100,000 or higher) and operation costs, specialized operator training, and a lack of portability, which substantially lengthens the amount of time required for sample processing.^{24,28}

A promising alternative to replace (or to complement) ICP is to use luminescence-based sensors for REE detection.^{24,26-28} Advantages to luminescent techniques include significantly lower instrumentation costs (particularly for home-built fluorescence spectrometers), simpler operation, and the ability to design portable systems for field deployment. Luminescence sensing methods would considerably lower both the monetary and time costs associated with identifying high-value waste

^a National Energy Technology Laboratory, 626 Cochrans Mill Road, Pittsburgh, PA 15236

^b † Footnotes relating to the title and/or authors should appear here.

Electronic Supplementary Information (ESI) available: [details of any supplementary information available should be included here]. See DOI: 10.1039/x0xx00000x

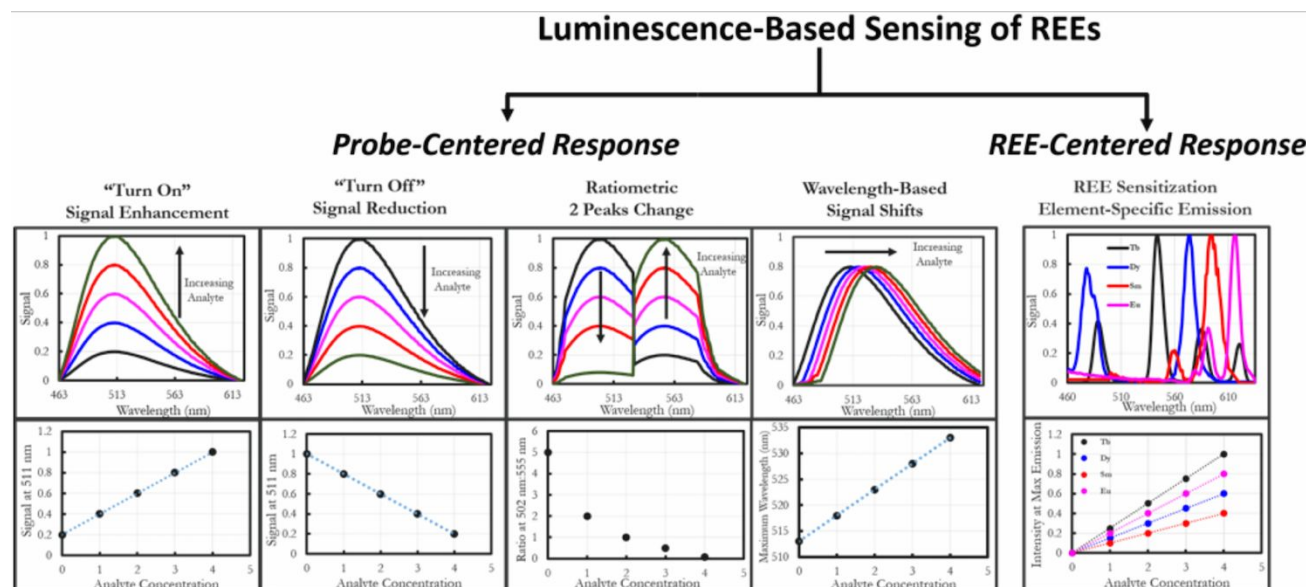


Figure 1. Schematic illustrating steady-state luminescence-based sensing techniques for REEs, with sample luminescent spectra readouts and calibration curves for each method. For probe-centered mechanisms, a material exhibits a luminescent signal that is modified by interactions with REEs. This can include either a signal enhancement or reduction, enhancements/reductions in two different peaks (i.e. ratiometric sensors), or a shift in the emission energy as a function of analyte concentration. Conversely, the chemical probe may transfer energy to luminescent REEs, which exhibit distinct, element-specific emission profiles with concentration-dependent emission intensities

streams, thus improving the economic viability of REE recovery. Notably, the luminescence-based detection of REEs is almost exclusively conducted in solution. The techniques outlined in this review may thus be directly used to rapidly identify high value liquid streams of REEs, such as natural waters,^{13,14} acid mine drainage,^{17,18,29} and industrial wastewaters.¹⁹ Additionally, the processing steps (i.e. extraction, purification, and concentration) associated with REE recovery from solid state sources are usually solution-based.^{16,30–32} Hence, luminescence-based techniques also present a rapid, low-cost method for characterizing downstream REE processing steps relative to ICP. This review begins with a discussion of general luminescent sensing approaches and REE optoelectronic properties, followed by more specific descriptions of different materials that have been used for REE detection (organic molecules, biomolecules, polymers, metal complexes/nanoparticles, and metal-organic frameworks) and their associated sensing mechanisms. The review concludes with a brief overview of portable luminescent spectrometer designs and a framework for future innovations that may advance the field.

2. REE Sensing Techniques

Steady-state luminescence-based detection of REEs can occur through two different mechanisms (**Figure 1**). In the first process, which will be referred to here as **“Probe-centered,”** the sensor selectively interacts with specific REEs, causing changes in the emission profile of the *probe* itself, such as emission quenching,³³ enhancement,²⁶ and/or a shift in the emission energy.³⁴ A “ratiometric” response in which changes in the intensity ratio of two different luminescence peaks are monitored as a function of analyte concentration³⁵ may also be used for REE detection.³⁶ The use of two peaks for detection

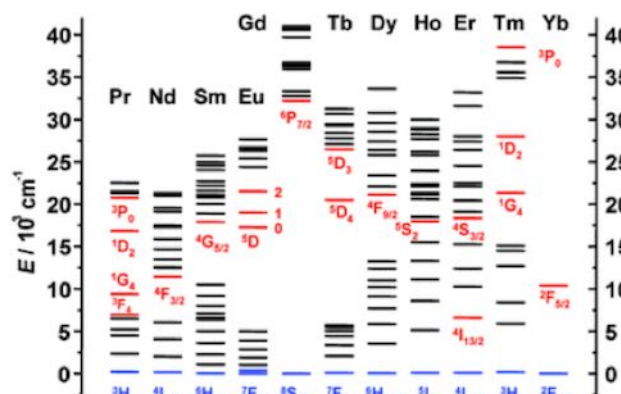


Figure 2. Partial energy diagrams for the lanthanide aquo ions, where the main luminescent transitions are drawn in red and the fundamental energy level is in blue. Reprinted with permission from ref. 44. Copyright 2005, the Royal Chemical Society.

may enable the sensor to be used over a wider concentration range and can sometimes provide an internal calibration against matrix interference effects, providing advantages over simpler “turn off” or “turn on” sensors.³⁷ Additionally, multivariate sensing techniques^{38–40} have recently been developed in which the response of multiple optical variables (i.e. luminescence, absorption, etc.) are measured for the sensor in the presence of each element of interest, and, by comparing the aggregate data, unique responses may be observed that differentiate individual elements.⁴¹ Potential drawbacks of “probe-centered” approaches is that these sensors often have the ability to only identify one element per sensor (for element-specific sensors),⁴² or, if the sensor responds to multiple REEs, the inability to distinguish signal from individual REEs, making it challenging to determine the true value of a waste stream²⁶ (*N.B.* certain REEs are considered more economically important than others, with the five most valuable being Eu, Nd, Tb, Dy, and Y, according to a 2011 US Department of Energy Report.)⁴³

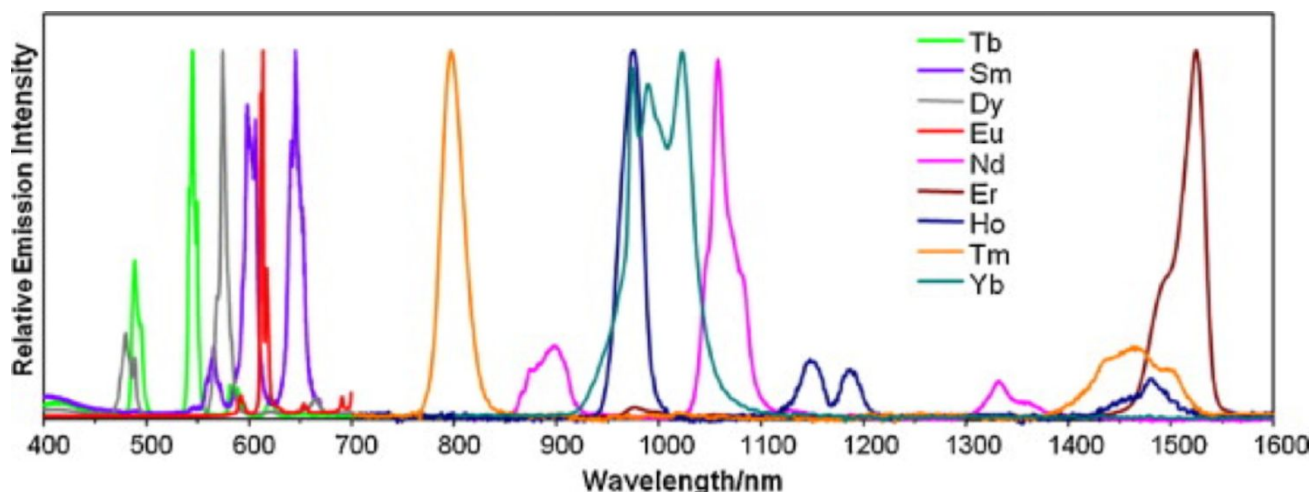
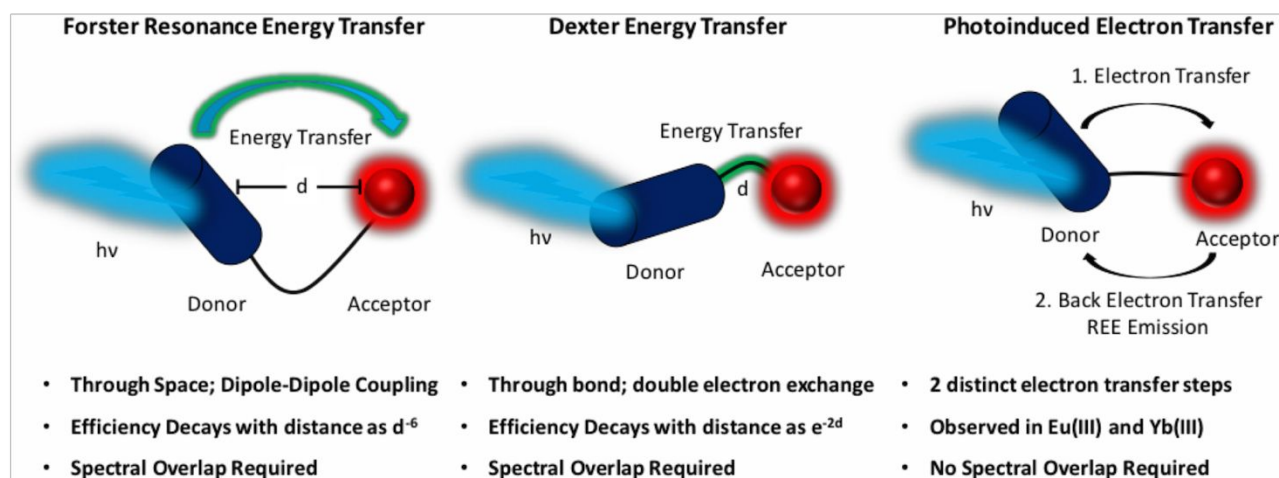


Figure 3. Normalized emission spectra of luminescent lanthanide complexes in solution, exhibiting characteristic, element-dependent, sharp emission bands with minimal overlap with respect to one another (*N.B.* the intensity and quantum yield of individual elements will vary significantly in water). Reprinted with permission from Ref. 45. Copyright 2010, Elsevier Masson SAS, all rights reserved.

In the second mechanism, the probe transfers energy to REEs, followed by REE-centered emission in a process dubbed “sensitization.” This “**REE-Centered**” approach exploits the inherent luminescent properties of certain trivalent REEs, including Gd, Tb, Sm, Dy, Eu, Ho, Tm, Yb, Pr, Nd, and Er (Figure 1). These 11 elements exhibit unique electronic transitions arising from f-orbital transitions (Figure 2)⁴⁴ which are shielded from the external environment by outer s and p-orbitals, producing characteristic line-like emission bands (Figure 3).⁴⁵ Importantly, the intrinsic quantum yields of individual REEs varies significantly by element type; the most emissive REEs have the largest energy gap between the highest energy ground state and lowest energy emissive state.^{44,46} Wide energy gaps reduce the likelihood of emission quenching via non-radiative energy loss. Hence, emission is most frequently observed from Tb and Eu, whereas the aqueous sensitization of other REEs such as Pr and Er is seldom observed.⁴⁴ Because the f-f transitions are parity forbidden, direct excitation of the REEs produces only weak emission.^{44,47} To circumvent this, a sensitizer material may first be excited, followed by energy transfer (typically *via* the

sensitizer triplet state) to the REE and subsequent REE-centered photoluminescence.^{44,48-51} This energy-transfer process may occur through space by donor-acceptor dipole-dipole coupling (i.e. Förster resonance energy transfer), a simultaneous through-bond electron exchange between the donor and acceptor (Dexter energy transfer), or via a photoinduced, redox-mediated pathway (Scheme 1).⁵² In general, sensitization requires the chromophore and REE to be in close proximity (~ 100 Å or less for a Förster process and a few angstrom or less for a Dexter mechanism), as well as spectral overlap between the energy donor and acceptor.⁵² Hence, a sensor material with suitable emission energy and in close proximity to an REE may be used to sensitize REE-centered emissions, allowing individual emissive REEs to be distinguished from one another.^{24,25} Solution-based REE sensitization can be challenging because REE-centered emission is susceptible to quenching from high-energy vibrational stretches (e.g. O-H, N-H, and C-H) which reduce emission signal, particularly in aqueous systems.^{44,53,54} However, this barrier may be circumvented by creating a bulky



Scheme 1. Illustration and summary of the three REE sensitization pathways: a through-space Förster resonance energy transfer, a through-bond Dexter energy transfer, and a photoinduced electron transfer followed by back electron transfer and REE-centered emission.

Table 1. Comparison of Steady-State and Time-Resolved Luminescent REE Sensing Techniques

| Method | Advantages | Disadvantages |
|----------------|--|--|
| Probe-Centered | Only method that can detect non-luminescent REEs such as Y, Sc, Lu, etc. | Can only detect one element per sensor, or can detect total REE content without information on individual REE concentrations |
| REE-Centered | Can detect multiple elements simultaneously | Cannot detect non-luminescent REEs such as Y, Sc, Lu, etc. |
| Time-Resolved | May be more robust against background emission, particularly for sensitized REEs with long-lived emission. Can also be used on solid-state samples | Requires more sophisticated equipment than steady-state approaches and is best suited for species with long-lived emission (i.e. luminescent REEs) |

chelation environment around the REE, protecting the REE from solvent. This is often achieved by using sensitizer materials with multidentate chelation sites or porous structures capable of REE encapsulation. A drawback of sensitization-based approaches is that non-luminescent REEs (e.g. Sc, Y, La, Lu, etc.) cannot be detected (although these REEs may still be detected using the “probe-centered response” approach shown in **Figure 1**).²⁵ The sensitization approach *does* enable detection of 4 of the 5 most economically critical REEs (Nd, Eu, Tb, and Dy).⁴³ The most complete picture of a waste stream’s value may best be obtained using both probe-centered and REE-centered approaches in tandem.

It is worth noting that time-resolved techniques may also be theoretically applied to improve REE detection, although such studies are less common relative to steady-state sensing experiments. Here, emission intensity as a function of time is measured either at the emission maximum of the sensing material (for probe-based approaches) or at the emission maximum of sensitized REEs (for REE-centered approaches) as

a function of time, enabling discernment and detection.⁵⁵ Because emissive lanthanides typically have long (microsecond or longer) emission lifetimes compared to potential interfering species, time-resolved techniques can be highly sensitive.^{46,56} Individual REEs may be distinguished by measuring the lifetime at the emission maximum for each REE, or by using time-gated techniques, in which the emission spectrum is recorded after a brief (i.e. tens of nanoseconds to microseconds) delay following pulsed excitation. During this delay, emission from other interfering species will often fully decay due to their shorter emission lifetime. The time-gated technique has been applied to characterize REE content in solids.⁵⁵ **Table 1** compares potential advantages and disadvantages of steady-state and time-resolved luminescent REE sensing approaches. For convenience, **Table 2** summarizes REE sensor properties including the detection limit, sensing mechanism, and selectivity from various studies in the literature.

Table 2. Summary of Properties for Reported Luminescence-Based Rare Earth Element Sensors

| REE | Detection Limit (ppb) | Material | Solvent | Mechanism ^a | Portable? ^b | Reusable? ^c | # of Interfering Ions Screened ^d | Response Time (s) ^e | Ref. |
|-----|-----------------------|----------------|--------------|------------------------|------------------------|------------------------|---|--------------------------------|------|
| Sc | 0.8 | Organic Ligand | Water | Turn-On | No | No | 21 | 600 | 57 |
| | 0.15 | Organic Ligand | Water | Turn-On | No | No | 42 | 0 | 58 |
| | 0.2 | Organic Ligand | Water | Turn-On | No | No | 59 | 0 | 59 |
| | 0.12 | Organic Ligand | Water | Turn-On | No | No | 36 | 600 | 60 |
| Y | 0.013 | Organic Ligand | THF | Turn-On | No | No | 11 | 0 | 61 |
| | 889 | Metal Complex | Benzonitrile | Turn-On | No | No | 12 | N/A | 62 |
| La | 65 | Organic Ligand | Ethanol | Turn-On | No | Yes | 18 | N/A | 63 |
| | 1.53 | Organic Ligand | Water | Turn-Off | No | No | 9 | N/A | 64 |
| | 16 | Organic Ligand | Water | Turn-On | No | Yes | 18 | N/A | 65 |
| | 0.2 | Organic Ligand | Water | Turn-Off | No | Yes | 11 | 120 | 66 |
| | 6.2 | Nanoparticle | Water | Peak Shift | No | No | 14 | N/A | 67 |
| Ce | 29 | Organic Ligand | Water | Turn-On | No | No | 18 | 0 | 68 |
| | 24 | Organic Ligand | Water | Turn-On | No | No | 15 | N/A | 69 |
| | 1.54 | Organic Ligand | Water | Turn-Off | No | No | 9 | N/A | 64 |
| | 2 | Organic Ligand | Water | Turn-On | Yes | No | 16 | 0 | 41 |
| | 0.94 | Metal Complex | Water | Sensitization | No | No | 14 | 0 | 70 |

| Journal Name | | | | | | | ARTICLE | | |
|--------------|--------|-------------------------|--------------|---------------|-----|-----|---------|------|----|
| | 31 | Nanoparticle | Water | Turn-Off | No | No | 15 | 0 | 71 |
| | 9 | Nanoparticle | Water | Ratiometric | No | No | 14 | 1800 | 72 |
| Ce(IV) | 11,200 | Organic Ligand | Water | Turn-On | No | No | 14 | 300 | 73 |
| | 96 | Organic Ligand | Water | Ratiometric | No | No | 20 | 60 | 74 |
| | .0001 | Organic Ligand | Ethanol | Turn-On | No | No | ≥60 | 300 | 75 |
| | 117 | Nanoparticle | Water | Turn-Off | No | No | 16 | 60 | 76 |
| Pr | 11 | Organic Ligand | Water | Turn-On | No | No | 18 | 0 | 77 |
| Nd | 100 | Metal-Organic Framework | Water | Sensitization | No | No | 2 | ~300 | 25 |
| Sm | 0.2 | Organic Ligand | Water | Sensitization | No | No | 16 | 600 | 78 |
| | 3800 | Metal Complex | Water | Sensitization | Yes | No | 0 | N/A | 24 |
| | 44 | Nanoparticle | Water | Turn-Off | No | No | 14 | N/A | 67 |
| | 360 | Metal-Organic Framework | Water | Sensitization | No | No | 2 | ~300 | 25 |
| Eu | 1500 | Organic Ligand | THF | Turn-On | No | No | ≥3 | N/A | 79 |
| | 30 | Organic Ligand | Acetonitrile | Ratiometric | No | No | 18 | N/A | 37 |
| | 131 | Organic Ligand | Water | Turn-On | No | No | 13 | N/A | 80 |
| | 11 | Organic Ligand | Water | Turn-On | Yes | No | 16 | 0 | 41 |
| | 61 | Organic Ligand | Water | Sensitization | No | No | 21 | 0 | 81 |
| | 7.3 | Organic Ligand | Water | Sensitization | No | No | 5 | 600 | 82 |
| | 2 | Organic Ligand | Water | Sensitization | Yes | No | 5 | 92 | 83 |
| | 0.88 | Organic Ligand | Water | Sensitization | No | No | 8 | 300 | 28 |
| | 0.22 | Organic Ligand | Water | Sensitization | No | No | 29 | 600 | 84 |
| | 0.2 | Organic Ligand | Water | Sensitization | No | No | 15 | N/A | 85 |
| | 0.02 | Organic Ligand | Water | Sensitization | No | No | 16 | 600 | 78 |
| | 50 | Metal Complex | Water | Sensitization | Yes | No | 0 | N/A | 24 |
| | 0.3 | Metal Complex | Acetonitrile | Sensitization | No | No | 19 | 60 | 86 |
| | 0.33 | Metal Complex | Acetonitrile | Sensitization | No | No | 21 | 60 | 87 |
| | 0.8 | Nanoparticle | Water | Turn-On | No | No | 18 | N/A | 88 |
| | 43 | Metal-Organic Framework | Water | Sensitization | No | No | 2 | ~300 | 25 |
| | 130 | Metal-Organic Framework | Water | Sensitization | No | No | 0 | 120 | 4 |
| | <150 | Metal-Organic Framework | Water | Sensitization | No | No | 1 | N/A | 89 |
| Gd | 2.2 | Biomolecule | Water | Multivariate | No | No | 16 | 2400 | 90 |
| Tb | 22.4 | Organic Ligand | Acetonitrile | Turn-Off | No | No | 19 | N/A | 91 |
| | 10 | Organic Ligand | Water | Turn-Off | No | Yes | 19 | 45 | 92 |
| | 86 | Organic Ligand | Water | Sensitization | No | No | 10 | N/A | 93 |
| | 143 | Organic Ligand | Water | Sensitization | No | No | 21 | 0 | 81 |
| | 0.46 | Organic Ligand | Water | Sensitization | Yes | Yes | 16 | 30 | 94 |
| | 79 | Metal Complex | Water | Sensitization | Yes | No | 0 | N/A | 24 |
| | 90 | Metal-Organic Framework | Water | Sensitization | No | No | 2 | ~300 | 25 |
| | ≤160 | Metal-Organic Framework | Water | Sensitization | No | Yes | 10 | 120 | 95 |
| | 0.3 | Metal-Organic Framework | DMF | Sensitization | No | No | 15 | 60 | 96 |
| | 16 | Metal-Organic Framework | Water | Sensitization | No | No | 7 | 1800 | 97 |
| | <16 | Metal-Organic Framework | Water | Sensitization | No | No | 1 | N/A | 89 |
| Dy | 0.01 | Organic Ligand | Water | Turn-Off | No | Yes | 19 | 35 | 98 |
| | 2000 | Metal Complex | Water | Sensitization | Yes | No | 0 | N/A | 24 |

| | | | | | | | | | |
|------|------|-------------------------|--------------|---------------|----|-----|----|------|-----|
| | 510 | Metal-Organic Framework | Water | Sensitization | No | No | 2 | ~300 | 25 |
| | 1800 | Metal-Organic Framework | DMF | Sensitization | No | No | 15 | 60 | 96 |
| Yb | 990 | Organic Ligand | Acetonitrile | Turn-On | No | Yes | 8 | 600 | 99 |
| | 21 | Organic Ligand | Acetonitrile | Ratiometric | No | No | 18 | 0 | 100 |
| | ≤120 | Nanoparticle | DMSO | Sensitization | No | Yes | 0 | ~60 | 101 |
| | 260 | Metal-Organic Framework | Water | Sensitization | No | No | 2 | ~600 | 25 |
| Lu | 150 | Organic Ligand | Water | Turn-On | No | No | 20 | N/A | 42 |
| | 9 | Organic Ligand | Water | Turn-On | No | No | 16 | 0 | 41 |
| | 14 | Nanoparticle | Water | Turn-On | No | No | 20 | N/A | 102 |
| | 7 | Nanoparticle | Water | Turn-On | No | No | 18 | N/A | 103 |
| All | 7 | Organic Ligand | Water | Turn-Off | No | No | 0 | N/A | 104 |
| REEs | 2 | Biomolecule | Water | Ratiometric | No | Yes | 5 | 60 | 26 |

*No reported fluorescence-based detection limits for Ho, Er, and Tm sensors. DMF: Dimethylformamide; DMSO: dimethylsulfoxide. N/A indicates that this information was not explicitly stated. ^aRefer to Figure 1 and Section 2 for illustrations of each mechanism; note that “Turn-on” refers to the emergence of an emission peak corresponding to the sensor material, whereas “sensitization” refers to the emergence of an REE-centered emission peak. ^bPortability indicates the sensing experiments were conducted on home-built instruments capable of field deployment, such as those described in Section 10. ^cReusable sensors have been demonstrated to undergo multiple REE loading and unloading cycles (see Table 2). ^dRefers to the total number of cations and anions added (along with the REE of interest) to determine whether these ions impact the sensor efficacy ^eResponse times of 0 indicate studies in which measurements were conducted immediately upon the exposure of the sensor material to REEs

3. Properties of an Ideal REE Sensor

As with any sensor, certain characteristics are essential: high selectivity and sensitivity, stability under relevant conditions, rapid response times, etc. Desirable sensor characteristics as well as experimental approaches for impactful evaluations of sensor performance are summarized in **Table 3**, and sample data is included in **Figure 4** to illustrate experimental “best practices” for evaluating potential REE sensors. Sensitivity and selectivity are particularly important for environmental REE detection, which may require evaluation in harsh matrices. One targeted area for REE detection includes acid mine drainage (AMD), which we emphasize as an example due to the extreme challenges such a harsh matrix presents: as demonstrated by **Table 4**, AMD waters often have REE content in the low part-per-million or part-per-billion range, and the concentration of interfering metal cations is often several orders of magnitude higher than the REE content, with pH values as low as 2. For sensors based on REE sensitization, quenching effects from water must also be mitigated, an additional challenge.

In this *Review*, we will discuss an array of materials that have been evaluated for their luminescent response to post-synthetic additions of REEs, ranging from relatively well-studied systems such as organic molecules to emerging, less-studied materials including nanoparticles. The sensing performance of each material class will be discussed in detail in the context of the criteria outlined in **Table 3**. A general overview of each material, with a list of advantages and disadvantages typically encountered in each material class, is summarized in **Scheme 2**, with more detailed discussions in the individual sections. While Scheme 2 illustrates that clear advantages and challenges may be observed from each material class, we emphasize here (and throughout this *Review*) that opportunities exist for designing composite materials comprised of multiple materials, which may synergistically combine the advantageous properties of the individual materials. For example, the selectivity of MOFs for REEs may be improved by functionalizing the MOF surface with REE-selective organic molecules,¹⁰⁵ producing a highly sensitive and selective sensor.

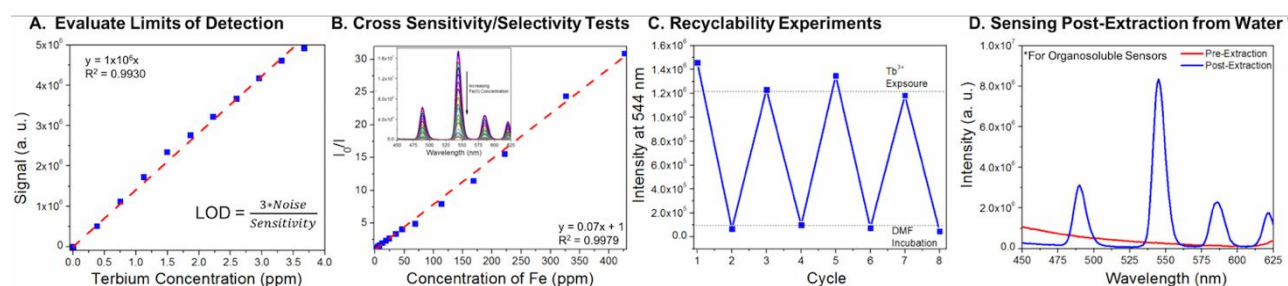


Figure 4. Recommended experiments for evaluating potential REE sensors. A. The limit of detection (which can be evaluated using the equation in the inset), B. cross-sensitivity against potential interfering elements (which can be evaluated using a Stern-Volmer plot), C. recyclability tests, and, for sensors that are only stable in organic media, D. demonstrating that the sensor may be used on REEs extracted from aqueous media.

Table 3. Important Considerations and Approaches for REE Sensor Design

| Property | Description | Experimental Approach |
|---|--|---|
| Sensitivity | Detecting low quantities of a given analyte. Environmental streams often have low ppm or ppb REE levels (Table 4) ^{10,17,29} | Estimate limits of detection and quantification for sensors (Table 2), typically taken as 3 times and 10 times the ratio of the noise:sensitivity (Figure 4-A). ¹⁰⁶ |
| Selectivity | Detecting an analyte of interest even in harsh matrices. For example, AMD waters may have > 100x higher concentrations of other metals than REEs with pH levels as low as 2 (Table 4) ^{14, 15, 74, 75} | Evaluate the sensor in environmentally relevant matrices and conditions and conduct cross-sensitivity studies. Stern-Volmer plots provide quantitative information on both quenching dynamics and mechanisms (Figure 4-B). ¹⁰⁷ |
| Scope | Establishing which REEs can be detected with a given sensor | Evaluate sensor on all REEs (in the case of a sensitization approach, evaluate on all emissive REEs) |
| Ease-of-Synthesis | Avoiding multiple and/or tedious synthetic steps, expensive materials or processes, and long synthesis times | Work with low-cost, commercially available materials and minimize tedious synthetic steps if possible |
| Water-Compatible | Maintaining stability when exposed to water. Most environmental sensing of REEs will be in aqueous conditions, unless REEs are first extracted into organics. ¹⁰⁸⁻¹¹¹ In some cases surfactants may aid sensing performance in water. ⁸⁴ | Evaluate sensing material in water and over extended time frames, or demonstrate sensor efficacy in organics following REE extraction from water (Figure 4-D) |
| Incorporation with Sensor Components | Depositing thin films of the sensor material onto sensor components, typically optical fibers, for portability and/or remote monitoring. ¹¹² | Use materials with practical protocols for thin film formation will facilitate development of portable REE detection systems. ^{83,113,114} |
| Response Time | The time required to attain maximum signal---ideally on the order of seconds/minutes instead of hours/days ⁸³ | Measure signal as a function of time until signal stabilizes |
| Recyclability | The ability to load and unload REEs from the sensor across multiple sensing cycles | Following REE exposure, remove REEs using fresh solvent, ¹¹⁵ a chelating agent, ⁶⁶ and/or a salt solution ⁹⁵ (Figure 4-C) |
| Non-Toxic | Materials that will not cause health or environmental harm | Avoid the use of toxic chemicals in sensor design when possible |

Table 4. Reported Rare Earth Element Concentrations and Other Characteristics of Acid Mine Drainage

| Location | pH | Total REE (ppm) | Fe (ppm) | Al (ppm) | Ca (ppm) | Mg (ppm) | Ref. |
|-------------------|------|-----------------|----------|----------|----------|----------|----------------|
| Sitai Mine, China | 3.61 | .0612 | 4.73 | 8.83 | 249 | 1.03 | ²⁹ |
| Clarion, PA | 4.4 | 1.134 | 385 | 9.1 | 149 | 236 | ¹⁷ |
| Pittsburgh, PA | 6.3 | 0.00029 | 22 | 0.1 | 66 | 20.1 | ¹⁷ |
| Germany | 4.8 | 0.073 | 0.01 | 4.01 | 405 | 193 | ¹¹⁶ |
| Germany | 3.8 | 4.7 | 404 | 88.2 | 57.8 | 1,139 | ¹¹⁶ |
| Romania | 3.0 | 1.58 | 1500 | 237 | 402 | 88.3 | ¹¹⁶ |
| Romania | 3.0 | 0.38 | 538 | 74.8 | 386 | 141 | ¹¹⁶ |
| Sweden | 3.2 | 0.035 | 6.3 | 1.10 | 396 | 57.4 | ¹¹⁶ |

4. Organic Molecules

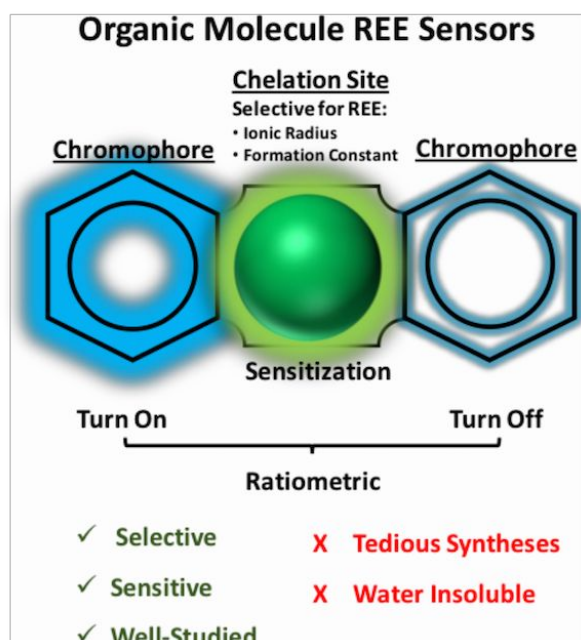
Organic molecules represent the most commonly-studied class of REE sensors, ranging in complexity from simple, commercially available compounds to rationally designed molecules that require multiple synthetic steps. As shown in **Scheme 3**, organic REE sensors typically include two components: an REE chelation site and an adjacent luminescent group that will provide a fluorescent response upon REE chelation. The REE chelation site is often either a macrocycle that binds to specific REEs based upon ionic size, or a functionality with a high binding affinity for REEs, such as a Schiff base (*vide infra*). The chromophoric group

may exhibit enhanced or quenched emission following REE chelation, or, conversely, may transfer energy to adjacent REEs and act as a sensitizer. In this section, we describe several classes of organic molecule REE sensor classes, including crown ethers, calixarenes, inclusion complexes, and Schiff bases (**Table 5**). The use of organic molecules in multivariate sensing techniques are also described. Note that in this section, we only consider organic complexes that have been demonstrated to spontaneously sensitize REE emission when added to REE-containing solutions, which would be necessary for use as a sensor. Hence, REE complexes that are first pre-formed and purified prior to photoluminescence characterization will not be discussed here but have been reviewed extensively elsewhere.^{44,117-119} It should be noted that

numerous organic molecules are known to sensitize multiple visible and NIR-emitting REE simultaneously and are likely strong candidates for REE detection applications.^{47-49,120-125}

| | Organic Compounds | MOFs | Biomolecules | Metal Complexes | Nanoparticles | Polymers |
|-------------------------------------|-------------------|------|--------------|-----------------|---------------|----------|
| Sensitive? | ✓ | ✓ | ✓ | ✓ | ? | ? |
| Selective? | ✓ | ✗ | ✓ | ✗ | ? | ? |
| Water Compatible? | ✗ | ✓ | ✓ | ✗ | ✗ | ✗ |
| Easy to Synthesize? | ✗ | ✓ | ✗ | ✗ | ✓ | ✗ |
| Incorporated into Portable Sensors? | ✓ | ✓ | ? | ? | ✓ | ✓ |

Scheme 2. General overview of the advantages and disadvantages of each material class used for REE detection based on existing literature (N.B. there are, of course, individual exceptions to the designations presented here; for example, while most organic compound REE sensors are used in organic conditions, several water-compatible compounds have been reported). Shortcomings of individual sensing materials may be overcome via the design of composite sensors, in which the advantageous properties of the constituent materials may be synergistically combined to improve performance.



Scheme 3. Overview of organic molecule-based detection of REEs. Typically, a strongly chelating species, such as a Schiff base or macrocycle, will selectively interact with the REE based on ionic radius or formation constant. The chelator is modified with chromophores that respond to the REE via emission enhancement, quenching, or a ratiometric response. Conversely, the REE may be sensitized. General advantages and disadvantages are listed.

However, because REE detection was typically not a focus of these studies, data on chelation kinetics, selectivity, and sensitivity are often not reported. Further studies are thus needed for existing sensitizers to evaluate their sensing efficacy.

Macrocyclic and Cavitand Compounds

A common strategy for designing highly selective REE sensors is to use macrocyclic or cavitand compounds such as crown

ethers, calixarenes, and inclusion complexes. Such compounds form chelating rings or cavities that interact with specific metals as a function of ion size. Chromophoric molecules are attached to the macrocyclic chelating group, enabling either REE sensitization or a probe-centered response (i.e. sensing is based on the enhancement and/or quenching of the molecule's emission, Figure 1). The latter is typically caused by electronic interactions between the chromophore and the chelated metal (energy transfer to the REEs, electron withdrawing effects, etc.).

Table 5. Classes of Organic REE Sensors

| Molecule Type | Selective Based Upon: | Elements Detected |
|----------------------|--------------------------------|---|
| Crown Ethers/Cyclens | Ionic Radii | Ce, ³³ Pr, ^{33,79} Nd, ^{33,79} Eu, ⁷⁹ La, ¹²⁶ Y, ¹²⁶ Tb ⁸¹ |
| Inclusion Complexes | Ionic Radii | Sc, ⁵⁸ La, ⁶⁴ Ce ⁶⁴ |
| Calixarenes | Ionic Radii & Binding Affinity | Yb, ^{127,128} Nd, ¹²⁹ Tb, ¹²⁹ Eu, ¹²⁹ Y, ¹³⁰ La ^{63,130} |
| Schiff Bases/Imines | Binding Affinity | Sc, ^{57,59,60} Eu, ^{80,131} Y, ⁶¹ Yb, ⁹⁹ Tb, ^{91,93} La, ⁶⁵ Pr, ⁷⁷ Lu, ⁴² Ce(IV) ^{73,74} |

Crown ethers are macrocyclic structures in which ether groups form rings with inward-facing oxygen atoms, providing a well-defined coordination site for REE cations. An example of a crown-ether based REE sensor is shown in **Figure 5A**. Here, a 1,4-diphenylethynyl-benzene chromophore with 18-crown-6 structures attached to either side for REE chelation selectively chelates Ce, Pr, and Nd (ionic radii: 112-114 pm), producing a "turn-off" response.³³ Another crown ether design exhibits a "turn on" response to Eu, Nd, and Pr (ionic radii ranging from 109 to 113 pm), where REE chelation prevents electronic donation between the chromophore and crown ether.⁷⁹ Cyclen and cyclam macrocycles, which have amino groups in the ring

interior instead of oxygen, have been used to selectively detect the non-emissive REEs La and Y,¹²⁶ and to sensitize Tb and Eu.⁸¹

Similar chelation effects have also been produced by adding two or more compounds, which can cooperatively chelate the REE.⁸⁴

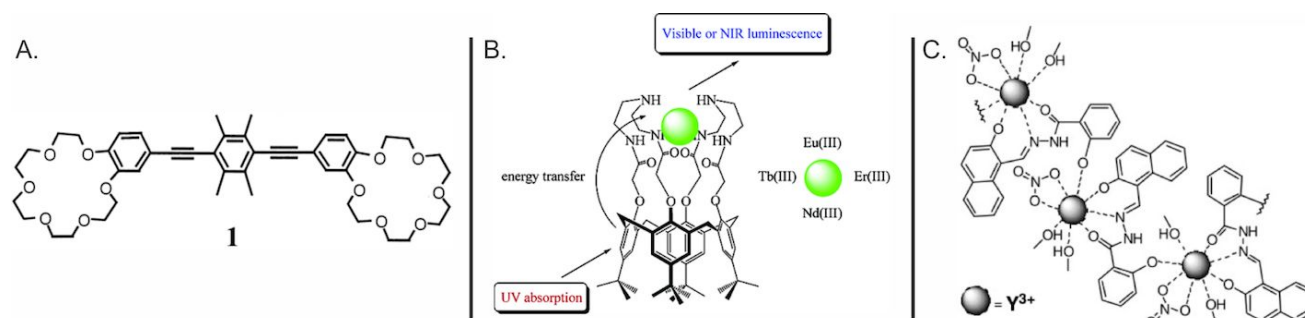


Figure 5. Examples of organic molecules used to sense REEs. **A.** The 18-crown-6-based sensor for Ce, Pr, and Nd developed by Schmehl and Li. Reprinted with permission from Ref. 33. Copyright 2000, Elsevier Inc. **B.** Schematic depicting the interaction between a calix[4]arene capped with aminopolyamide bridges with REEs, as well as the energy transfer from the calixarene to the REEs. Reprinted with permission from Ref. 129. Copyright 2006, American Chemical Society. **C.** Example of a Schiff base compound chelating the rare earth element yttrium(III). Reprinted with permission from Ref. 61. Copyright 2009, Elsevier.

Inclusion complexes, in which one molecule interacts with the cavity of another chemical structure via Van der Waals forces, also sense analytes based upon atomic radii. For example, a highly selective “turn on” sensor for Sc(III) was developed using quinizarin embedded in the cavity of β -cyclodextrin, (detection limit: 15 ppb).⁵⁸ The complex was most effective in basic conditions and was tolerant to a wide range of potential interfering ions.⁵⁸ Similarly, a complex formed from tetramethylcucurbit[6]uril and 2-(4-methoxyphenyl)-1H-imidazo[4,5-f][1,10]phenanthroline can detect 1.5 ppb of aqueous Ce(III) and La(III) via a quenching mechanism.⁶⁴

Calixarenes contain hydrophobic chalice-like cavities capable of encapsulating analytes of interest and are formed via hydroxylation between phenol and aldehyde groups.¹³² The chelation environment inside the calixarene may be developed to selectively interact with specific analytes. An example of a calixarene-based sensor is shown in **Figure 5B**. Here, a calix[4]arene base is capped by aminopolyamide bridges that chelate REEs. This calix[4]arene sensitizes Tb, Eu, and Nd, with particularly efficient emission from Tb (quantum yield: 12%).¹²⁹ Other calixarenes have been developed that exhibit selective “probe-centered” emission quenching or enhancement in the presence of Y(III),¹³⁰ La(III)^{63,130}, and Yb(III).^{127,128}

Schiff Bases, Imines, and Related Compounds

Schiff bases, which consist of RC=NR' groups, and related compounds, have also been widely investigated as selective fluorescent sensors for REEs (**Figure 5C**). Schiff base and related chelators exhibit high selectivity for REEs based upon the formation constant of the Schiff base-metal complex. One remarkable example is 1-(2-hydroxy-3-methoxybenzaldehyde)-4-aminosalicylhydrazide (HMB-ASH), which was exposed to 1000 ppm of 31 different metal cations in water. Luminescence was only observed in the presence of Sc(III), with a detection limit of ~ 0.8 ppb.⁵⁷ Other Schiff bases have been used to selectively detect Eu(III),¹³¹ Y(III),⁶¹ Yb(III),⁹⁹ and Tb(III)⁹¹ with ppb-level detection limits in organic solvents, using either “turn-on” or “turn-off” sensing mechanisms.

Schiff-based sensors have also been designed for use in water. For instance, aqueous, selective, and sensitive (16 ppb detection limit) sensing of La(III) under biologically relevant

conditions was enabled by an 8-hydroxyquinoline conjugate of amino-glucose. Complexation with La(III) produced a 60-fold enhancement of complex quantum yield, observable to the naked eye. The sensor did not exhibit any response to other metals tested and could be recycled: phosphate or fluoride anions could be added to turn off emission, which could then be turned on once again via the addition of La. The compound was integrated into filter paper for test strip detection and was also used for intracellular La imaging (**Figure 6**).⁶⁵ Schiff bases have also been developed to selectively detect ppb-level concentrations of Pr(III),⁷⁷ Eu(III),⁸⁰ and Lu(III)⁴² in water.

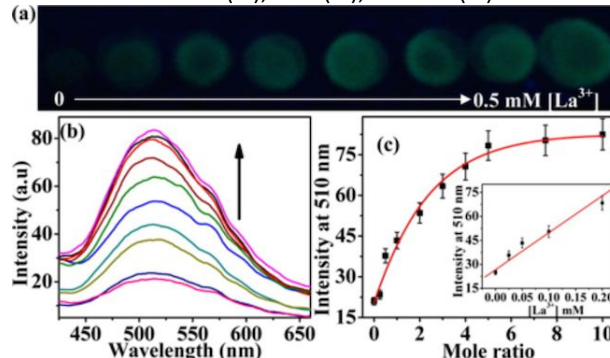


Figure 6. (a) Photograph of the sensor N-[3-methyl]-2-[pyridine-2-amido] phenyl pyridine-2-carboxamide deposited on Whatman cellulose filter paper exposed to increasing concentrations of La under 365 nm UV light. (b) Corresponding spectra obtained in fluorescence titration of the sensor ($\lambda_{\text{exc}} = 360$ nm) with La^{3+} on cellulose filter paper. (c) Plot of intensity vs $[\text{La}^{3+}]/[\text{Sensor}]$ mole ratio at 510 nm. Inset: The linear concentration region for the intensity vs $[\text{La}^{3+}]$ for the sensor L. Reprinted from Ref. 65 with permission from American Chemical Society, 2015.

In addition to the REEs listed above, Schiff bases have been designed to target Ce(IV) in water. Cerium is distinct among the REEs in that it can be tetravalent, while the other REEs are typically trivalent in solution; this unique redox property provides an additional pathway for selective sensor design using organic molecule sensors. A “turn on” sensor using a rhodamine derivative with a N,N-dimethylaniline moiety was developed that could be selectively oxidized by Ce(IV), causing both a colorimetric and luminescent response. An 11 ppm detection limit was observed in acetonitrile, while no optical response was observed in the presence of other trivalent REE, including Ce(III).⁷³ A 100-fold improvement in the detection limit was later obtained using two rhodamine groups linked by a

carbazole molecule, which was then integrated into TLC plates for simple colorimetric “dip-stick” studies.⁷⁴ Remarkably, recent

work has exploited the oxidative properties of Ce(IV) to produce a sensor capable of picomolar limits of detection.⁷⁵

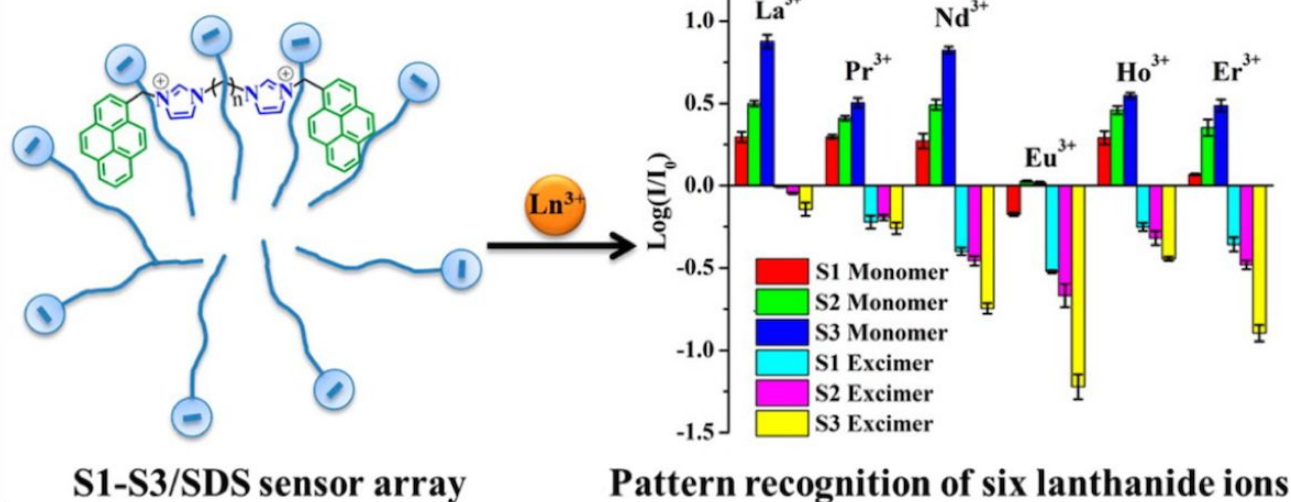


Figure 7. Schematic illustrating REE luminescent detection using an array of anionic surfactants and cationic bispyrene derivatives (left). REE-dependent responses are observed for each bispyrene monomer and excimer emission, making it possible to distinguish individual REEs based upon the fluorescent response (right). Reprinted from Ref. 134 with permission from the American Chemical Society, copyright 2014.

In addition to luminescent enhancement and quenching mechanisms, ratiometric Schiff base sensors have been used to detect La(III),³⁶ Yb(III) (21 ppb limit of detection)¹⁰⁰ and Eu(III) (30 ppb limit of detection),³⁷ even in the presence of interfering ions. While less common, there are also a few examples of Schiff bases and related compounds that sensitize REE emission. For example, tetrasodium-4,4',6,6'-tetracarboxy-2,2'-bipyridine spontaneously sensitizes Eu, Nd, Gd, and Tb in water, suggesting that this molecule might be well-suited for sensing applications.¹³³ Sensitization of Tb(III) has been observed using the commercially available compound thiabendazole. A fluorescence response was only observed when Tb was present, and the method was successfully used on Tb-spiked river water samples, with an 86 ppb detection limit.⁹³

Multivariate Organic Sensors

Multivariate sensing techniques, in which multiple types of sensor responses are analyzed to identify, distinguish, and quantify different analytes, have more recently been developed for REEs, primarily using organic compounds. In 2014, Ding and co-workers developed a sensor array consisting of assemblies of anionic surfactants and three cationic bispyrene derivatives (S1-S3), which exhibit both excimer and monomer emission peaks. The intensities of the monomer and excimer peaks each behave differently (i.e. quenched, enhanced, or not impacted) depending upon the REE being analyzed. By comparing the aggregate data, it was possible to distinguish La, Pr, Nd, Eu, Ho, and Er in solution (**Figure 7**). Importantly, divalent metals did not interfere with the observed signal.¹³⁴ In 2018, a sensing protocol for all 14 lanthanides was developed measuring the absorption and emission properties of curcumin, an inexpensive, commercially available, naturally occurring compound. Measurements were conducted at different pH values before and after chelation with each lanthanide, and

distinct responses were found for each element. As a proof-of-concept, colorimetric experiments were conducted in a pondwater matrix (pH of 6.5) using curcumin from over-the-counter turmeric powder, a UV flashlight, and a smart phone camera equipped with a spectrophotometer, providing a low-cost, portable method for REE sensing.⁴¹ Similarly, a combination of three different cavitand host molecules and two guest fluorophores have been used to sense heavy metals, including REEs, where chelation of metal ions produced distinct enhancement or quenching behaviors for each fluorophore, enabling the differentiation of metals at micromolar levels.¹³⁵

Organic Molecules Embedded in Polymer Membranes

One pathway towards the development of portable sensors is to immobilize the sensing molecule of interest into a polymer membrane. These “optode membranes” may then be integrated onto a sensor device, typically via deposition on an optical fiber tip, enabling remote detection.¹³⁶ For example, a quenching-based sensor was developed for Dy(III) by integrating the sensor molecule, 5-(dimethylamino)-N-(furan-2-yl-methylene)-naphthalene-1-sulfonylhydrazide, into a polyvinylchloride (PVC) membrane, enabling detection limits as low as 0.01 ppb, with successful tests in spiked river water matrices.⁹⁸ Similar sensors have been developed for Tb(III)⁹² and La(III),⁶⁶ providing rapid (45-120 seconds) detection times and low (tens of ppb) detection limits. Significantly, the La(III) sensor could be reused by soaking the sensor in a solution of EDTA, which removed the La from the sensor.⁶⁶

Sensitization-based optical membranes have also been produced: immobilization of 2-pyridone, a commercially available molecule, into a polystyrene membrane enabled the selective detection of down to 0.46 ppb Tb(III) in 30 s.⁹⁴ A tridentate bis(phosphinic acid)phosphine oxide sensor embedded in a Nafion membrane was developed in 2012 that

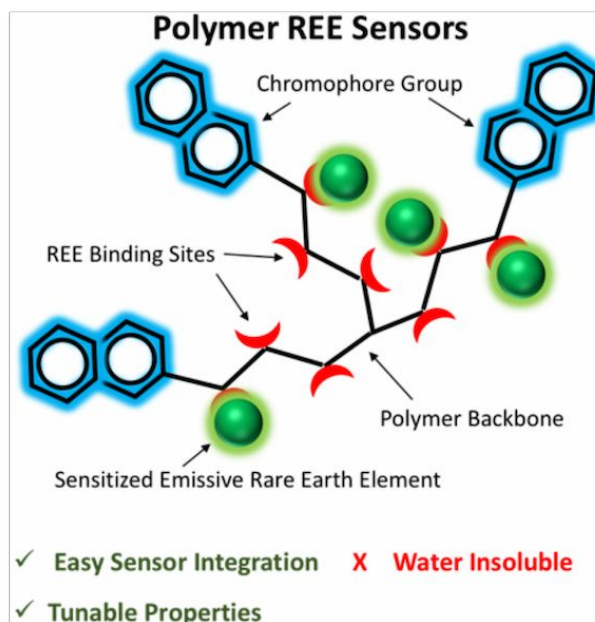
exhibited high selectivity for Eu(III), with a 5 minute response time in aqueous solutions and a detection limit of 0.88 ppb.²⁸ Similar results for Eu(III) have also been attained using a PVC membrane,⁸² which was later incorporated into a portable, fiber-based sensor for Eu-detection (see Section 10).⁸³

5. Polymers

Similar to organic molecules, polymeric materials typically include rigid, aromatic structures for light harvesting and tunable chelation environments to bind to REEs. However, polymers can be rationally designed for enhanced rigidity, solubility, chelation sites, photostability, and light absorption capacity relative to low-molecular weight molecules, and these advantages make polymers an attractive material for REE sensitization (Scheme 4).¹³⁷⁻¹³⁹ Polymeric coatings are also often applied to optical fibers, creating a natural path for polymer-based sensitizers to be integrated into portable systems.¹⁴⁰ However, polymer-based REE detection has not been studied extensively, nor have these materials been evaluated for detection limits, response time, or selectivity. Water compatibility can also be a challenge for certain polymers. Given the high performance of REE sensitization from porous materials such as metal-organic frameworks (MOFs, Section 9), further investigation into porous polymeric REE sensors is clearly warranted and will likely aid in the discovery of new sensors and high-performance emissive materials.

Dendrimers

Polymer-based sensitization of REEs typically involves dendrimers, which are bulky polymers consisting of repeating branch units. In 2002, Balzani and Vögtle sensitized Nd, Er, and Yb using a dendrimer comprised of a benzene core with (dialkyl)-carboxamine linkers coupled to six aliphatic amide groups for REE chelation and eight 5-(dimethylamino)-1-naphthalenesulfonyl (dansyl) units, which act as light harvesters.¹⁴¹ Protonation of the dansyl units also enabled sensitization of Tb and Eu at 77 K.¹⁴² The authors later modified the dendrimer system by introducing molecular "clips" consisting of two anthracene molecules linked to a benzene ring with two sulfate groups. Combining Nd, the dendrimer, and the molecular clip led to spontaneous self-assembly of the components, leading to Nd-centered emission that was resistant to oxygen quenching.¹⁴³



Scheme 4. Overview of polymer-based sensing of REEs. Of the few examples of polymer-based REE sensors, all have used a sensitization mechanism, in which sites within the polymer chelate the REEs, and chromophoric structures in the polymer are used to sensitize the REE emission. General advantages and disadvantages are listed.

Nd has also been sensitized by a dendrimer with a macrocyclic 1,4,8,11-tetraazacyclotetradecane core with polyamidoamine (PAMAM) branches, terminated by dansyl groups. The authors observed that increasing the number of branches (and, by extension, chromophoric dansyl groups) led to more efficient REE sensitization, which may aid in the design of future polymer-based REE sensors.¹⁴⁴ Petoud and co-workers used a PAMAM dendrimer containing 60 internal amine groups for REE chelation and 32 external 2,3-naphthalimide groups as light harvesters for Eu(III) sensitization in DMSO (Figure 8A-B), with sufficiently strong emission for naked eye detection.¹⁴⁵

Porous Organic Polymers (POPs)

Porous organic polymers, as their name implies, are a class of porous polymeric materials characterized by high surface area and tunable structure (Figure 8C-D). Such structures may be advantageous for REE detection: chromophoric monomers can sensitize REEs, tunable pore sizes may promote selectivity

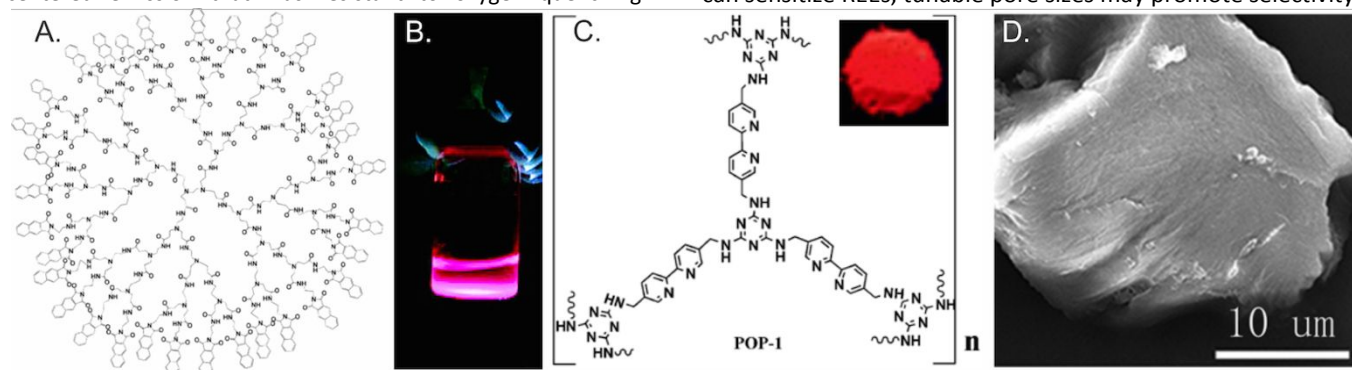


Figure 8. Examples of polymer-based REE sensitizers. A) Structure of the PANAM dendrimer with 60 internal amine groups for REE chelation and 32 external 2,3-naphthalimide groups as light harvesters for Eu(III) sensitization, with B) photograph of Eu sensitized by PANAM in DMSO under UV light. Reprinted from Ref. 145 with permission from the American Chemical Society, 2004. C) Structure of POP-1 (Inset: Photograph of POP-1/Eu powder under UV illumination) and D) scanning electron microscope (SEM) image of POP-1/Eu. Reprinted from Ref. 146 with permission from Centre National de la Recherche Scientifique (CNRS) and the Royal Society of Chemistry, Copyright 2018.

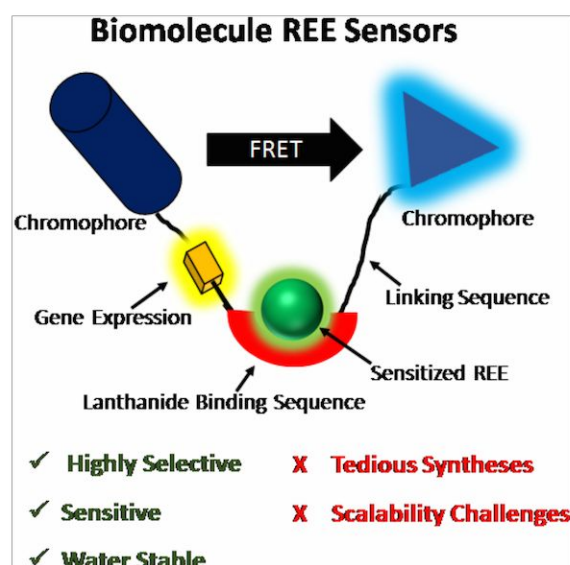
for certain ions, and encapsulation may also protect REEs from solvent-based quenching. Despite these potential advantages, POPs have not yet been widely studied for REE sensing applications. An exception is POP-1, comprised of melamine and 5,5'-bis(bromomethyl)-2,2'-bipyridine. While not evaluated directly for REE detection, POP-1 could both encapsulate and sensitize Eu. Upon excitation with UV light, Eu-centered emission could be observed visibly in both water and in the solid state, which was then used to sense other analytes.¹⁴⁶

6. Biomolecules

Biomolecules, such as peptides, proteins, and bacteria, can exhibit high selectivity for REEs and have emerged as an impactful class of REE sensors (Scheme 5).^{151,152} Indeed, it has been demonstrated REEs contribute to biological processes in harsh, REE-rich environments such as volcanoes. For example, growth of *Methylobacterium extroquens* can be enhanced by adding certain REEs to its growth media, and it is known that REEs contribute to their ability to catalytically oxidize methanol.¹⁵¹ Biomolecules that bind selectively to REEs have been used in the design of "probe-based" sensors, which rely on chelation-induced gene expression¹⁴⁷ or Förster resonance energy transfer (FRET) mechanisms for sensing.²⁶ Research in the field of bio-chelation has also spurred the design of "lanthanide binding tags (LBTs)," which are peptides that exhibit high selectivity for REEs.^{147,150,152-155} These LBTs have been incorporated into "sensitization-based" sensors. DNA has also been exploited for REE detection.^{90,148}

Clear advantages of biomolecule-based REE sensors include high selectivity for REEs over possible interferants, in addition to being water-tolerant. High performance sensors have been developed to give total REE concentrations,²⁶ or to sensitize specific REEs.¹⁵⁰ Integration of biomolecules onto optical fiber-based sensors has also been previously demonstrated, indicating that there is potential for the development of portable, biotechnology-based REE sensors for field use.¹⁵⁶ Disadvantages may include sophisticated syntheses and/or scalability challenges. Table 6 summarizes the experimental

approaches used with biomolecules for REE detection, and more detailed discussions are included in this section.



Scheme 5. Overview of biomolecule-based sensing of REEs. Selective peptide binding sequences or proteins interact selectively with REEs, and depending upon the sensor, this can promote fluorescent signal via gene expression, a FRET mechanism, or sensitization of the REE itself via a nearby chromophore. General advantages and disadvantages are listed.

Gene Expression Techniques

One bio-based sensing strategy is to use gene expression for REE detection. In a 2013 study the iron(III)-binding motif used by *Salmonella* to detect extracellular iron (III) via a two-component PmrA/PmrB system was replaced with a LBT. The system was engineered such that, in the presence of REE ions, a gene encoded with a green fluorescent protein (GFP) was expressed, and the GFP emission could be monitored to detect REE content within the cell (Figure 9A). The signal was selectively enhanced by sub-micromolar REE concentrations (using Tb as a representative REE), whereas other common extracellular metal ions such as iron, copper, zinc, and calcium did not impact the emission signal, highlighting the high selectivity of this method.¹⁴⁷

FRET-Based Techniques

More recently, Cotruvo et al. designed a REE sensor using the protein lanmodulin (LanM), which exhibits a high binding affinity (K_d s of 5-25 pM) for REEs. Here, LanM was used as a bridge between enhanced cyan fluorescent protein (ECFP) and the fluorescent yellow protein citrine, which act as a FRET pair. Upon REE chelation, LanM undergoes a conformational change, decreasing the distance between the ECFP and citrine and hence leading to FRET. The system acts as a ratiometric sensor, where emission from the ECFP centered at 475 nm decreases while the signal from the citrine at 529 nm is enhanced. Minimal interference was observed when other secondary metals were tested (Figure 9B). Signal was obtained within 1

Table 6. Summary of Biomolecular REE Sensing Approaches

| Technique | Approach |
|-------------------------------|--|
| Gene Expression | REE chelation "turns on" expression of luminescent gene ¹⁴⁷ |
| FRET | REE chelation-induced conformational change turns on FRET signal ²⁶ |
| RNA Cleaving | DNAzyme with REE co-factor cleaves fluorescently labelled RNA ⁹⁰ |
| Multivariate DNA-Based Sensor | Statistical analysis of changes in the time-gated luminescence response of different emissive DNA complexes in the presence of various metal ions ¹⁴⁸ |
| Sensitization | LBTs that chelate REEs are excited via tryptophan groups or appended chromophores ^{149,150} |

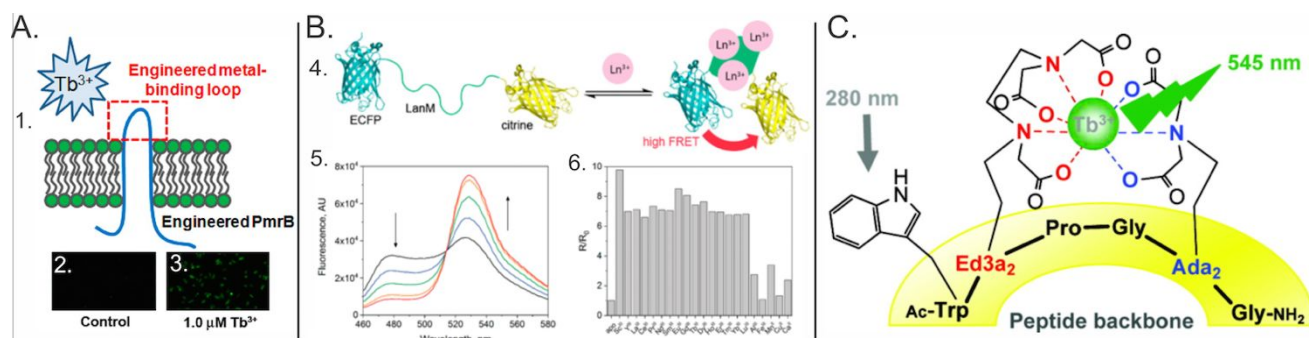


Figure 9. Examples of biotechnology-based detection of REEs. **A.** 1) The Fe(III)-binding loop in *Salmonella* is replaced with an LBT and engineered to express a gene encoded with GFP. Images show the sensor before (2) and after (3) the chelation of Tb. Reprinted with permission from Ref. 147. Copyright 2013, American Chemical Society. **B.** Schematic illustrating the FRET-based luminescent sensing of REEs using LaMP1. (lanmodulin-based protein sensor 1). Here, the REE binding group LanM selectively interacts with REEs and folds, bringing the citrine and enhanced cyan fluorescent protein (ECFP) into close proximity, enabling FRET (4). The fluorescent response of the LaMP1 sensor as a function of increasing REE content (1 to 4 equivalents) is shown in plot 5, while the selectivity of the sensor is shown in plot 6: REEs produce a ~ 7 -10 fold enhancement of emission whereas interfering metals exhibit only a ~ 1 -3 fold enhancement. Reprinted from Ref. 26 with permission from the American Chemical Society, 2019. **C.** Example of a peptide sequence modified with a chelating agent for selective REE chelation and sensitization. Here, terbium is chelated by an ethylenediamine triacetate functional group, and is sensitized via energy transfer from an excited tryptophan molecule. Reprinted with permission from Ref. 149. Copyright 2012, American Chemical Society.

minute of aqueous REE exposure at concentration levels as low as 10 nM (~ 2 ppb depending upon the REE being analyzed). The sensor is particularly well-suited for applications in which information on the *total* REE content is desired, as it cannot be used to differentiate between individual REEs.²⁶

DNA-Based Sensors

DNAzymes refer to DNA-based biocatalysts that can cleave RNA in the presence of certain metal ion cofactors. The ability of certain REEs to act as DNAzyme cofactors has enabled the development of selective sensors for REEs. For these experiments, RNA was modified with a fluorescent molecule at one terminus and a quenching molecule on the other. As the DNAzyme cleaved the RNA as a function of REE concentration, emission from the released fluorescent molecule could be tracked, and the technique could detect down to 2.2 ppb Gd.⁹⁰ A multivariate sensor comprised of 5 different DNAzyme arrays was developed to distinguish between 14 individual REEs in water at sub-micromolar concentrations.⁹⁰ A second multivariate sensor based upon the time-gated luminescence signal from Tb sensitized by DNA has also been developed to distinguish metal ions, including individual REEs.¹⁴⁸

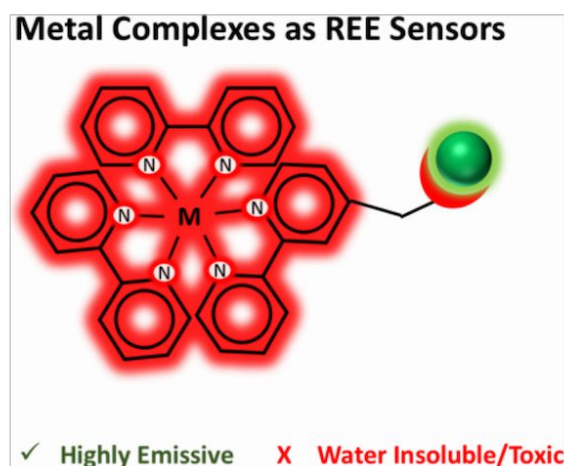
Bio-based REE Sensitizers

A fourth type of bio-inspired REE sensor uses LBTs modified with sensitizer molecules and/or chelating groups. These sensors have the ability to distinguish individual REEs while maintaining a high degree of selectivity. One such example has been demonstrated by Bonnet and Gunnaugsson, who modified the calcium-binding loop of the parvalbumin protein by attaching a 1,8-naphthalimide functionality to the N-terminus.¹⁵⁰ The sensor can excite both Tb(III) and Eu(III) upon photoexcitation of 1,8-naphthalimide, with signal obtained at micromolar concentrations in aqueous 0.1 M NaCl at pH 7. Importantly, the modification to the peptide did not alter its binding affinity for REEs. Selectivity for REEs was demonstrated over Zn(II), Cu(II), and Ca(II).¹⁵⁰ Similarly, Delangle's group functionalized a peptide backbone with ethylenediamine triacetate for REE chelation (Figure 9C).¹⁴⁹ Tb(III) sensitization was demonstrated by exciting a nearby tryptophan residue at 280 nm, and no difference in the emission intensity was observed in water or deuterium oxide, indicating that the REE is completely

protected from solvent. REE affinity down to femtomolar concentrations was estimated for the peptide sequence.¹⁴⁹

7. Metal Complexes

Transition metal complexes have been widely explored for their remarkable luminescent properties, which often include high quantum yields, strong absorption, long lifetimes, and triplet-state emission, typically through metal-to-ligand charge transfer states.¹⁵⁷ Pioneering work by van Veggel in the early 2000s demonstrated that NIR-emitting lanthanides could be sensitized using transition metal complexes such as ferrocene and [Ru(bipy)₃]²⁺ derivatives, which has since spurred significant research in this area, leading to the development of transition-metal complex-based sensors for REEs (Scheme 6).^{158,159}



Scheme 6. Overview of metal complexes as REE sensors. Typically, at least one organic ligand on an emissive metal complex is modified with an REE chelating group to hold the REE in close proximity to the emissive complex. Photoexcitation of the complex initiates energy transfer to the REE, followed by REE-centered emission. General advantages and disadvantages are listed.

Despite the fact that a multitude of metal complexes have been investigated for REE sensitization,¹⁶⁰ studies evaluating their sensing efficacy have been limited. Significant advancements in the effectiveness of metal complex-based REE detection could be achieved via synthetic modifications to the organic ligands to enhance selectivity for REEs—for example, using macrocycles, Schiff bases, or lanthanide-binding tags (*vide*

supra). Further, the development of new water-compatible emissive metal complexes is needed, as most evaluations of REE sensitization reviewed here were conducted in organic solvent (*N.B. aqueous sensitization has been conducted with gold-cyanide complexes, but cyanide is highly toxic*).

Ru/Os Bipy Complexes

Successful sensitization of REEs using transition metal complexes requires both a highly emissive metal complex and available sites for REEs to interact with the complex. In one design, a dendrimer containing a cyclam chelating group was found to spontaneously assemble with the emissive complex $[\text{Ru}(\text{bpy})_2(\text{CN})_2]$ in the presence of Nd, leading to sensitized Nd emission.¹⁶¹ The Ward group similarly used $[\text{Ru}(\text{bipy})_3]^{2+}$ and $[\text{Os}(\text{bipy})_3]^{2+}$ as REE sensitizers by modifying one bipy ligand with an aza-18-crown-6-macroclyce group for REE chelation (**Figure 10**). The Ru complex sensitized Nd, while the Os complex sensitized both Yb and Nd in acetonitrile.¹⁶² Several compounds containing a ruthenium(II) bipyridine complex coupled with different calix[4]arenes (*vide supra*) were developed by Maestri and co-workers for the detection of Nd, Eu, and Tb.¹⁶³ Different luminescent responses were observed for each element: Nd was sensitized, Tb enhanced Ru(bipy) emission due to a reduction in vibrational quenching, and Eu^{3+} generally quenched emission from the complexes tested.¹⁶³

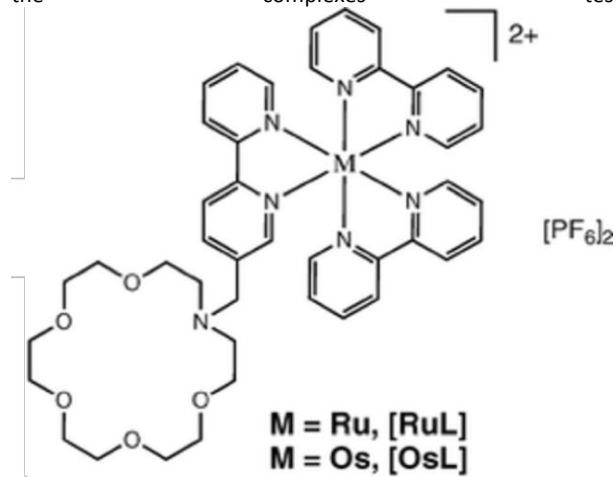


Figure 10. Structure of the Ru or $[\text{Os}(\text{bipy})_3]^{2+}$ modified with an aza-18-crown-6-macroclyce group for REE chelation. Energy transfer was demonstrated to the NIR-emitting Yb(III) and Nd(III). Reprinted with permission from Ref. 162. Copyright 2009, Royal Society of Chemistry.

d^{10} Metal-Cyanide Compounds

Clusters formed from coinage metals (Cu, Ag, and Au) in the +1 oxidation state with cyanide (e.g. $[\text{Au}(\text{CN})_2]_n$, where $n \geq 2$) exhibit unique emissive properties due to metal-metal bonded excimers and exciplexes that are sensitive to both the number of monomer units (n) and cluster geometry. Emission from these complexes can be efficiently transferred to luminescent REEs. Indeed, energy transfer from d^{10} -cyanide complexes to REEs was demonstrated by Patterson and co-workers, who optimized the concentration of $[\text{K}[\text{Au}(\text{CN})_2]]$ in aqueous solution to sensitize Tb emission.¹⁶⁴ Later, clusters of Cu, Ag, and Au with cyanide were shown to sensitize both Tb and Eu emission in organic media.¹⁶⁵ Notably, during the evaluation of a portable spectrometer (Section 10) for aqueous REE detection, d^{10} -

cyanide complexes were used to sensitize REEs: concentrations as low as 3800 ppb (Sm), 2000 ppm (Dy), 79 ppb (Tb), and 50 ppb (Eu) were detected.²⁴

Zinc Complexes

Complexes of zinc with REE chelators such as porphyrin or Schiff bases have been developed for selective detection of specific REEs. In 2004, Fukuzumi's group developed a zinc porphyrin-quinone dyad (ZnP-CONH-Q) that exhibited selective emission enhancement following chelation of the non-luminescent REE Y(III). Excitation of the zinc-porphyrin complex resulted in rapid electron transfer to the quinone group, quenching its emission. Chelation of Y prevented this energy transfer process, leading to enhanced emission from the zinc-porphyrin complex. The selectivity of the system for Y was ascribed to a combination of Lewis acidity and ionic radii factors: metal ions with weaker Lewis acidity than Y, such as Lu, Eu, Yb, and others, did not interact strongly enough with the quinone group to influence the energy transfer rate, and elements such as iron, copper, and scandium, which have higher Lewis acidity than Y, were too small to interact with both quinone carbonyl oxygens (**Figure 11**). No detection limits were reported, but signal was observed for 889 ppb Y in benzonitrile.⁶²

A zinc-based luminescence enhancement system containing N-(3-methoxysalicylidene)-2-aminopyridine (a Schiff base), 1,10-phenanthroline and zinc detected Eu content as low as 0.3 ppb in acetonitrile. Combining Eu with all three chemicals dramatically enhanced the intensity of Eu-centered luminescence, and each chemical contributed to the enhanced emission. The sensor was tested in the presence of interfering ions and in different matrices, with high selectivity and sensitivity for Eu signal.⁸⁶ Subsequent work using N-*o*-vanilin)-1,8-diaminonaphthalene as the Schiff base also produced an Eu sensor that was resistant to metal cation interferants.⁸⁷

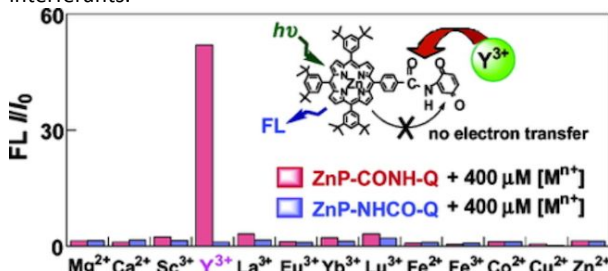


Figure 11. Fluorescence-based detection of trivalent yttrium using the zinc porphyrin/quinone dyad (ZnP-CONH-Q), which shows a unique luminescent response to Y relative to a variety of other secondary metals. The response is lost when the zinc porphyrin is linked to quinone via the NC connection (ZnP-NHCO-Q) versus the CN connection. Reprinted with permission from Ref. 62. Copyright 2004, American Chemical Society.

8. Nanoparticles

Nanoparticles, loosely defined as materials with at least one dimension between 1 to 100 nm in size, exhibit unique optical properties that are not observed in their bulk counterparts.¹⁶⁶ A diverse range of nanomaterial classes have been developed, including noble metal (e.g. gold, silver, etc.) particles, carbon-based materials (e.g. graphene), semiconducting metal chalcogenides (e.g. CdSe), metal oxide particles, polymeric nanoparticles, and silica, to name a few. The optical properties

arising at the nanoscale range from field enhancement effects via localized surface plasmon resonances (which can enhance the luminescent signal of nearby luminophores)¹⁶⁷ to intense, tunable band-gap based emission.¹⁶⁶ Further, these optical properties can typically be tuned by alterations to the particle size, shape, composition, and surface chemistry: in considering luminescence, critical to REE sensitization, the emission energy of CdSe quantum dots can be tuned with size,¹⁶⁶ the emission energy of InP quantum dots can be altered via changes to surface composition,¹⁶⁸ and gold nanoclusters exhibit luminescent properties that are sensitive to core geometry¹⁶⁹ as well as both the identity and structure of the stabilizing surface molecules (often referred to as “capping ligands”).¹⁷⁰

As shown in **Scheme 7**, nanomaterials typically consist of a particle core as well as capping ligands that passivate the particle surface. Both the core and ligands may play a role in the sensing mechanism. For instance, the core may transfer energy to REEs that either intercalate into the core itself or are held in the ligand shell, or it can simply serve as a scaffold for organic or polymeric sensitizers. Conversely, the ligand and/or core may exhibit emission properties that are enhanced or quenched following interaction with an REE, enabling a diverse array of nanoparticle-based sensing strategies. **Table 7** provides a summary of core and ligand properties facilitate nanoparticle-based REE sensitization: high energy, intense emission from the core can sensitize REEs, and short, bulky, REE-chelating ligands facilitate Dexter and Förster energy transfer processes.

Table 7. Core and Ligand Properties Needed for Sensitization

| Core Properties | Ligand Properties |
|--|--|
| <ul style="list-style-type: none"> High Energy Emission Intense Emission | <ul style="list-style-type: none"> Short Length Bulky Sites for REE Chelation |

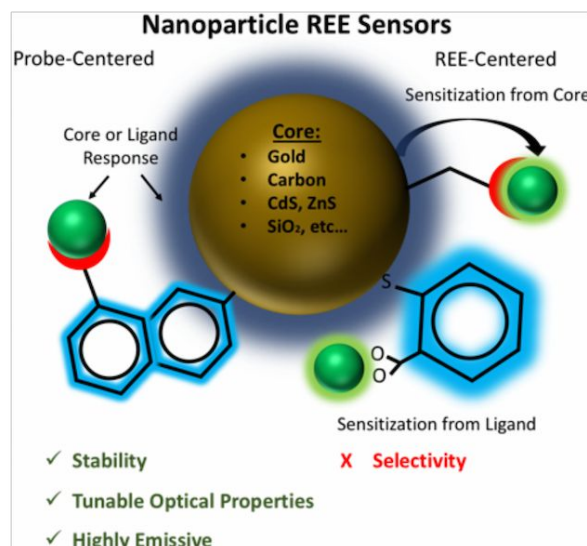
The tremendous diversity in strategies for tuning nanomaterial emission properties and the multitude of available organic ligands for surface functionalization has spurred significant interest in exploring nanoparticles for REE sensitization. The inherent stability of hard inorganic particles may also aid in the development of recycling strategies for re-use across multiple sensing cycles.¹⁷¹ Unlike more mature sensitizer classes, such as organic molecules, nanomaterials have not been extensively evaluated as sensor materials for REEs, and further development is needed in this area: simply screening other high-performance emissive nanomaterials such as InP quantum dots and perovskites for post-synthetic

REE sensitization should advance the field of nanoparticle-based REE sensing. Future designs using ligands with high selectivity for REEs (such as macrocyclic ligands or lanthanide binding tags) could be an intriguing path for producing selective nanoparticle-based sensors. This section will not cover emissive REE-containing upconversion nanoparticles such as NaYF₄:Yb because the REEs are added during synthesis, however these materials are reviewed elsewhere.¹⁷²⁻¹⁷⁴

Metal-Chalcogenide Semiconductor Nanoparticles

Semiconductor metal-chalcogenide nanoparticles, often referred to as “quantum dots,” exhibit band-gap emission that is directly correlated to particle size, and can produce high energy emission with quantum yields approaching unity, meeting the criteria listed in **Table 7**.¹⁷⁵ There has thus been interest in designing quantum dot-

based systems for REE sensitization, which would combine the broad absorption features of quantum dots with the narrow emission bands of REEs.¹⁷⁶⁻¹⁷⁸ This has often been accomplished by doping REE ions into the quantum dots such as CdS¹⁷⁹ during the nanoparticle synthesis. However, recent progress has been made in the post-synthetic sensitization of REEs using quantum dots, which is more relevant for REE sensing applications.



Scheme 7. Overview of nanoparticle-based REE detection. Sensing may be “probe-based,” where core or ligand emission properties are enhanced or quenched following REE chelation. Additionally, the nanoparticle core and/or organic ligands may sensitize REE emission. A wide range of core and ligand structures may be accessed experimentally. General advantages and disadvantages are listed.

Work from Waldeck and Petoud demonstrated that ZnS and CdS could sensitize Tb and Eu added post-synthetically, following REE intercalation into the particle (**Figure 12**).¹⁸⁰ This work was followed up by Mukherjee, who screened CdSe and ZnS against ten different emissive REEs using the post-synthetic addition technique. It was found that CdSe was capable of only sensitizing Tb and Eu, while ZnS could sensitize Tb, Eu, and Yb.¹⁸¹

Rather than intercalating into the particle core, REEs may also be sensitized upon chelation by the ligand shell. Ana de Bettencourt-Dias’ group demonstrated that water-soluble CdS nanoparticles can sensitize Eu, Nd, and Yb bound to 3-mercaptopropionic acid (3-MPA) ligands (**Figure 13**),¹⁸² a short chelating ligand (**Table 7**). Infrared and ¹H nuclear magnetic resonance (NMR) spectroscopy techniques confirmed that the REEs were coordinated to the terminal carboxylates of the ligand shell. Energy transfer efficiencies of ~0.01% were observed in water.¹⁸² The same group conducted analogous experiments on MPA-capped ZnS nanoparticles.¹⁸³ It is important to note that MPA alone cannot sensitize REE emission, hence the core itself must be the sensitizer.

However, there are instances where the ligand alone *does* act as the sensitizer. In these cases, the nanoparticle simply acts as a scaffold for ligand-REE interactions. Such an example was demonstrated with thiosalicylic acid-capped ZnS and CdS. The excitation spectrum of Tb interacting with free ligand was compared to the excitation spectra of Tb in the presence of the ligand-capped quantum dots, and no difference was observed¹⁸⁴ leading the authors to conclude that sensitization was coming from the ligand alone. Interestingly, some

differences in the Tb lifetime and intensity as a function of the quantum dot core were observed, and these differences were attributed to different coordination modes of the thiosalicyclic ligand on the NP surface, highlighting the importance of both ligand identity and arrangement for REE sensitization. In fact, disruptions to the ligand shell as a result of REE binding can induce a “turn-off” response, which has been exploited with ZnS quantum dots in the development of a selective Ce(III) sensor.⁷¹

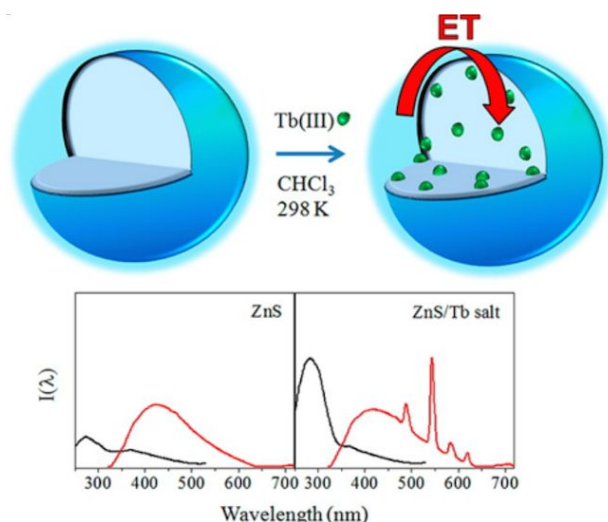


Figure 12. Schematic illustrating the post-synthetic sensitization of REEs using energy transferred from ZnS (top). REEs added to ZnS post-synthetically intercalate into the spherical particles, enabling sensitization. Excitation (black, monitored at 545 nm) and emission spectra (red) recorded before and after Tb(III) addition are shown at the bottom. Reprinted with permission from Ref. 180. Copyright 2013, American Chemical Society.

Carbon Nanomaterials

Carbon nanodots and related compounds are an emerging class of nanomaterials comprised of pseudospherical sp^2 -conjugated carbon cores often passivated by an organic ligand or polymer, usually with sub-10 nm diameters.^{185,186} Carbon nanodots are often relatively polydisperse in terms of their size and shape,¹⁸⁷ making it a challenge to establish structure-property correlations or to even classify the material.¹⁸⁸ However, advantages including tunable excitation/emission properties, ease of functionalization and synthesis, high stability, water solubility, and low cost (using abundant

precursors such as folic acid⁶⁷ and acetic acid¹⁸⁹) have motivated the study of carbon nanodots as REE sensitizers.

Work from Ana de Bettencourt-Dias' group demonstrated energy transfer from crystalline, ~4-5 nm carbon dots to Tb and Eu ions in acetonitrile. Fourier transform infrared spectroscopy (FT-IR) indicated the presence of surface carbonyl and carboxylate groups, which chelated REE cations added post-synthetically.¹⁸⁹ Tb(III) sensitization has also been observed in water using both carbon nanodots¹⁸⁷ and graphene quantum dots.¹⁹⁰ Huang and co-workers demonstrated that cysteine-functionalized carbon nanodots spontaneously formed hierarchical structures following the addition of Eu(III) in aqueous media. Eu(III)-centered emission visible to the naked eye was detected under UV illumination (**Figure 14a-f**).³⁴

In addition to acting as an REE sensitizer, carbon nanomaterials have also been used to detect REEs via quenching or wavelength shifts in response to specific REEs. An oxygen-rich, N-doped, blue-emitting graphene quantum dot has been developed that exhibits selective quenching in the presence of Ce(IV) in water, with detection limits as low as 117 ppb.⁷⁶ Similar quenching-based sensing mechanisms have been observed in negatively charged nitrogen-doped carbon nanodots: in response to the emissive REEs (Pr, Nd, Sm, Eu, Gd, Tb, Dy, Ho, Er, Yb, and Tm), quenching alone was observed. However, when non-emissive La, Y, and Lu REEs were tested, a 20 nm red-shift in emission was observed during the quenching process.⁶⁷ Using Sm and La as representatives of the quenching and wavelength shift mechanisms, respectively, the authors measured detection limits of 6.3 ppb for La and 44 ppb for Sm. The response of the sensor to non-REE metals was not reported.⁶⁷ “Turn-off” detection of Sm and Eu has also been demonstrated with carbon nanodots functionalized with the metal chelator 2-thenoyltrifluoroacetone.¹⁹¹

Silica Nanomaterials

Mesoporous silica (SiO_2) nanoparticles functionalized with chromophores have been analyzed for the detection of Lu and Eu by Hosseini and co-workers.^{88,102,103} SiO_2 is relatively inexpensive and easy to functionalize, providing a convenient material for REE detection. Further, the rigidity of the SiO_2 walls can improve emission performance relative to free chromophores in solution. High transparency to visible light and

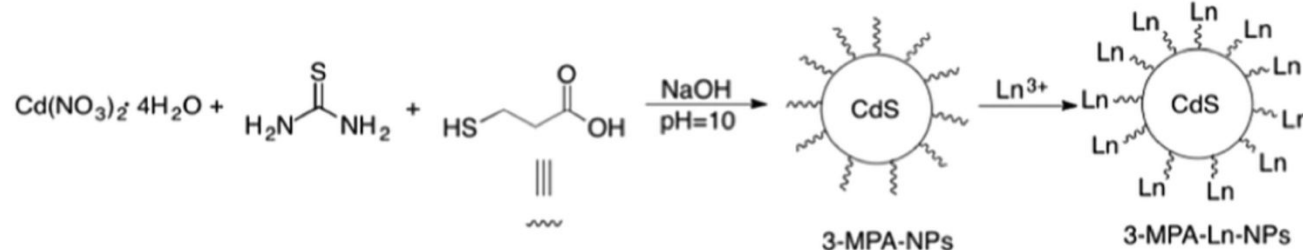


Figure 13. Schematic illustrating the synthesis of 3-mercaptopropionic acid (3-MPA)-capped cadmium sulfide nanocrystals. Trivalent lanthanides (Ln^{3+}) added post-synthetically bind to the terminal carboxylate group on the 3-MPA ligand, holding them near the CdS surface and enabling energy transfer and sensitization. Reprinted with permission from Ref. 182. Copyright 2018, Royal Society of Chemistry.

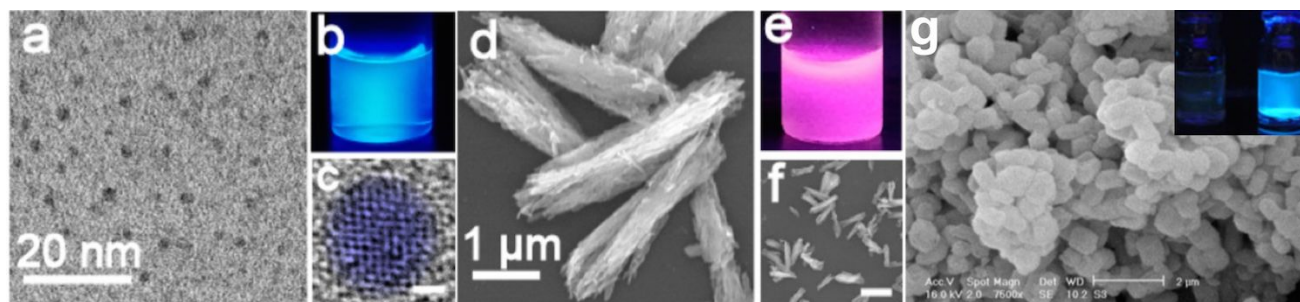


Figure 14. a) transmission electron image (TEM) of the L-cysteine-functionalized carbon quantum dots, b) photograph of the carbon quantum dots in water under UV illumination, c) high resolution image of the carbon quantum dots (scale bar 0.5 nm), d) TEM of the Eu@carbon quantum dots, e) photograph of the Eu@carbon dots in water under UV illumination, and f) wideout TEM image of the Eu@carbon nanodots (scale bar: 4 μm). Reprinted from Ref. 34 with permission from the American Chemical Society, 2019. g) Scanning electron micrograph of the hexagonally structured mesoporous SiO_2 functionalized with 8-hydroxyquinoline. Inset shows a photograph of the sensor under UV illumination with (right) and without (left) Lu added. Reprinted with permission from Ref. 103. Copyright 2013, Elsevier.

ease of integration into optical fibers also make SiO_2 nanoparticles attractive for fluorescence sensing applications.

The detection of Lu was accomplished using the chromophoric molecule 8-hydroxyquinoline grafted onto mesoporous SiO_2 (LUS-1)¹⁰² and the hexagonally structured mesoporous SiO_2 , SBA-15.¹⁰³ For both systems, Lu chelation with the 8-hydroxyquinoline “turned on” emission at ~ 480 nm, enabling detection limits of 14 ppb Lu in water for LUS-1¹⁰² and 7 ppb for the SBA-15 (Figure 14g).¹⁰³ The sensor was selective for Lu and was successfully applied to soil and fly ash, although the source of selectivity is unclear. A similar strategy in which cinchonidine molecules were grafted onto SiO_2 -coated magnetite (Fe_3O_4) was used to detect down to 0.8 ppb Eu.⁸⁸

Gold Nanoparticles

Gold nanoparticles (AuNPs) with diameters in the ~ 1 -3 nm range can exhibit relatively weak visible or near-infrared emission that is known to be sensitive to the identity and structure of surface capping ligands used to stabilize the particle.^{170,192} Emissive AuNPs are intriguing for applications such as biological imaging due to high molar absorptivity in the UV-visible range, biologically relevant near-infrared emission, and biocompatibility, but suffer from broad emission peaks.^{101,170} To circumvent this, Millstone and co-workers investigated emissive AuNPs as REE sensitizers, focusing

specifically on Yb(III), which absorbs near-infrared light and has one emission band. Yb(III) was titrated into a solution containing *ortho*-mercaptobenzoic acid (oMBA)-functionalized AuNPs in DMSO (Figure 15), leading to a decrease in AuNP-centered emission at 875 nm coupled with an increase in the Yb peak at 980 nm, indicative of efficient energy transfer.¹⁰¹ The structure of the ligand was once again essential to the energy transfer process, as shorter ligands produced more efficient sensitization via a Dexter mechanism. Additionally, Yb emission was rapidly quenched using straight-chain ligands versus bulkier aromatic ligands (Table 7).¹⁰¹ The sensitization process could also be reversed by adding a chelating agent. While the detection limit was not evaluated, spectral features corresponding to Yb-centered emission were observed at concentrations as low as 120 ppb Yb.¹⁰¹

It is worth noting that the unique, visible plasmonic features of larger AuNPs have also been exploited for colorimetric sensing applications. For example, Hutchison's group functionalized plasmonic gold nanoparticles with a tetramethylmalonamide binding group that selectively binds trivalent lanthanides, causing chelation-induced aggregation and a corresponding red-shift and broadening of the localized surface plasmon resonance peak.¹⁹³ Similar strategies have been employed to develop a AuNP-based La(III) sensor¹⁹⁴ and a AgNP-based Yb(III) sensor.¹⁹⁵

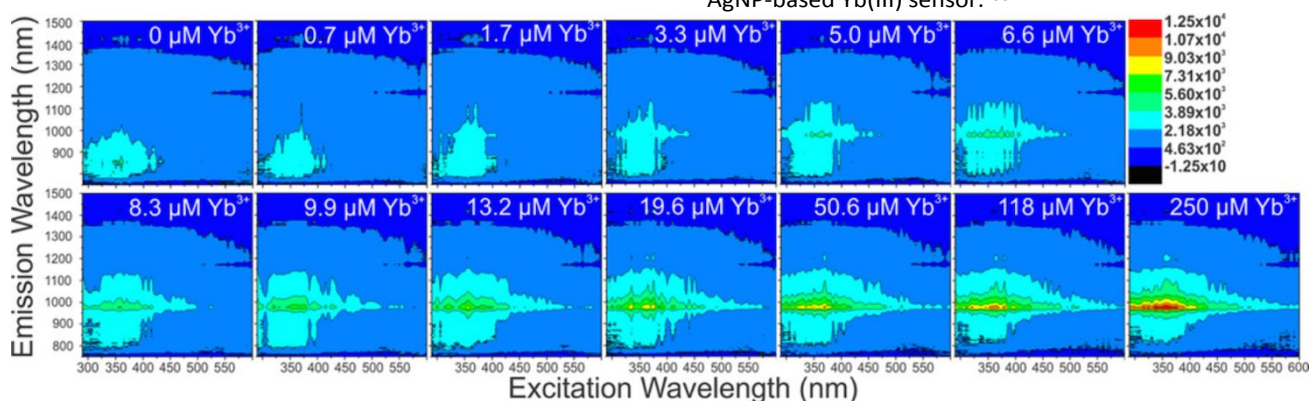


Figure 15. Excitation/emission contour plots of *ortho*-mercaptobenzoic acid-capped gold nanoparticles in the presence of increasing concentrations of Yb^{3+} ions in DMSO. The AuNP peak at 875 nm gradually weakens, while the Yb-centered peak emerges at 980 nm during the energy transfer. Reprinted from Ref. 101 with permission from the American Chemical Society, copyright 2017.

9. Metal-Organic Frameworks/Coordination Polymers

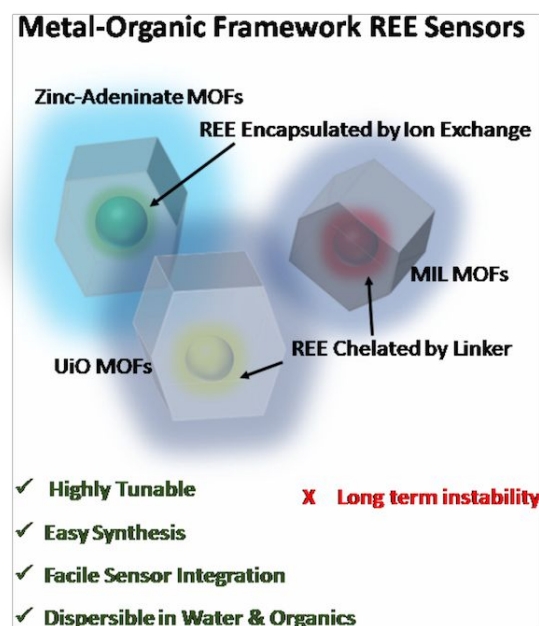
Metal-organic frameworks (MOFs) are crystalline, ordered, highly porous materials consisting of metal centers linked by organic ligands.¹⁹⁶ MOF structural variables such as pore size can be precisely tuned via careful selection of the linker or by post-synthetic modifications, making them attractive as selective sensors. Further, a nearly limitless combination of metal centers and organic linkers can be used for the design of MOFs, enabling a range of exciting properties that can be optimized for applications including gas capture/separation, drug delivery, and sensing.¹⁹⁶ Along with structural tunability, the optical features of the MOF may also be controlled by judicious choice of the linker and metal centers, facilitating their use as REE sensitizers.^{197,198}

REEs can either be encapsulated into the pores of MOFs via post-synthetic addition (**Scheme 8**) or they can be used as metal centers during MOF synthesis. The latter strategy has been exploited to design high-performance luminescent MOFs,^{199,200} but this *Review* will focus only on MOFs capable of sensitizing REEs post-synthetically. Following REE encapsulation, chromophoric linkers on the MOF are excited, followed by energy transfer to the REE and REE-centered emission.²⁵

MOFs may offer many advantages for REE sensing applications. Their well-defined pores often provide a rigid environment around the REE, reducing vibrational quenching and interaction with solvent molecules such as water.⁵³ Consequently, REEs can be sensitized in a variety of solvents.²⁵ While some MOFs require custom-synthesized linkers, many MOFs can be synthesized from commercially available, inexpensive chemicals with relatively simple reaction protocols. MOFs can also be synthesized using non-toxic chemicals, which is advantageous relative to, for example, metal cyanide complexes or CdSe quantum dots described earlier (*vide supra*). Numerous strategies have been developed to integrate MOF films onto sensor components including optical fibers, making them well-suited for field deployment or remote sensing with portable instrumentation.^{113,114,201,202} Finally, many MOFs can rapidly sensitize multiple REEs simultaneously, even at part-per-billion concentration levels,^{4,25,53,96,203-206} while other MOFs have been designed to selectively sensitize individual REEs.²⁰⁷ These properties, taken together, point towards MOFs as a particularly promising sensor class for luminescent REE detection. While most reports on MOF-based REE sensitization have not directly evaluated REE sensing efficacy (i.e. reporting sensitization kinetics, detection limits, selectivity, etc.), **Table S1** summarizes over 75 reports on MOF-based sensitization of REEs, each of which may be useful for REE detection.

There are, however, multiple challenges that must be overcome for the development of a robust MOF-based sensor. Many MOFs are not stable in water, or at the low pH levels in which REEs are often extracted. MOFs that *do* require custom-made linkers can be expensive both in terms of material cost and in the number of synthetic steps required. For environmental applications, such as deployment in acid mine

drainage where secondary metal concentrations are orders of magnitude higher than REE content, highly selective sensors will be needed (**Table 4**).³ One promising avenue for enhancing the selectivity of REE uptake is the post-synthetic functionalization of the MOF with chelating groups that have a high affinity for REEs, as demonstrated by Ahn and co-workers.¹⁰⁵ Comparable materials such as covalent organic frameworks (COFs) may also emerge as an equally intriguing sensor platform.²⁰⁸ Like MOFs, COFs are highly ordered, porous structures, but rather than being linked by metal centers, organic molecules are instead linked through covalent bonds. A recent strategy of post-synthetic encapsulation of Eu with a COF was demonstrated, suggesting that COFs may also have utility as REE sensors.²⁰⁸



Scheme 8. Overview of REE sensing using metal-organic frameworks (MOFs). Anionic MOFs, such as the zinc-adeninate series, may encapsulate REEs via a cation-exchange process, whereas other MOFs such as the UiO and MIL series, utilize linkers with extra chelation sites that bind REEs. Following REE encapsulation, the REEs are sensitized through the chromophoric linkers in the MOF structure, enabling detection. A nearly limitless combination of metal centers and linkers may be used for MOF formation. General advantages and disadvantages are listed.

Zinc-Adeninate MOFs

One of the first examples of an anionic MOF post-synthetically encapsulating an REE was demonstrated by Rosi and Petoud using the zinc-adeninate MOF dubbed “bioMOF-1.” The MOF, comprised of zinc metal centers with adenine (ad) and biphenyldicarboxylate (BPDC) linkers, is anionic with dimethylammonium cations residing in its pores (structural formula = $[Zn_8(ad)_4(BPDC)_6O \cdot 2Me_2NH_2, 8DMF, 11H_2O]$).⁵³ The dimethylammonium cations exchange with REE cations via incubation in DMF, leading to efficient sensitization of Tb(III), Sm(III), Eu(III), and Yb(III), even after dispersion in water.⁵³ Since this ground-breaking study, REE@bioMOF-1 systems have been developed for use as sensors,²⁰⁹⁻²¹² solid-state white lighting displays,²¹¹ and optical barcodes.²¹³ To date, bioMOF-1 is known to sensitize Tb, Sm, Eu, Yb, and Nd. The related anionic MOF JXNU-4 (structural formula = $\{(Me_2NH_2)_2[Zn_6(\mu_4-O)(ad)_4(BPDC)_4]\}_n$) also sensitizes Tb emission.²¹⁴

Inspired by the bioMOF-1 and JXNU-4 work, we investigated the REE sensing efficacy of bioMOF-100, which contains the same metal and linkers as bioMOF-1/JXNU-4 but forms the mesoporous structure $\text{Zn}_8(\text{ad})_4(\text{BPDC})_6\text{O}_2 \cdot 4\text{Me}_2\text{NH}_2 \cdot 49\text{DMF} \cdot 31\text{H}_2\text{O}$.²⁵ We hypothesized that the high porosity of bioMOF-100 would facilitate rapid REE uptake and sensitization, even when evaluated directly in water (**Figure 16**). BioMOF-100 was screened for sensitization of 10 emissive REEs, producing part-per-billion limits of detection for Tb, Dy, Sm, Eu, Yb, and Nd in water (**Table 2**).²⁵ Kinetics studies revealed maximum emission signal was obtained within ~5 to 10 minutes, depending upon the REE. Additionally, the sensor performance was evaluated in matrices containing metal interferants (FeSO_4) and acid to simulate conditions expected from environmental samples. Signal was still obtained at sub-3 pH and >100 ppm Fe, however quenching effects were clearly observed, indicating that interferant mitigation strategies will be needed for successful field work. One potential strategy would be to first use an extracting agent to separate the REEs from interferants in the field. As a proof-of-concept, Eu and Nd in water were extracted into hexanes using trioctylphosphine oxide (TOPO), and signal was obtained in hexanes using bioMOF-100.²⁵

UiO MOFs

The UiO (University of Oslo) family of MOFs have been extensively explored for REE sensitization due to their stability even in relatively harsh aqueous conditions such as high or low pH.²¹⁶ Typically, REE uptake into UiO is facilitated via functionalization of the linker with extra amine or carboxylate sites to provide interaction sites. Interestingly, reports on UiO-based sensitization of REEs have mainly focused only on Eu(III).

UiO-66, made up of terephthalic acid linkers and zirconium metal centers, has been modified in several different ways to facilitate Eu sensitization, summarized in **Table 8**. Interestingly, Yan's group found that the sensitization of Eu by UiO-66 modified with 1,2,4,5-benzenetetracarboxylic acid could be enhanced following exposure to Cd ions. This emission enhancement was attributed to either a) reduced vibrational quenching from Cd chelation, b) enhanced intermolecular energy transfer from the linker to Eu(III) due to the "heavy atom" effect, and/or c) Cd-mediated alterations to the excited state energy of the ligand, leading to better energy matching between the linker and Eu.²¹⁷ These results suggest that pre-incubating MOFs in solutions of "heavy atoms" such as Cd could improve MOF-based detection of REEs. Similarly, Bai and Liu modulated the number of carboxylate groups available for Eu

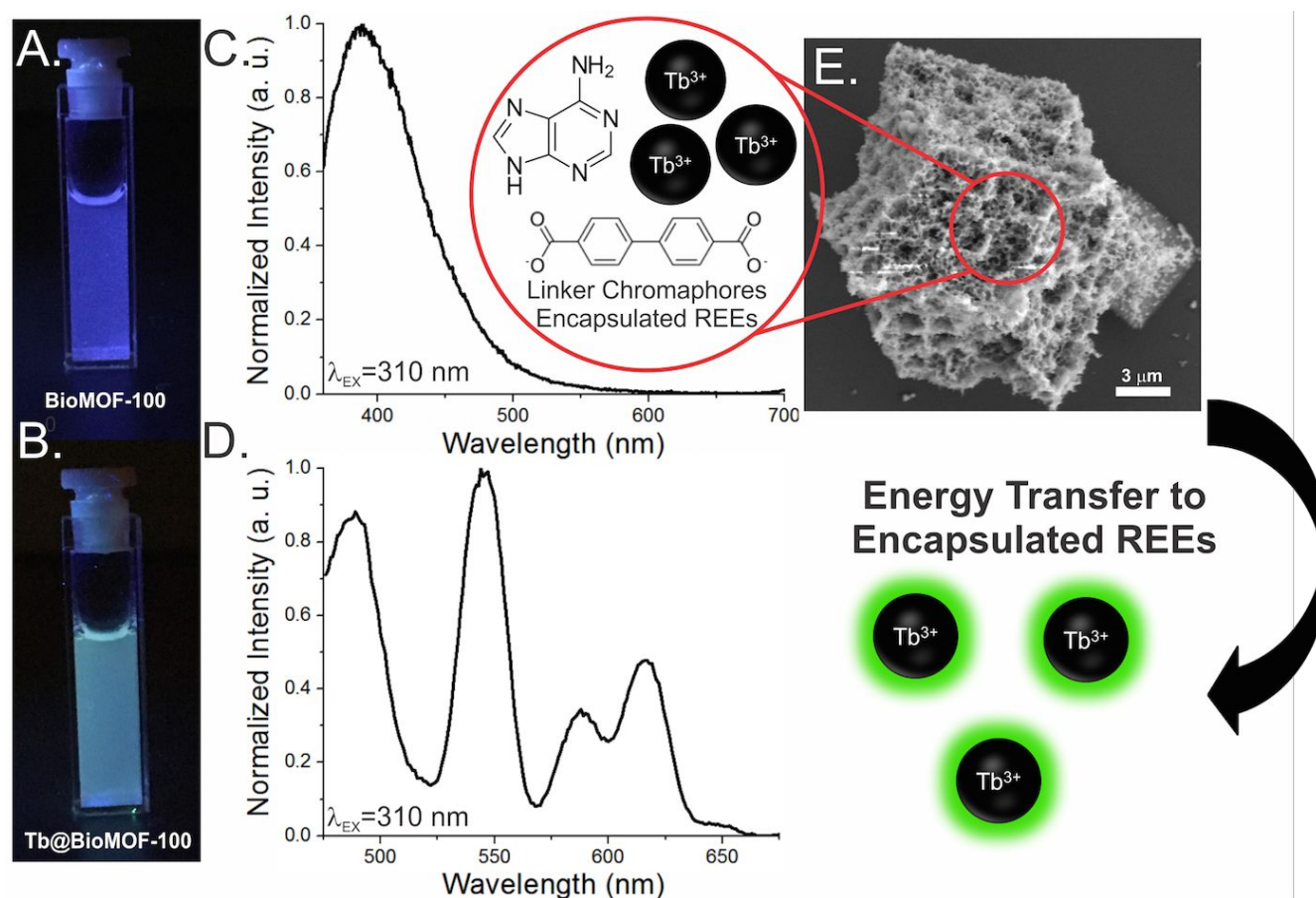


Figure 16. Schematic illustrating sensitization of REEs by BioMOF-100. Aromatic, luminescent linkers in BioMOF-100 are first excited by UV light, followed by energy transfer to REEs encapsulated within the pores of BioMOF-100, leading to REE-centered emission. A: image of BioMOF-100 in water under 365 nm illumination. B: image of BioMOF-100 in an aqueous solution of 8 ppm Tb^{3+} under 365 nm illumination. C: normalized emission spectra of BioMOF-100 in water, excited at 310 nm. D: normalized emission spectra of the Tb^{3+} excited at 310 nm. E: scanning electron micrograph of BioMOF-100. Reprinted with permission from Ref. 25. Copyright 2019, American Chemical Society.

Table 8. Modifications of UiO-66 to Facilitate Eu Uptake

| Ligand | Binding Site | Ref. |
|-------------------------------------|---------------|---------|
| 1,2,4-benzenetricarboxylic acid | Extra -COOH | 218 |
| 1,2,4,5-benzenetetracarboxylic acid | 2 Extra -COOH | 218,217 |
| terephthalic acid/isophthalic acid | Defect Sites | 216,219 |
| 2,6-pyridinedicarboxylic acid | Extra Amine | 220 |

binding by varying the terephthalic acid:isophthalic acid ratio used in the synthesis; increasing the isophthalic acid content created defect sites in the MOF to which the Eu and Tb could bind. Finally, UiO-66/REE interactions can be promoted by introducing an amine group instead of a carboxylate functionality by using 2,6-pyridinedicarboxylic acid as the linker.

An intriguing use of UiO-66 for REE uptake was demonstrated by Wang and co-workers, who integrated UiO-66-2COOH with polyacrylonitrile nanofibers and monitored their ability to absorb Tb and Eu in solution. Loadings of up to 60% by weight were recorded, with sensitized emission observed from Tb, Eu, and a combination of Eu/Tb (Figure 17). Remarkably, the absorbent could be regenerated via incubation in HCl, indicating the material can be recycled and reused.²²¹

Similar modifications have been made to UiO-67, consisting of zirconium metal centers linked by biphenyldicarboxylates. For example, Cui and Qian introduced nitrogen groups into their linker by using 2,2-bipyridine-5,5-dicarboxylic acid (bpydc) in the MOF synthesis, providing additional sites for Eu interaction. Eu could be sensitized even at sub-2 pH levels, highlighting the stability of the UiO system in acidic conditions.²²²

MIL MOFs

The MIL (Materials of Institut Lavoisier) series of MOFs have also shown promise for REE sensitization. Like the UiO series, the bulk of experiments involving REE functionalization have focused on using sensitized REE emission to detect other analytes, rather than using the MOF to detect the REEs themselves. Modified linkers with additional functional groups for REE binding are again often used during the MIL synthesis. However, unlike the UiO system that was evaluated only on Tb and Eu, the MIL systems have been demonstrated to sensitize Tb, Dy, Sm, Eu, Yb, Nd, and even Er.^{204,205}

Al-MIL-53-COOH, comprised of aluminum metal centers and trimellitic acid, was used by the Yan group for Eu and Tb sensitization. The trimellitic acid linker provides an extra carboxylate site for REE absorption, facilitating REE uptake.²²³ A composite material consisting of carbon dots (*vide supra*) encapsulated in Al-MIL-53-COOH has also demonstrated efficacy in sensitizing Eu.²²⁴ Other MIL Eu(III) sensitizers are summarized in Table 9, which includes two examples of REE detection using MOFs in the solid-state: thin films of MIL-124(In) sensitize Eu, while MIL-100 solvothermally grown onto silicon²²⁵ and indium tin oxide²²⁶ substrates sensitizes Tb, Sm, Eu, and Dy. Such studies are important for portable sensing work, as the MOFs may be immobilized onto optical fibers.¹¹⁴ Among the intriguing innovations in MIL-based REE sensitization is the use of silver ions to enhance REE emission intensity. Similar to the “heavy atom” effects observed in the UiO-66 system loaded with Cd ions (*vide supra*), post-synthetic addition of Ag⁺ to REE-loaded MIL MOFs significantly enhanced the luminescence signal. For example, MIL-121, comprised of Al metal centers with 1,2,4,5-benzenetetracarboxylic acid linkers, can sensitize Tb and Eu by itself.²²⁷ However, adding Ag⁺ post-

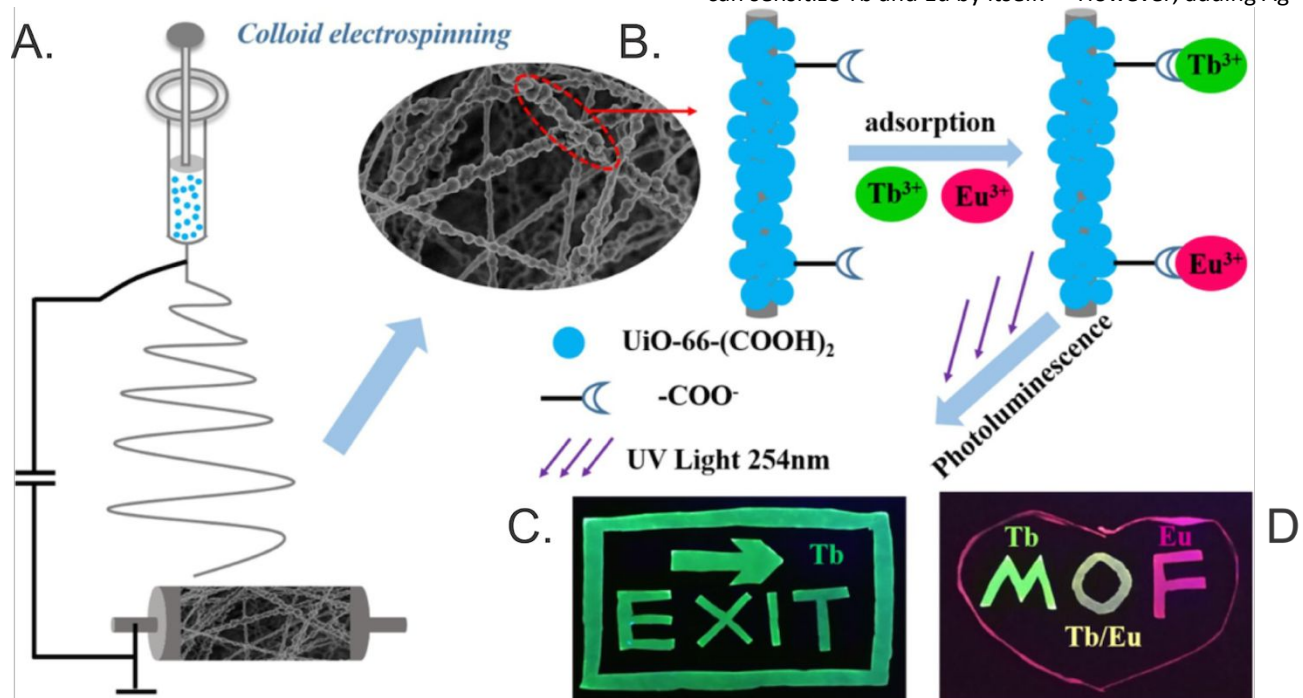


Figure 17. A. Schematic illustrating the colloid electrospinning-based production of UiO-66-(COOH)₂ nanofiber membranes with (B) and SEM image of the MOF-coated fibers. Carboxylate groups in the MOF bind REEs, enabling MOF-based REE sensitization upon UV excitation. The inset are photographs of nanofiber films exposed to Tb (C) and Tb, Eu, and Tb/Eu (D) under UV excitation. Reprinted with permission from Ref. 221. Copyright 2019, Elsevier, Inc.

Table 9. MIL Series MOFs for REE Sensitization

| Name | Metal | Linker | Sensitized REE | Ref. |
|----------|-------|---------------------------------|----------------|---------|
| MIL-124 | Ga | 1,2,4-benzenetricarboxylate | Eu | 228,229 |
| MIL-125 | Ti | 2-aminoterephthalic acid | Eu | 230 |
| MIL-116 | Al | benzenehexacarboxylate | Eu | 231 |
| MIL-140C | Zr | biphenyl-4,4'-dicarboxylic acid | Eu | 232 |
| MIL-124 | In | 1,2,4-benzenetricarboxylate | Eu | 233 |
| MIL-100 | In | benzene-1,3,5-tricarboxylate | Tb, Sm, Eu, Dy | 225,226 |

synthetically to Eu@MIL-121 enhances Eu emission 5-fold (Figure 18),²³⁴ Sm emission 30-fold, Dy emission 20 fold, and enables sensitization of the NIR-emitting elements Yb, Nd, and Er.²³⁴ Further, addition of Ag⁺ to MIL-61 (gallium metal, 1,2,4,5-benzenetetracarboxylic acid linker) enhances sensitization of Yb, Nd, Er, Sm, Tb, Dy, and Eu.²⁰⁴

Taken together, MIL represents a powerful class of MOF-based REE sensitizers, capable of sensitizing up to 7 different REEs. While it is not clear if adding Ag⁺ prior to REE exposure will enhance the sensitization process, the use of heavy atoms to improve sensor sensitivity is an intriguing strategy that warrants further investigation. It has also been shown with MIL-101 that the MOF can be functionalized with selective chelating groups for REE extraction, and coupling this strategy with luminescent sensing experiments may improve selectivity for REEs.¹⁰⁵

Other MOF-based REE Sensitizers

While the three MOF classes described above have been extensively studied for their ability to sensitize REE emission, there are other MOFs that exhibit intriguing REE sensitization properties. Here we highlight MOFs that show promise in their demonstrated ability to sensitize multiple REEs, detect low quantities of an REE, and/or rapidly obtain signal following REE exposure. Many of these MOFs are included in Table 10, with a more comprehensive list of over 75 MOFs capable of post-synthetic REE sensitization included in Table S1 (*N.B.* because many of these MOFs were not designed specifically for REE sensing, long loading times were often used to ensure complete REE loadings. However, based on the performance of MOFs that have been evaluated for REE sensing, it is likely that significantly shorter times may be used).

Several MOFs have been evaluated directly for their efficacy in detecting REEs via luminescence-based techniques. Notably, in 2015 Sun and co-workers developed a series of cadmium MOFs with hexa[4-(carboxyphenyl)oxamethyl]-3-oxapentane acid linkers, modified with different space-directing N-donors, including the V-shaped 2,2-bipyridine (bipy), I-shaped 4,4'-di(1*H*-imidazol-1-yl)-1,1'-biphenyl (bib), and Y-shaped 1,3,5-tri(1*H*-imidazol-1-yl)benzene (tib) (Figure 19).⁹⁷ Each of the three MOFs were screened as sensors for 9 different REEs in water, and selective sensitization of Tb was observed in all three cases. The MOF containing the Y-shaped tib ligand yielded a

detection limit of ~16 ppb for Tb, whereas the bib and bipy linkers had detection limits of ~1600 ppb. Kinetics studies indicated that Tb signal could be observed within half an hour, with gradual increase in intensity over the course of 72 hours.⁹⁷ This work highlights the importance of correlating MOF structure with sensitization efficacy, an area not widely studied to date. A separate study found that the MOF linker could be used to tune selectivity for Eu versus Tb: an indium and 5',5''-oxybis(2'-methoxy[1,1':3',1''-terphenyl]-4,4''-dicarboxylic acid) could sensitize Tb emission at concentrations as low as 10⁻⁷ M (~16 ppb), with Eu emission observed at ~10⁻⁶ M (~150 ppb) in water.⁸⁹ Using 5',5''-oxybis([1,1':3',1''-terphenyl]-4,4''-dicarboxylic acid) as the linker decreased the MOF's ability to sensitize Tb by several orders of magnitude but led to an order of magnitude increase in Eu sensitization, again highlighting the importance of the MOF structure for REE sensing.⁸⁹

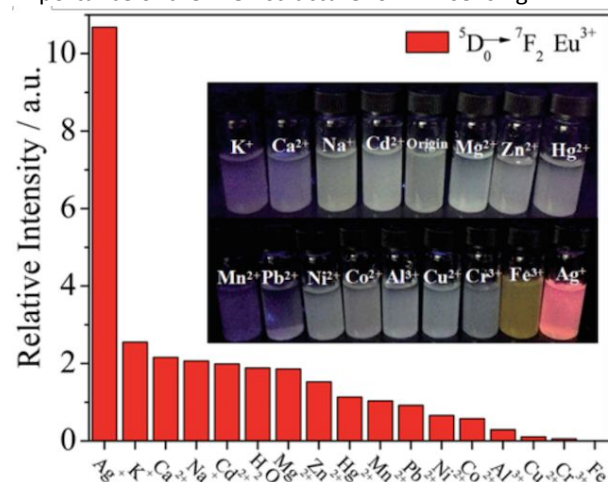


Figure 18. Luminescent response of Eu@MIL-121 exposed to 10 mM concentrations of different ions. The signal is enhanced 5-fold in the presence of Ag⁺, with no response or quenching in the presence of other ions. Inset: photograph of each sample under 254 nm illumination, where characteristic red Eu-based emission is clearly observed only with Ag⁺. Reprinted with permission from Ref. 234. Copyright 2014, Royal Society of Chemistry.

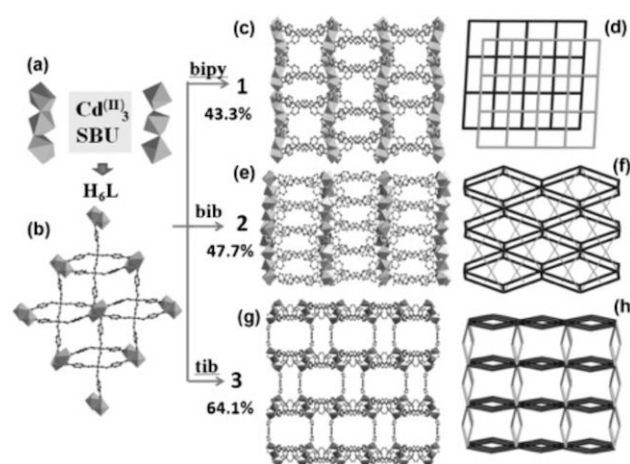


Figure 19. Schematic illustration of MOF structures evaluated for REE detection with hierarchical free-pore volumes and interesting topological nets constructed by (Cd²⁺)₃ secondary binding units (SBUs), extendable hexatopic ligands (H₆L), and different N donors (i.e., V-shaped bipy, I-shaped bib, and Y-shaped tib ligands). Linker-induced structural changes in the MOF structure impacts the ability of the MOF to sensitize Tb. Reprinted with permission from Ref. 97. Copyright 2015, John C. Wiley and Sons, Inc.

Table 10. Summary of MOF-Based REE Sensitizers

| Name | Elements Sensitized | Loading Solvent | Loading Time | Measured Solvent | Ref. |
|--|----------------------------|-----------------------|--------------|---|-------------|
| [[Cd(4,4'-bipy)(H ₂ O)(L)]·(4,4'-bipy)·11(H ₂ O)] | Tb, Eu, Nd | H ₂ O | 1.5 hours | N/A | 235 |
| [(CH ₃) ₂ NH ₂][In(L)]·CH ₃ CH ₂ OH | Tb, Eu, Dy, Sm | DMF | 72 hours | N/A | 236 |
| [Cd ₃ (L)(tib)(DMF) ₂] | Tb, Dy, Eu | H ₂ O | 0.5 hours | H ₂ O | 97 |
| [Cu(HCPOC) ₂] _n | Tb | H ₂ O | 0.5-72 hours | H ₂ O | 237 |
| [Cu ₂ (3,3'-dpdc) ₂ (bpp)] | Tb, Eu | H ₂ O | N/A | H ₂ O | 238 |
| [Cu ₂ (3,4-pydc) ₂ (H ₂ O) ₅] _n ·2nH ₂ O | Tb | H ₂ O | 1 minute | H ₂ O | 95 |
| [HDMA] ₂ [Zn ₂ (BDC) ₃ (DMA)]·6DMF | Eu, Tb, Sm, Dy, Nd, Yb | DMF | 72 hours | N/A | 206 |
| [NH ₄] ₂ [ZnL]·6H ₂ O | Eu, Tb | H ₂ O | N/A | H ₂ O | 239 |
| [Pb ₂ (TZI)(μ ₃ -OH)(H ₂ O)·(H ₂ O)] _n | Tb, Eu, Sm, Dy | H ₂ O | 48 hours | N/A | 240 |
| [Zn(O-OBA)(BPP)]·0.5H ₂ O | Tb, Eu, Dy, Sm | H ₂ O | 72 hours | H ₂ O | 241 |
| [Zn(μ-L)(μ-1,3-dpp)] | Tb, Eu | H ₂ O | ~5 minutes | H ₂ O | 242 |
| [Zn ₂ (btb) ₂ (bbis)](Me ₂ NH ₂) ₂ ·6DMF | Tb, Eu, Sm, Dy | EtOH | 48 hours | Various Organic | 243 |
| [Zn ₂₁ (BTC) ₁₁ (μ ₃ -OH) ₃ (μ ₄ -O) ₃ (H ₂ O) ₁₈] _n ·21EtOH | Tb, Eu | EtOH | 2 hours | N/A | 244 |
| [Zn ₃ (Hbptc) ₂ (DMF) ₂] _n ·2DMF | Tb, Sm, Eu, Dy | Acetone | 72 hours | N/A | 245 |
| [Zn ₃ (L) ₂ (4,4'-bipy)(DMF) ₂] _n ·2H ₂ O | Tb, Eu | H ₂ O | 24 hours | N/A | 246 |
| [Zn ₇ L ₆](H ₂ NMe ₂) ₄ ·(H ₂ O) ₄₅ | Tb, Eu | Acetonitrile | 35 seconds | Acetonitrile | 225 |
| {(Me ₂ NH ₂)[Zn(L)(H ₂ O)]·DMF} _n | Tb, Eu, Sm, Dy | DMF | 48 hours | N/A | 247 |
| {[(CH ₃) ₂ NH ₂] ₂ [Zn ₅ (TDA) ₄ (TZ) ₄] _n ·4DMF} _n | Tb, Eu | MeOH | 24 hours | H ₂ O | 248 |
| {[In(FDA)(HFDA)(H ₂ O) ₄] _n ·2H ₂ O} | Eu, Dy | H ₂ O | 2 min | H ₂ O | 4 |
| {[Me ₂ NH ₂] _{0.125} [In _{0.125} (H ₂ L) _{0.25}] _n ·xDMF} _n | Eu, Dy, Sm, Tb | EtOH | 48 hours | N/A | 203 |
| {[Zn(H ₂ thca) _{0.5} (tib)] _n ·5H ₂ O} | Eu, Tb | H ₂ O | 48 hours | H ₂ O | 249 |
| Al-MIL-53-COOH | Eu, Tb | EtOH | 48 hours | H ₂ O | 223 |
| BioMOF-1 | Tb, Eu, Sm, Yb, Nd | DMF | 72 hours | H ₂ O, DMF, D ₂ O | 53,210-213 |
| BioMOF-100 | Tb, Eu, Dy, Sm, Yb, Nd | H ₂ O | 5 minutes | H ₂ O | 25 |
| Cd(ii)-MOF | Eu, Tb | H ₂ O | 2 to 8 hours | N/A | 250 |
| C-dots@MIL-53-COOH | Eu | EtOH | N/A | H ₂ O | 224 |
| COK-15 | Eu, Tb, Sm, Dy | EtOH/H ₂ O | 48 hours | N/A | 251 |
| HNU-25 | Tb, Dy | DMF | 1 minute | DMF | 96 |
| HPU-14 | Tb, Eu | H ₂ O | 0.5 hours | N/A | 252 |
| IFMC-10 | Eu, Sm, Tb | DMF | 48 hours | DMF | 115 |
| IFMC-2 | Tb, Dy, Eu | DMF | 48 hours | N/A | 253 |
| IFMC-3 | Tb, Dy, Eu, Sm | DMF | 48 hours | N/A | 254 |
| IRMOF-3 | Nd, Eu, Tb | EtOH | 72 hours | N/A | 255,256 |
| JXNU-4 | Tb, Eu | H ₂ O | 12 hours | H ₂ O | 214,257 |
| Mg-MOF | Eu, Tb | H ₂ O | 30 seconds | H ₂ O | 207 |
| MIL-100 | Eu, Tb, Dy, Sm | DMF | 48 hours | N/A | 225,258,259 |
| MIL-116 | Eu | EtOH | 48 hours | H ₂ O | 231 |
| MIL-121 | Sm, Dy, Nd, Yb, Er | H ₂ O | 24 hours | H ₂ O | 227,234,260 |
| MIL-124 | Eu | EtOH | 24 hours | H ₂ O | 229,233 |
| MIL-125-(Ti)-NH ₂ -AM | Eu | MeOH | 6 hours | Various Organic | 230 |
| MIL-140C | Eu | DMF | 24 hours | H ₂ O | 232 |
| MIL-61 | Eu, Dy, Sm, Tb, Er, Nd, Yb | H ₂ O | 24 hours | H ₂ O | 204,261,262 |
| MOF-808 | Tb | Ethanol | 6 hours | Various, incl. H ₂ O | 263 |
| MOF-SO ₃ ⁻ | Tb, Eu | H ₂ O | 12 hours | H ₂ O | 264 |
| NENU-522 | Eu, Tb, Sm, Dy | DMF | 48 hours | DMF | 265 |
| Ni-BTC | Tb, Dy, Sm, Eu | EtOH | 12 hours | H ₂ O | 266,267 |
| Pb ₂ L ₂ | Eu, Tb | H ₂ O | 3 hours | H ₂ O | 268 |
| Sc-MOF | Eu | EtOH | 10 hours | H ₂ O | 269 |
| UiO-66(DPA) | Eu | H ₂ O | 24 hours | H ₂ O | 220 |
| UiO-66(Zr)-(COOH) ₂ | Eu | EtOH/H ₂ O | 20 hours | H ₂ O | 217,270,271 |
| UiO-66-COOH | Eu | EtOH | 24 hours | N/A | 218,221 |
| UiO-66-IPA | Eu, Tb | H ₂ O | 24 hours | H ₂ O | 216,219 |
| UiO-67 | Eu | MeOH | 12 hours | H ₂ O | 226 |
| UiO-67(Bypdc) | Eu | MeOH | 120 hours | H ₂ O | 222 |

Zn-Hbtc-BPY

Tb, Eu

EtOH

24 hours

H₂O and others

272

*EtOH: Ethanol; MeOH: Methanol; DMF: Dimethylformamide; DMA: Dimethylacetamide. N/A indicates that this information was not provided or that the measurements were conducted in the solid state. Highly sensitive (0.3 ppb detection limit) sensors for Tb(III) were developed by Pan's group using MOFs comprised of zinc metal centers with tetrazole and 5-[bis(4-carboxylbenzyl) amino] isophthalic acid ligands (HNU-25 and HNU-26).⁹⁶ REE binding was achieved through both tetrazole nitrogen atoms and oxygen atoms from the carboxylic acid, enabling Tb to be detected within 1 minute of exposure. Weak sensitization was observed in the presence of Dy, and no sensitization was observed for the other REE.⁹⁶ More recently, a copper(II) 3,4-pyridine dicarboxylic acid MOF was developed for Tb detection.⁹⁵ The MOF underwent a cation exchange where Tb displaced Cu in the MOF structure. Signal could be obtained within 1 minute, and although no limits of detection were reported, clear signal was obtained at 1 μM concentrations (~ 160 ppb) in water. Importantly, the sensor could be regenerated by incubating the MOF in copper nitrate; the Cu cations would exchange with Tb(III), producing MOF crystals with the same XRD pattern as the original Cu-MOF. Other emissive REEs were not evaluated.

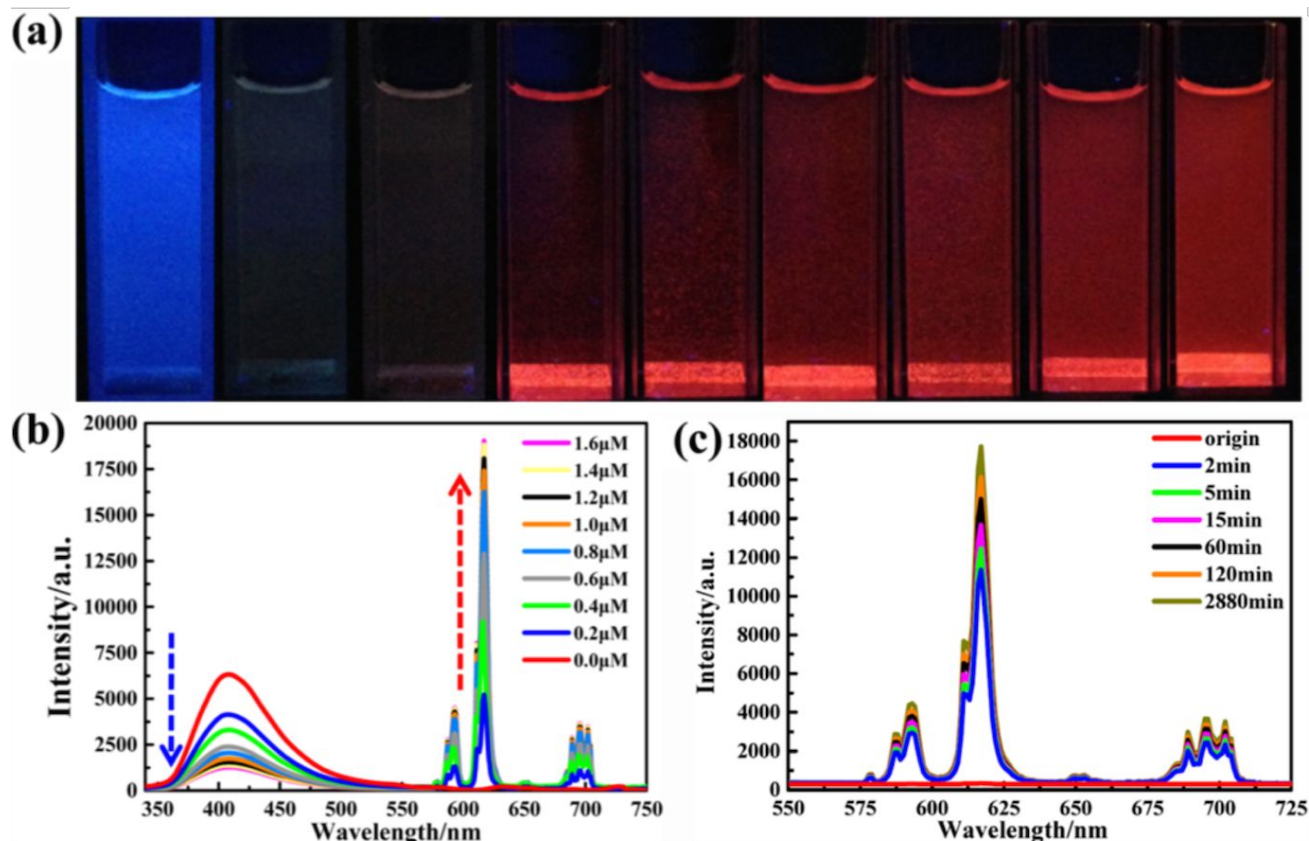


Figure 20. Sensitization of Eu(III) using $[\text{In}(\text{FDA})(\text{HFDA})(\text{H}_2\text{O})_4]\cdot 2\text{H}_2\text{O}$. (A) Photographs of the MOF-Eu composite under UV light with Eu concentration ranging from 0 μM to 1.6 μM moving from left to right. (b) Emission profile of the MOF-Eu composite as a function of Eu concentration; with increasing Eu, the MOF-centered emission peak at 408 nm decreases while the Eu-centered peak at 617 nm increases. (c) Emission profile of the MOF-Eu composite as a function of time after Eu addition. Over 50% maximum signal is obtained within 2 minutes. Reprinted with permission from Ref. 4. Copyright 2017, the American Chemical Society.

The exploration of MOF-lanthanide interactions have often been motivated by the development of white-light emitting materials, and these studies have also uncovered promising REE-sensor materials.^{4,246,249,265,273,274} For instance, an indium and furan-2,5-dicarboxylic acid MOF was demonstrated to sensitize both Dy(III) and Eu(III) in water, with a 130 ppb detection limit for Eu.⁴ Significantly, kinetics studies revealed that intense Eu signal could be observed within 2 minutes, with a gradual increase in intensity over 2 days (Figure 20).⁴ Similarly, Ni and co-workers investigated MOF/REE composites for white-light applications by encapsulating Tb and Eu using MOF microspheres comprised of zinc, benzene-1,3,5-tricarboxylate (BTC), and 4,4'-bipyridine (bipy). REE emission could be detected in a multitude of solvents and across a range of pH values, and the MOF could be synthesized at room temperature and ambient atmosphere, an advantage for mass-production²⁷²

Several MOFs (in addition to the MIL and zinc-adeninate structures described above) can simultaneously sensitize emission from multiple REEs beyond Tb and Eu. Three such MOFs have been developed at the Institute of Functional Materials Chemistry (IFMC) for lanthanide sensitization. IFMC-2, comprised of zinc and 4,5-di(1H-tetrazol-5-yl)-2H-1,2,3-triazole linkers, is unique in that it is one of the few to efficiently sensitize Dy emission in addition to Tb (Figure 21).²⁵³ IFMC-3, made up of zinc, 5-methyl-1H-tetrazole and phosphoric acid, sensitized emission from Eu, Tb, Dy, and Sm, although emission from the latter two REEs was weak.²⁵⁴ Reversible sensitization of Tb, Eu, and Sm was achieved within 30 minutes using IFMC-10 (zinc and 4',4'',4'''-(2,4,6-trimethylbenzene-1,3,5-triyl)tris(methylene)tribiphenyl-4-carboxylate linkers). Interestingly, the Eu could be removed from the IFMC-10 by incubation in DMF for 24 hours, indicating recyclability.¹¹⁵

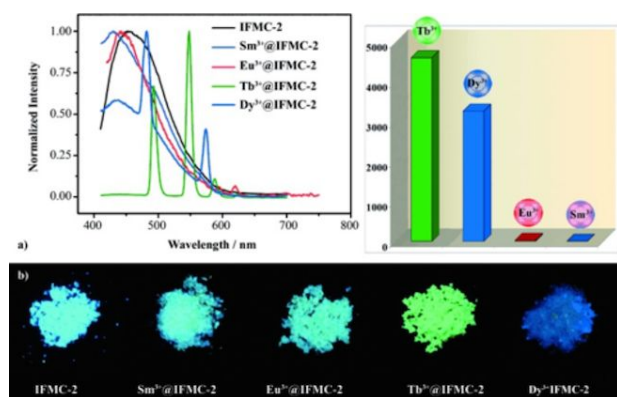


Figure 21. Emission spectra of IFMC-2 and REEs encapsulated by IFMC-2 (top left). Maximum intensity at the characteristic emission wavelength for each REE following encapsulation by IFMC-2 (top right). Photographs of MOF powders illuminated by UV light before and after exposure to each REE. Reprinted with permission from Ref. 253. Copyright 2014, John C. Wiley and Sons, Inc.

The Yan group demonstrated that an anionic zinc-benzene-1,4-dicarboxylate MOF could sensitize emission from both visible and near-infrared REEs, including Tb, Dy, Sm, Eu, Yb, and Nd via a cation-exchange mechanism.²⁰⁶ Given the rapid uptake of REEs reported for anionic MOFs,²⁵ the zinc-benzene-1,4-dicarboxylate's ability to sensitize multiple REEs makes it a promising candidate for further sensing-based evaluations, including investigating its loading kinetics, water stability, REE selectivity, and detection limits. Many other MOFs have been evaluated as sensitizers for the visible-emitting REEs, with the ability to induce emission from Tb, Dy, Sm, and Eu using a single material.^{240,241,243,245,247,265} Among these, a zinc MOF with 2,2'-oxybis(benzoate) and 1,3-di(4-pyridyl)propane linkers underwent both REE loading and emission measurements in water, an important consideration for sensing in environmental systems such as e-waste processing streams,²⁴¹ as did a cadmium(II) MOF with a custom-designed ethylene glycol ether-bridging dicarboxylate ligand and 4,4'-bipyridine linkers.²³⁵ A Ni-BTC coordination polymer exhibited intense sensitization of Tb and moderate sensitization of Dy, Sm, and Eu.²⁶⁶ Following Tb sensitization, the MOF exhibited resistance to quenching in the presence of 1 mM concentrations of a variety of secondary metals, including several that would be encountered in AMD systems such as Fe(II), Al(III), and Ca(II). Quenching was observed with Cu(II) and Fe(III). Such studies are

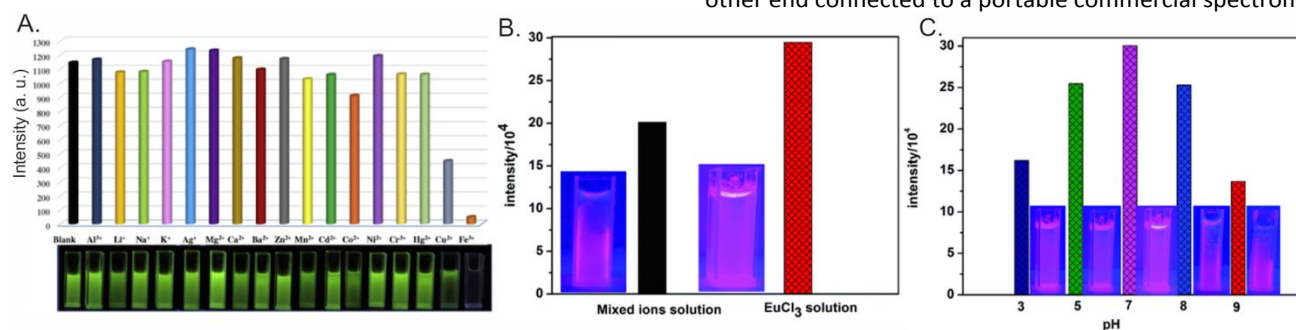


Figure 22. Quenching studies of REE@MOFs in the presence of metals and acids. A) Emission intensity of Tb encapsulated by Ni-BTC in the presence of aqueous 1 mM concentrations of different cations. The inset shows the corresponding photographs of each Tb@Ni-BTC sample under UV illumination. Strong quenching is observed only from Cu(II) and Fe(III). Reprinted with permission from Ref. 266. Copyright 2020, Elsevier, Inc. B) Plot of maximum Eu emission sensitized by a Mg-MOF intensity with and without the presence of equal concentrations of transition metal cations and C) as a function of pH. Insets show a photograph of each sample under UV light. Reprinted with permission from Ref. 207. Copyright 2014, Royal Society of Chemistry.

critical for evaluating “real world” systems in which sensors can be practically deployed (**Figure 22A**).²⁶⁶

Conversely, some MOFs have been reported to selectively sensitize Eu(III) but no other visible-emitting REEs.^{207,275,276} This selectivity may be useful in situations where only one REE is targeted, particularly if the MOF is robust against other cationic interferants. A MOF made of magnesium and (4,4'-(pyrazine-2,6-diyl)) dibenzoic acid not only showed selectivity for Eu sensitization, but also produced signal within 30 seconds in water. Further, the Eu emission was robust across a range of pH values (3 to 9), and in the presence of equal concentrations of interfering cations such as Fe and Cu (**Figure 22B-C**).²⁰⁷

10. Portable Luminescent Sensors

A key advantage of luminescence-based sensors over the more commonly-used ICP-MS characterization (in addition to cost savings) is the portability of fluorescence spectrometers. Small, simplistic sensor designs have been developed with low power requirements, enabling them to be carried into the field to characterize REE-rich streams, providing significant time savings over competing techniques. Portable designs typically involve a light source, such as a broadband lamp or light-emitting diode (LED), a detector, and optical fibers to direct exciting light to the sample and/or emitted light to the detector.

One such example is shown in **Figure 23**. Here, the tip of an optical fiber was coated with a PVP membrane containing a bis(phosphinic acid)phosphine oxide sensitizer, producing an inexpensive and portable Eu(III) sensor with a 92 second response time and a 2 ppb detection limit.⁸³ In this set-up, an external UV lamp is used, enabling sensing in solution or in air after Eu exposure. A similar design has been introduced using a 280 nm LED excitation source, with an optical fiber to guide emitted light from the sample cuvette to a detector. In this case, the sensitizer is pre-mixed with the solution, rather than being deposited on the fiber itself.²⁷

In a separate design, a Y-shaped bifurcated optical fiber bundle is used, in which two separate fiber cables meet at a single tip. In this study, the bifurcated fiber tip was placed in an REE-containing solution along with the sensitizer material. One end of the fiber was connected to a 365 nm LED source, and the other end connected to a portable commercial spectrometer

(Scheme 9).²⁴ When a gold-cyanide sensitizer was used, part-per-billion detection of the visible-emitting REEs (Tb, Eu, Sm, and Dy) were achieved. Such a set-up may be modified to accommodate different sensitizers, light sources, and detectors, providing a versatile platform for REE detection.

As described in Section 2, time-resolved luminescent techniques show promise for REE detection.^{55,277} Several portable time-resolved designs have been developed over the past two decades,^{278,279} including one that used signal from Eu to detect trace amounts of pharmaceuticals.⁵⁶ These spectrometers consist of a pulsed excitation source (e.g. xenon flash lamp, overdriven pulsed LEDs, and/or pulsed laser diodes), and a photomultiplier tube is often used as the detector. Such designs may be useful for deployment in the field to sense REEs.

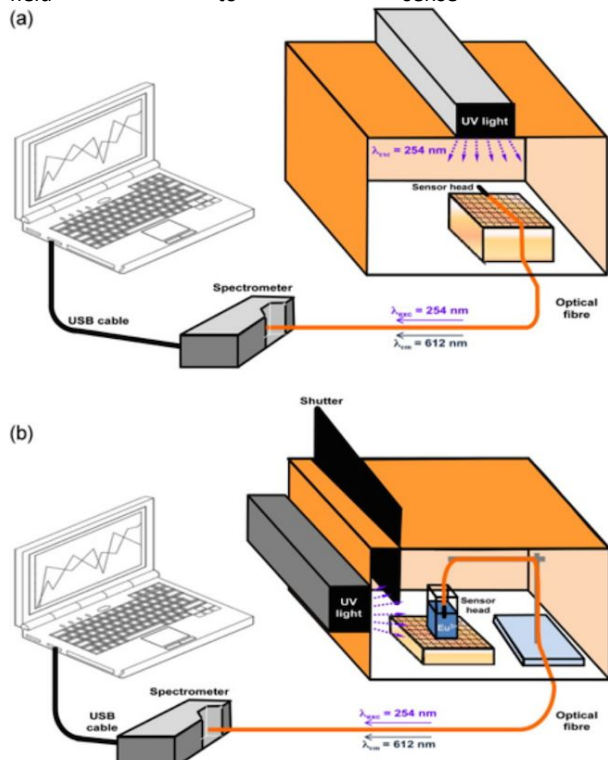
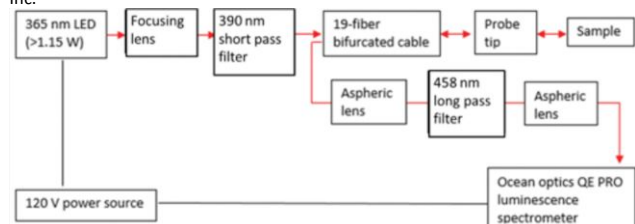


Figure 23. Experimental set-up for the optical fiber-based detection of Eu luminescence in (a) aerial and (b) solution using the $\text{PhPO}-(\text{C}_6\text{H}_4\text{POPhN}(\text{CH}(\text{CH}_3)_2)_2)_2$ sensor embedded into a PVP membrane. Reprinted with permission from Ref. 83. Copyright 2012, Elsevier, Inc.



Scheme 9. Schematic of an optical fiber-based portable luminescent sensor equipped with an LED excitation source. Reprinted with permission from Ref. 24. Copyright 2017, Institute of Electrical and Electronics Engineers.

11. Conclusions and Opportunities

Monopolistic global economic conditions, environmental concerns, and the projected increase in demand for REE-intensive technologies has spurred interest in the recovery of REEs from various non-conventional sources.^{5,25} A key challenge to attaining a stable, sustainable REE supply is the development of rapid, quantitative, and

inexpensive methods for locating high value REE-containing streams in the field. Fluorescent sensors exploiting the unique optoelectronic properties of REEs have emerged as a promising avenue for meeting this challenge.^{24-26,79,191} As demonstrated in this Review, advances in the field of materials science have spurred an array of high-performance materials that are promising for REE detection. While relatively mature sensor technologies have been developed for probing total REE content²⁶ or individual REEs^{28,42,66,126} with high degrees of selectivity and sensitivity, the ability to simultaneously detect and distinguish multiple REEs within the complex matrices of environmental samples remains challenging.²⁵ This is compounded by the fact that many materials which show promise in sensitizing REE emission are often not evaluated for their sensing efficacy. Additionally, studies that *do* evaluate sensor performance are often not evaluated under environmentally-relevant conditions. Included here are recommendations for sensor evaluations, spectrometer development, and next steps in material design that we anticipate will advance the field of REE sensor development:

1. Evaluate Prospective Sensors for the Criteria Outlined in Table 2 and Figure 4: researchers in the REE field will benefit greatly from having information on the sensitivity, selectivity, and operating conditions of potential sensors. This information will enable the researcher to choose the optimal sensor while establishing trends upon which other sensors may be designed.

2. Choose Appropriate Sensors Depending on Experimental Task REE sensing techniques are needed across a range of processing steps, from identifying valuable waste streams to characterizing extraction, concentration, and purification steps of REE samples. In each case, ideally the simplest, most cost-effective sensor possible should be used. For characterizing waste streams, which typically will have challenging matrices, highly selective sensors are needed, such as biomolecules. However, during processing steps in which REEs are purified and concentrated, simpler sensors can likely be used. **Table 11** provides examples of REE processing steps and the types of sensors best suited for each task.

3. Integration of Sensors with Portable Systems: maximum benefit in terms of time and financial costs will be obtained using portable spectrometers that can be taken directly to REE sources. As outlined in Section 10, several low-cost designs have already been reported, which typically rely on low-powered LED light sources and optical fibers connecting the sample with the excitation source and/or detector.^{24,27} Improved signal from portable spectrometers may be obtained by immobilizing the sensor material onto the optical fiber itself.⁸³ Therefore, continued development of chemical strategies will be needed to integrate a diverse array of sensing materials onto optical fibers. Conducting evaluations of REE sensing materials on portable systems will also provide results that are more meaningful for field deployment. Finally, evaluating the performance of portable time-resolved spectrometers for REE sensing applications represents an exciting opportunity for future development in the field.

4. Develop Sensors for Near-Infrared Emitting REEs: The detection of near-infrared emission can be challenging in part due to higher equipment costs. However, several economically important REEs, including Nd and Yb, emit strongly in the near-infrared region. Few, if any, studies have investigated the

Table 11. Recommended Sensors for Various REE Processing Steps

| Experimental Task | Key Sensor Properties | Recommended Sensor |
|--|--|---|
| Probe total REE content in a waste stream | Scope, selectivity, sensitivity, water compatibility | Sensors that probe "All REEs" from Table 1 |
| Probe individual REE content in a waste stream | Selectivity, sensitivity, water compatibility | Biomolecules or water-compatible organic sensitizers |
| Probe "high value" REE content post-purification | Scope, response time, ease-of-synthesis | MOFs or simple organic sensitizers |
| Differentiate between REEs post-purification | Scope, selectivity | Multivariate sensors |
| Quantify a specific REE | Selectivity, sensitivity | Sensors with "probe based" response for specific element (or sensitizers of specific elements), listed in Table 1 |
| Characterize purified REEs | Ease-of-Synthesis, Response time, Recyclable | MOFs, Nanoparticles, simple organic molecules, particularly if they can be regenerated |

sensitization-based detection of Er, Pr, Tm, and Ho, which emit in the near-infrared. Materials capable of sensitizing these elements would facilitate their recovery and would also create new markets for these REEs by exploiting their emission properties.^{120,121,123} While most REE sensitizers are only evaluated on Tb and Eu, it is worthwhile to also screen the other emissive REEs using the sensitizer: Sm, Dy, Tm, Pr, Ho, Yb, Nd, and Er. Equally important is the integration of near-infrared detectors with portable spectrometer systems.

5. Design of Composite Materials: As highlighted throughout this *Review*, each material class has advantages and disadvantages for REE detection. Developing composite materials may yield sensors that synergistically combine the advantageous properties of individual materials. For instance, functionalizing nanoparticles with peptide lanthanide binding tags could combine the strong light-harvesting properties and recyclability of nanoparticles with the high REE selectivity of the peptide. In general, regardless of sensing mechanism, high-performance sensors require a strongly-emitting chromophore that responds to REE interactions, and a chelating group that selectively interacts with REEs. **Table 12** summarizes potential combinations of chromophores and REE binding groups that may potentially be used in the development of new composite REE sensor materials.

Table 12. Core and Ligand Properties Needed for Sensitization

| Chromophore | REE Binding Group |
|----------------------------|-------------------------|
| -Aromatic Organic Molecule | -Schiff Base |
| -Emissive Nanoparticle | -Macrocyclic Compound |
| -Metal Complex | -Lanthanide Binding Tag |
| -MOF | |

6. Computational Modeling to Design Selective REE Sensors: in tandem with experimental approaches, computational modeling of material interactions with REEs will significantly aid in the screening and discovery of new high-performance sensor materials.²⁸⁰ Indeed, computational simulations have played a crucial role in engineering biomaterials,²⁸¹ ligands,^{280,282} inorganic layered materials,²⁸³ surfactants,²⁸⁴ and other materials for selective REE interactions. The continued

development of new techniques in quantum computation is expected to facilitate further progress in the design of highly selective materials for REE binding,²⁸⁵ while machine learning methods are being increasingly used to optimize sensor design and performance.^{286,287}

REE detection by luminescence-based techniques, particularly in harsh environments such as acid mine drainage, remains a challenge that requires innovations in both material development and spectrometer design. Such innovations will have benefits not only in REE recovery and processing, but also in the design of new luminescent materials, improved, low-cost luminescence sensing platforms, and in the detection of other valuable ions in waste streams. Significant progress has been made recently in the design of low-cost REE sensors, however overcoming remaining barriers for practical field deployment will require additional research from the materials science and photonics communities alike.

Conflicts of interest

The authors declare no conflicts of interest.

Acknowledgements

This project was funded by the Department of Energy, National Energy Technology Laboratory, an agency of the United States Government. Neither the United States Government nor any agency thereof, nor any of their employees, makes any warranty, express or implied, or assumes any legal liability or responsibility for the accuracy, completeness, or usefulness of any information, apparatus, product, or process disclosed, or represents that its use would not infringe privately owned rights. Reference herein to any specific commercial product, process, or service by trade name, trademark, manufacturer, or otherwise does not necessarily constitute or imply its endorsement, recommendation, or favoring by the United States Government or any agency thereof. The views and opinions of authors expressed herein do not necessarily state or reflect those of the United States Government or any agency thereof. SEC is grateful for funding through the National Energy

Technology Research Participation Program, sponsored by the U.S. Department of Energy and administered by the Oak Ridge Institute for Science Education.

Notes and references

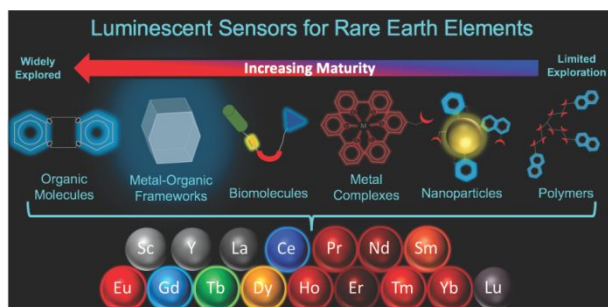
- 1 Franus, W.; Wiatros-Motyka, M. M.; Wdowin, M. *Environ. Sci. Pollut. Res.* **2015**, *22*, 9464.
- 2 Wells Jr, W.; Wells, V. L. *Patty's Toxicology* **2001**.
- 3 Lin, R.; Soong, Y.; Granite, E. J. *Int. J. Coal Geol.* **2018**, *192*, 1.
- 4 Du, X.; Fan, R.; Qiang, L.; Wang, P.; Song, Y.; Xing, K.; Zheng, X.; Yang, Y. *Cryst. Growth Des.* **2017**, *17*, 2746.
- 5 Dutta, T.; Kim, K.-H.; Uchimiya, M.; Kwon, E. E.; Jeon, B.-H.; Deep, A.; Yun, S.-T. *Environ. Res.* **2016**, *150*, 182.
- 6 Binnemans, K.; Jones, P. T.; Blanpain, B.; Van Gerven, T.; Yang, Y.; Walton, A.; Buchert, M. *J. Clean. Prod.* **2013**, *51*, 1.
- 7 Gholz, E. *Rare earth elements and national security*; Council on Foreign Relations, 2014.
- 8 Barteková, E.; Kemp, R. *Resour. Policy* **2016**, *49*, 153.
- 9 Chen, Y.; Zheng, B. *Sustainability* **2019**, *11*, 1288.
- 10 Hedin, B. C.; Capo, R. C.; Stewart, B. W.; Hedin, R. S.; Lopano, C. L.; Stuckman, M. Y. *Int. J. Coal Geol.* **2019**, *208*, 54.
- 11 Du, X.; Graedel, T. E. *Environ. Sci. Technol.* **2011**, *45*, 4096.
- 12 Alonso, E.; Sherman, A. M.; Wallington, T. J.; Everson, M. P.; Field, F. R.; Roth, R.; Kirchain, R. E. *Environ. Sci. Technol.* **2012**, *46*, 3406.
- 13 Johannesson, K. H.; Tang, J.; Daniels, J. M.; Bounds, W. J.; Burdige, D. J. *Chem. Geol.* **2004**, *209*, 271.
- 14 Wen, B.; Shan, X.-q.; Xu, S.-g. *Analyst* **1999**, *124*, 621.
- 15 Dai, S.; Finkelman, R. B. *Int. J. Coal Geol.* **2018**, *186*, 155.
- 16 Honaker, R.; Zhang, W.; Werner, J. *Energy Fuels* **2019**.
- 17 Stewart, B. W.; Capo, R. C.; Hedin, B. C.; Hedin, R. S. *Int. J. Coal Geol.* **2017**, *169*, 28.
- 18 Ayora, C.; Macías, F.; Torres, E.; Lozano, A.; Carrero, S.; Nieto, J.-M.; Pérez-López, R.; Fernández-Martínez, A.; Castillo-Michel, H. *Environ. Sci. Technol.* **2016**, *50*, 8255.
- 19 Li, C.; Zhuang, Z.; Huang, F.; Wu, Z.; Hong, Y.; Lin, Z. *ACS Appl. Mater. Interfaces* **2013**, *5*, 9719.
- 20 Tansel, B. *Environ. Int.* **2017**, *98*, 35.
- 21 Song, G.; Yuan, W.; Zhu, X.; Wang, X.; Zhang, C.; Li, J.; Bai, J.; Wang, J. *J. Clean. Prod.* **2017**, *151*, 361.
- 22 Sprecher, B.; Kleijn, R.; Kramer, G. J. *Environ. Sci. Technol.* **2014**, *48*, 9506.
- 23 Ding, Y.; Harvey, D.; Wang, N.-H. L. *Green Chem.* **2020**.
- 24 Ahern, J. C.; Poole, Z. L.; Baltrus, J.; Ohodnicki, P. R. *IEEE Sens. J.* **2017**, *17*, 2644.
- 25 Crawford, S. E.; Gan, X. Y.; Lemaire, P. C.; Millstone, J. E.; Baltrus, J. P.; Ohodnicki Jr, P. R. *ACS Sens.* **2019**, *4*, 1986.
- 26 Mattocks, J. A.; Ho, J. V.; Cotruvo Jr, J. A. *J. Am. Chem. Soc.* **2019**, *141*, 2857.
- 27 Lan, H.; Crawford, S.; Splain, Z.; Boyer, T.; Ohodnicki, P.; Baltrus, J.; Zou, R.; Wang, M.; Chen, K. P. In *CLEO: QELS Fundamental Science*; Optical Society of America: 2019, p JW2A. 14.
- 28 Sainz-Gonzalo, F.; Popovici, C.; Casimiro, M.; Raya-Barón, A.; López-Ortiz, F.; Fernández, I.; Fernández-Sánchez, J.; Fernández-Gutiérrez, A. *Analyst* **2013**, *138*, 6134.
- 29 Zhao, F.; Cong, Z.; Sun, H.; Ren, D. *Int. J. Coal Geol.* **2007**, *70*, 184.
- 30 Tunsu, C.; Petranikova, M.; Ekberg, C.; Retegan, T. *Sep. Purif. Technol.* **2016**, *161*, 172.
- 31 Sinclair, L.; Baek, D. L.; Thompson, J.; Tester, J.; Fox, R. V. *J. Supercrit. Fluids* **2017**, *124*, 20.
- 32 Taggart, R. K.; Hower, J. C.; Hsu-Kim, H. *Int. J. Coal Geol.* **2018**, *196*, 106.
- 33 Xia, W.-S.; Schmehl, R. H.; Li, C.-J. *Tetrahedron* **2000**, *56*, 7045.
- 34 Li, R. S.; Liu, J. H.; Yang, T.; Gao, P. F.; Wang, J.; Liu, H.; Zhen, S. J.; Li, Y. F.; Huang, C. Z. *Anal. Chem.* **2019**, *91*, 11185.
- 35 Huang, X.; Song, J.; Yung, B. C.; Huang, X.; Xiong, Y.; Chen, X. *Chem. Soc. Rev.* **2018**, *47*, 2873.
- 36 Hosseini, M.; Ganjali, M. R.; Abkenar, S. D.; Veismohammadi, B.; Riahl, S.; Norouzi, P.; Salavati-Niasari, M. *Anal. Lett.* **2009**, *42*, 1029.
- 37 Ganjali, M. R.; Hosseini, M.; Hariri, M.; Norouzi, P.; Khandar, A. A.; Bakhtiari, A. *Mater. Sci. Eng. C* **2010**, *30*, 929.
- 38 Daszykowski, M.; Kaczmarek, K.; Vander Heyden, Y.; Walczak, B. *Chemom. Intell. Lab. Syst.* **2007**, *85*, 203.
- 39 Brown, S. D.; Blank, T. B.; Sum, S. T.; Weyer, L. G. *Anal. Chem.* **1994**, *66*, 315.
- 40 Brereton, R. G. *Multivariate pattern recognition in chemometrics: illustrated by case studies*; Elsevier, 1992.
- 41 Roy, B.; Roy, T. S.; Rahaman, S. A.; Das, K.; Bandyopadhyay, S. *ACS Sens.* **2018**, *3*, 2166.
- 42 Faridbod, F.; Sedaghat, M.; Hosseini, M. e.; Ganjali, M.; Khoobi, M.; Shafiee, A.; Norouzi, P. *Spectrochim. Acta A* **2015**, *137*, 1231.
- 43 Chu, S. *Critical materials strategy*; DIANE Publishing, 2011.
- 44 Bünzli, J.-C. G.; Piguet, C. *Chem. Soc. Rev.* **2005**, *34*, 1048.
- 45 Uh, H.; Petoud, S. *C. R. Chim.* **2010**, *13*, 668.
- 46 Moore, E. G.; Samuel, A. P.; Raymond, K. N. *Acc. Chem. Res.* **2009**, *42*, 542.
- 47 Chow, C. Y.; Eliseeva, S. V.; Trivedi, E. R.; Nguyen, T. N.; Kampf, J. W.; Petoud, S. p.; Pecoraro, V. L. *J. Am. Chem. Soc.* **2016**, *138*, 5100.
- 48 Comby, S.; Imbert, D.; Chauvin, A.-S.; Bünzli, J.-C. G. *Inorg. Chem.* **2006**, *45*, 732.
- 49 Law, G. L.; Pham, T. A.; Xu, J.; Raymond, K. N. *Agnew. Chem. Int. Ed.* **2012**, *51*, 2371.
- 50 Feng, J.; Zhang, H. *Chem. Soc. Rev.* **2013**, *42*, 387.
- 51 Binnemans, K. *Chem. Rev. (Washington, DC, U. S.)* **2009**, *109*, 4283.
- 52 Ward, M. D. *Coord. Chem. Rev.* **2010**, *254*, 2634.
- 53 An, J.; Shade, C. M.; Chengelis-Czegan, D. A.; Petoud, S.; Rosi, N. L. *J. Am. Chem. Soc.* **2011**, *133*, 1220.
- 54 Beeby, A.; M. Clarkson, I.; S. Dickens, R.; Faulkner, S.; Parker, D.; Royle, L.; S. de Sousa, A.; A. Gareth Williams, J.; Woods, M. *J. Chem. Soc., Perkin Trans. 2* **1999**, 493.
- 55 Gaft, M.; Panczer, G.; Reisfeld, R.; Uspensky, E. *Phys. Chem. Miner.* **2001**, *28*, 347.
- 56 Chen, G. *Rev. Sci. Instrum.* **2005**, *76*, 063107.
- 57 Yamada, H.; Kojo, M.; Nakahara, T.; Murakami, K.; Kakima, T.; Ichiba, H.; Yajima, T.; Fukushima, T. *Spectrochim. Acta A* **2012**, *90*, 72.
- 58 Sánchez, F. G.; Lopez, M. H.; Gomez, J. M. *Analyst* **1987**, *112*, 1037.
- 59 Pozo, M. U.; de Torres, A. G.; Pavón, J. C.; Rojas, F. S. *Analyst* **1991**, *116*, 757.
- 60 Tang, B.; Wang, Y.; Zhang, X.; Zhang, C.; Du, M. *Analyst* **1998**, *123*, 283.
- 61 Zhang, D.; Zang, Z.; Zhou, X.; Zhou, Y.; Tang, X.; Wei, R.; Liu, W. *Inorg. Chem. Commun.* **2009**, *12*, 1154.
- 62 Okamoto, K.; Fukuzumi, S. *J. Am. Chem. Soc.* **2004**, *126*, 13922.
- 63 Mummidivarapu, V. S.; Nehra, A.; Hinge, V. K.; Rao, C. P. *Org. Lett.* **2012**, *14*, 2968.
- 64 Huang, Y.-H.; Geng, Q.-X.; Jin, X.-Y.; Cong, H.; Qiu, F.; Xu, L.; Tao, Z.; Wei, G. *Sens. Actuators, B* **2017**, *243*, 1102.
- 65 Areti, S.; Bandaru, S.; Teotia, R.; Rao, C. P. *Anal. Chem.* **2015**, *87*, 12348.
- 66 Shamsipur, M.; Mohammadi, M.; Taherpour, A. A.; Lippolis, V.; Montis, R. *Sens. Actuators, B* **2014**, *192*, 378.
- 67 Wang, S.; Liu, S.; Zhang, J.; Cao, Y. *Talanta* **2019**, *198*, 501.
- 68 Liu, M.; Xu, Z.; Song, Y.; Li, H.; Xian, C. *J. Lumin.* **2018**, *198*, 337.
- 69 Luo, X.; Chen, D.; Xu, Z.; Song, Y.; Li, H.; Xian, C. *J. Rare Earths* **2019**.

- 70 Akseli, A.; Rakicioğlu, Y. *Talanta* **1996**, *43*, 1983.
- 71 Rofouei, M. K.; Tajarrud, N.; Masteri-Farahani, M.; Zadmand, R. *J. Fluoresc.* **2015**, *25*, 1855.
- 72 Nemati, F.; Zare-Dorabei, R. *Talanta* **2019**, *200*, 249.
- 73 Huang, L.; Liu, Y.; Ma, C.; Xi, P.; Kou, W.; Zeng, Z. *Dyes Pigm.* **2013**, *96*, 770.
- 74 Goswami, S.; Paul, S.; Manna, A. *RSC Adv.* **2014**, *4*, 43778.
- 75 Ahmed, M. J.; Islam, M. T.; Farhana, F. *RSC Adv.* **2019**, *9*, 25609.
- 76 Chu, X.; Wang, S.; Cao, Y. *New J. Chem.* **2020**.
- 77 Ganjali, M.; Hosseini, M.; Ghafarloo, A.; Khoobi, M.; Faridbod, F.; Shafiee, A.; Norouzi, P. *Mater. Sci. Eng. C* **2013**, *33*, 4140.
- 78 Si, Z.; Jiang, W.; Ding, Y.; Hu, J. *Fresenius. J. Anal. Chem.* **1998**, *360*, 731.
- 79 Bekiari, V.; Judeinstein, P.; Lianos, P. *J. Lumin.* **2003**, *104*, 13.
- 80 Yang, F.; Ren, P.; Liu, G.; Song, Y.; Bu, N.; Wang, J. *Spectrochim. Acta A* **2018**, *193*, 357.
- 81 Vaněk, J.; Lubal, P.; Ševčíková, R.; Poláček, M.; Hermann, P. *J. Lumin.* **2012**, *132*, 2030.
- 82 Sainz-Gonzalo, F.; Casimiro, M.; Popovici, C.; Rodríguez-Diéguez, A.; Fernández-Sánchez, J.; Fernández, I.; López-Ortiz, F.; Fernández-Gutiérrez, A. *Dalton Trans.* **2012**, *41*, 6735.
- 83 Sainz-Gonzalo, F.; Elosua, C.; Fernández-Sánchez, J.; Popovici, C.; Fernández, I.; Ortiz, F.; Arregui, F.; Matias, I.; Fernández-Gutiérrez, A. *Sens. Actuators, B* **2012**, *173*, 254.
- 84 Yang, W.; Teng, X.-l.; Chen, M.; Gao, J.-z.; Yuan, L.; Kang, J.-w.; Ou, Q.-y.; Liu, S.-x. *Talanta* **1998**, *46*, 527.
- 85 Si, Z. K.; Jiang, W.; Wang, L.; Ma, G.; Hu, J. T. *Microchim. Acta* **2002**, *138*, 19.
- 86 Zhang, L.; An, Y.; Ahmad, W.; Zhou, Y.; Shi, Z.; Zheng, X. *J. Photochem. Photobiol. A* **2013**, *252*, 167.
- 87 Zhou, Y.; Ahmad, W.; An, Y.; Zhang, L.; Zheng, X. *Luminescence* **2014**, *29*, 531.
- 88 Ganjali, M. R.; Hosseini, M.; Khobi, M.; Farahani, S.; Shaban, M.; Faridbod, F.; Shafiee, A.; Norouzi, P. *Talanta* **2013**, *115*, 271.
- 89 Gao, X.; Sun, G.; Ge, F.; Zheng, H. *Inorg. Chem.* **2019**, *58*, 8396.
- 90 Huang, P.-J. J.; Vazin, M.; Lin, J. J.; Pautler, R.; Liu, J. *ACS Sens.* **2016**, *1*, 732.
- 91 Ganjali, M.; Veismohammadi, B.; Hosseini, M.; Norouzi, P. *Spectrochim. Acta A* **2009**, *74*, 575.
- 92 Hosseini, M.; Ganjali, M. R.; Veismohammadi, B.; Faridbod, F.; Abkenar, S. D.; Norouzi, P. *Anal. Chim. Acta* **2010**, *664*, 172.
- 93 Chen, Q.; Zuo, J.; He, X.; Mo, X.; Tong, P.; Zhang, L. *Talanta* **2017**, *162*, 540.
- 94 Essawy, A. A. *Sens. Actuators, B* **2014**, *196*, 640.
- 95 Moghzi, F.; Soleimannejad, J.; Sañudo, E. C.; Janczak, J. *Mater. Res. Bull.* **2019**, *110*, 683.
- 96 Li, M.; Ren, G.; Wang, F.; Li, Z.; Yang, W.; Gu, D.; Wang, Y.; Zhu, G.; Pan, Q. *Inorg. Chem. Front.* **2019**, *6*, 1129.
- 97 Yi, F. Y.; Li, J. P.; Wu, D.; Sun, Z. M. *Chem. Eur. J* **2015**, *21*, 11475.
- 98 Ganjali, M. R.; Gupta, V. K.; Hosseini, M.; Hariri, M.; Faridbod, F.; Norouzi, P. *Sens. Actuators, B* **2012**, *171*, 644.
- 99 Zapata, F.; Caballero, A.; Espinosa, A.; Tárraga, A.; Molina, P. *Eur. J. Inorg. Chem.* **2010**, *2010*, 697.
- 100 Hosseini, M.; Ganjali, M. R.; Veismohammadi, B.; Norouzi, P.; Alizadeh, K.; Abkenar, S. D. *Mater. Sci. Eng. C* **2010**, *30*, 348.
- 101 Crawford, S. E.; Andolina, C. M.; Kaseman, D. C.; Ryoo, B. H.; Smith, A. M.; Johnston, K. A.; Millstone, J. E. *J. Am. Chem. Soc.* **2017**, *139*, 17767.
- 102 Hosseini, M.; Ganjali, M. R.; Rafiei-Sarmazdeh, Z.; Faridbod, F.; Goldooz, H.; Badiie, A.; Nourozi, P.; Ziarani, G. M. *Anal. Chim. Acta* **2013**, *771*, 95.
- 103 Hosseini, M.; Ganjali, M. R.; Aboufazeli, F.; Faridbod, F.; Goldooz, H.; Badiie, A.; Norouzi, P. *Sens. Actuators, B* **2013**, *184*, 93.
- 104 Berregi, I.; Durand, J. S.; Casado, J. A. *Talanta* **1999**, *48*, 719.
- 105 Lee, Y.-R.; Yu, K.; Ravi, S.; Ahn, W.-S. *ACS Appl. Mater. Interfaces* **2018**, *10*, 23918.
- 106 Harris, D. C. *Quantitative chemical analysis*; Macmillan, 2010.
- 107 Coutinho, A.; Prieto, M. J. *Chem. Educ.* **1993**, *70*, 425.
- 108 Sato, T. *Hydrometallurgy* **1989**, *22*, 121.
- 109 Wang, J.; Xie, M.; Liu, X.; Wang, H. *Sep. Purif. Technol.* **2018**, *194*, 188.
- 110 Wang, J.; Liu, X.; Fu, J.; Xie, M.; Huang, G.; Wang, H. *Sep. Purif. Technol.* **2019**, *209*, 789.
- 111 Du, R.-B.; An, H.; Zhang, S.; Yu, D.; Xiao, J.-C. *RSC Adv.* **2015**, *5*, 104258.
- 112 Zhang, H.; Ye, J.; Wang, X.; Zhao, S.; Lei, R.; Huang, L.; Xu, S. *J. Mater. Chem. C* **2019**, *7*, 15269.
- 113 Crawford, S. E.; Kim, K.-J.; Yu, Y.; Ohodnicki, P. R. *Cryst. Growth Des.* **2018**, *18*, 2924.
- 114 Kim, K.-J.; Lu, P.; Culp, J. T.; Ohodnicki, P. R. *ACS Sens.* **2018**, *3*, 386.
- 115 Chen, L.; Tan, K.; Lan, Y.-Q.; Li, S.-L.; Shao, K.-Z.; Su, Z.-M. *Chem. Commun. (Cambridge, U. K.)* **2012**, *48*, 5919.
- 116 Grawunder, A.; Merten, D.; Büchel, G. *Environ. Sci. Pollut. Res.* **2014**, *21*, 6812.
- 117 Wei, C.; Ma, L.; Wei, H.; Liu, Z.; Bian, Z.; Huang, C. *Sci. China Technol. Sci.* **2018**, *61*, 1265.
- 118 Bünzli, J.-C. G. *Coord. Chem. Rev.* **2015**, *293*, 19.
- 119 Bünzli, J.-C. G. *Acc. Chem. Res.* **2006**, *39*, 53.
- 120 Zhang, J.; Badger, P. D.; Geib, S. J.; Petoud, S. *Agnew. Chem. Int. Ed.* **2005**, *44*, 2508.
- 121 Zhang, J.; Petoud, S. *Chem. Eur. J* **2008**, *14*, 1264.
- 122 Petoud, S.; Cohen, S. M.; Bünzli, J.-C. G.; Raymond, K. N. *J. Am. Chem. Soc.* **2003**, *125*, 13324.
- 123 Moore, E. G.; Szigethy, G.; Xu, J.; Pålsson, L. O.; Beeby, A.; Raymond, K. N. *Agnew. Chem. Int. Ed.* **2008**, *47*, 9500.
- 124 de Bettencourt-Dias, A.; Barber, P. S.; Viswanathan, S. *Coord. Chem. Rev.* **2014**, *273*, 165.
- 125 de Bettencourt-Dias, A.; Beeler, R. M.; Zimmerman, J. R. *J. Am. Chem. Soc.* **2019**, *141*, 15102.
- 126 Aoki, S.; Kawatani, H.; Goto, T.; Kimura, E.; Shiro, M. *J. Am. Chem. Soc.* **2001**, *123*, 1123.
- 127 Bayrakçı, M.; Kursunlu, A. N.; Güler, E.; Ertul, Ş. *Dyes Pigm.* **2013**, *99*, 268.
- 128 Yilmaz, B.; Bayrakçı, M. *J. Macromol. Sci. A* **2018**, *55*, 513.
- 129 Oueslati, I.; Sá Ferreira, R. A.; Carlos, L. D.; Baleizao, C.; Berberan-Santos, M. N.; de Castro, B.; Vicens, J.; Pischel, U. *Inorg. Chem.* **2006**, *45*, 2652.
- 130 Liu, J.-M.; Chen, C.-F.; Zheng, Q.-Y.; Huang, Z.-T. *Tetrahedron Lett.* **2004**, *45*, 6071.
- 131 Tolpygin, I.; Tikhomirova, K.; Revinskii, Y. V.; Bren, Z. V.; Dubonosov, A.; Bren, V. *Russ. J. Org. Chem.* **2017**, *53*, 1651.
- 132 Gutsche, C. D. *Acc. Chem. Res.* **1983**, *16*, 161.
- 133 Butler, C.; Goetz, S.; Fitchett, C. M.; Kruger, P. E.; Gunnlaugsson, T. *Inorg. Chem.* **2011**, *50*, 2723.
- 134 Wang, S.; Ding, L.; Fan, J.; Wang, Z.; Fang, Y. *ACS Appl. Mater. Interfaces* **2014**, *6*, 16156.
- 135 Liu, Y.; Mettry, M.; Gill, A. D.; Perez, L.; Zhong, W.; Hooley, R. J. *Anal. Chem.* **2017**, *89*, 11113.
- 136 Morf, W. E.; Seiler, K.; Rusterholz, B.; Simon, W. *Anal. Chem.* **1990**, *62*, 738.
- 137 de Bettencourt-Dias, A.; Rossini, J. S. *Inorg. Chem.* **2016**, *55*, 9954.
- 138 Vancaeyzeele, C.; Ornatsky, O.; Baranov, V.; Shen, L.; Abdelrahman, A.; Winnik, M. A. *J. Am. Chem. Soc.* **2007**, *129*, 13653.
- 139 Sun, W.; Yu, J.; Deng, R.; Rong, Y.; Fujimoto, B.; Wu, C.; Zhang, H.; Chiu, D. T. *Agnew. Chem. Int. Ed.* **2013**, *52*, 11294.

- 140 Aernecke, M. J.; Walt, D. R. *Sens. Actuators, B* **2009**, *142*, 464.
- 141 Vögtle, F.; Gorka, M.; Vicinelli, V.; Ceroni, P.; Maestri, M.; Balzani, V. *ChemPhysChem* **2001**, *2*, 769.
- 142 Vicinelli, V.; Ceroni, P.; Maestri, M.; Balzani, V.; Gorka, M.; Vögtle, F. *J. Am. Chem. Soc.* **2002**, *124*, 6461.
- 143 Branchi, B.; Ceroni, P.; Balzani, V.; Klärner, F. G.; Vögtle, F. *Chem. Eur. J* **2010**, *16*, 6048.
- 144 Pillai, Z. S.; Ceroni, P.; Kubeil, M.; Heldt, J. M.; Stephan, H.; Bergamini, G. *Chem. Asian J.* **2013**, *8*, 771.
- 145 Cross, J. P.; Lauz, M.; Badger, P. D.; Petoud, S. *J. Am. Chem. Soc.* **2004**, *126*, 16278.
- 146 Li, G.; Fang, H.; Jiang, D.; Zheng, G. *New J. Chem.* **2018**, *42*, 19734.
- 147 Liang, H.; Deng, X.; Bosscher, M.; Ji, Q.; Jensen, M. P.; He, C. *J. Am. Chem. Soc.* **2013**, *135*, 2037.
- 148 Xue, S.-F.; Chen, Z.-H.; Han, X.-Y.; Lin, Z.-Y.; Wang, Q.-X.; Zhang, M.; Shi, G. *Anal. Chem.* **2018**, *90*, 3443.
- 149 Niedźwiecka, A.; Cisnetti, F.; Lebrun, C.; Delangle, P. *Inorg. Chem.* **2012**, *51*, 5458.
- 150 Bonnet, C. S.; Devocelle, M.; Gunnlaugsson, T. *Org. Biomol. Chem.* **2012**, *10*, 126.
- 151 Vu, H. N.; Subuyuj, G. A.; Vijayakumar, S.; Good, N. M.; Martinez-Gomez, N. C.; Skovran, E. *J. Bacteriol.* **2016**, *198*, 1250.
- 152 Horrocks, W. D.; Collier, W. E. *J. Am. Chem. Soc.* **1981**, *103*, 2856.
- 153 Franz, K. J.; Nitz, M.; Imperiali, B. *ChemBioChem* **2003**, *4*, 265.
- 154 Nitz, M.; Sherawat, M.; Franz, K. J.; Peisach, E.; Allen, K. N.; Imperiali, B. *Agnew. Chem. Int. Ed.* **2004**, *43*, 3682.
- 155 Ancel, L.; Niedźwiecka, A.; Lebrun, C.; Gateau, C.; Delangle, P. *C. R. Chim.* **2013**, *16*, 515.
- 156 Barozzi, M.; Manicardi, A.; Vannucci, A.; Candiani, A.; Sozzi, M.; Konstantaki, M.; Pissadakis, S.; Corradini, R.; Selleri, S.; Cucinotta, A. *J. Lightwave Technol.* **2016**, *35*, 3461.
- 157 Xu, L.-J.; Xu, G.-T.; Chen, Z.-N. *Coord. Chem. Rev.* **2014**, *273*, 47.
- 158 Klink, S. I.; Keizer, H.; Hofstraat, H. W.; van Veggel, F. C. *Synth. Met.* **2002**, *127*, 213.
- 159 Klink, S. I.; Keizer, H.; van Veggel, F. C. *Agnew. Chem. Int. Ed.* **2000**, *39*, 4319.
- 160 Ward, M. D. *Coord. Chem. Rev.* **2007**, *251*, 1663.
- 161 Giansante, C.; Ceroni, P.; Balzani, V.; Vögtle, F. *Agnew. Chem. Int. Ed.* **2008**, *47*, 5422.
- 162 Lazarides, T.; Tart, N. M.; Sykes, D.; Faulkner, S.; Barbieri, A.; Ward, M. D. *Dalton Trans.* **2009**, 3971.
- 163 Beer, P. D.; Szemes, F.; Passaniti, P.; Maestri, M. *Inorg. Chem.* **2004**, *43*, 3965.
- 164 Guo, Z.; Yson, R. L.; Patterson, H. H. *Chem. Phys. Lett.* **2007**, *433*, 373.
- 165 Guo, Z.; Yson, R. L.; Patterson, H. H. *Chem. Phys. Lett.* **2007**, *445*, 340.
- 166 Murray, C.; Norris, D. J.; Bawendi, M. G. *J. Am. Chem. Soc.* **1993**, *115*, 8706.
- 167 Abadeer, N. S.; Brennan, M. R.; Wilson, W. L.; Murphy, C. *J. ACS Nano* **2014**, *8*, 8392.
- 168 Stein, J. L.; Mader, E. A.; Cossairt, B. M. *J. Phys. Chem. Lett.* **2016**, *7*, 1315.
- 169 Malola, S.; Kaappa, S.; Häkkinen, H. *J. Phys. Chem. C* **2019**, *123*, 20655.
- 170 Crawford, S. E.; Hartmann, M. J.; Millstone, J. E. *Acc. Chem. Res.* **2019**, *52*, 695.
- 171 Zhang, J.; Yu, S.-H. *Nanoscale* **2014**, *6*, 4096.
- 172 Han, S.; Deng, R.; Xie, X.; Liu, X. *Agnew. Chem. Int. Ed.* **2014**, *53*, 11702.
- 173 Gnach, A.; Bednarkiewicz, A. *Nano Today* **2012**, *7*, 532.
- 174 DaCosta, M. V.; Doughan, S.; Han, Y.; Krull, U. J. *Anal. Chim. Acta* **2014**, *832*, 1.
- 175 McBride, J.; Treadway, J.; Feldman, L. C.; Pennycook, S. J.; Rosenthal, S. J. *Nano Lett.* **2006**, *6*, 1496.
- 176 Swabeck, J. K.; Fischer, S.; Bronstein, N. D.; Alivisatos, A. P. *J. Am. Chem. Soc.* **2018**, *140*, 9120.
- 177 Chengelis, D. A.; Yingling, A. M.; Badger, P. D.; Shade, C. M.; Petoud, S. *J. Am. Chem. Soc.* **2005**, *127*, 16752.
- 178 Mukherjee, P.; Shade, C. M.; Yingling, A. M.; Lamont, D. N.; Waldeck, D. H.; Petoud, S. *J. Phys. Chem. A* **2010**, *115*, 4031.
- 179 Planelles-Aragó, J.; Cordoncillo, E.; Ferreira, R. A.; Carlos, L. D.; Escribano, P. *J. Mater. Chem.* **2011**, *21*, 1162.
- 180 Mukherjee, P.; Sloan, R. F.; Shade, C. M.; Waldeck, D. H.; Petoud, S. *J. Phys. Chem. C* **2013**, *117*, 14451.
- 181 Debnath, G. H.; Rudra, S.; Bhattacharyya, A.; Guchhait, N.; Mukherjee, P. *J. Colloid Interface Sci.* **2019**, *540*, 448.
- 182 de Bettencourt-Dias, A.; Tigaa, R. *J. Mater. Chem. C* **2018**, *6*, 2814.
- 183 Tigaa, R. A.; Lucas, G. J.; de Bettencourt-Dias, A. *Inorg. Chem.* **2017**, *56*, 3260.
- 184 Tiseanu, C.; Mehra, R. K.; Kho, R.; Kumke, M. *J. Phys. Chem. B* **2003**, *107*, 12153.
- 185 Zheng, X. T.; Ananthanarayanan, A.; Luo, K. Q.; Chen, P. *Small* **2015**, *11*, 1620.
- 186 Chan, K. K.; Yap, S. H. K.; Yong, K.-T. *Nano-Micro Lett.* **2018**, *10*, 72.
- 187 Vostrikova, A. M.; Kokorina, A. A.; Demina, P. A.; German, S. V.; Novoselova, M. V.; Tarakina, N. V.; Sukhorukov, G. B.; Goryacheva, I. Y. *Sci. Rep.* **2018**, *8*, 16301.
- 188 Cayuela, A.; Soriano, M.; Carrillo-Carrion, C.; Valcarcel, M. *Chem. Commun. (Cambridge, U. K.)* **2016**, *52*, 1311.
- 189 Tigaa, R. A.; Monteiro, J. H.; Silva-Hernandez, S.; de Bettencourt-Dias, A. *J. Lumin.* **2017**, *192*, 1273.
- 190 McDowell, M.; Metzger, A.; Wang, C.; Bao, J.; Tour, J. M.; Martí, A. A. *Chem. Commun. (Cambridge, U. K.)* **2018**, *54*, 4325.
- 191 Dolai, S.; Bhunia, S. K.; Zeiri, L.; Paz-Tal, O.; Jelinek, R. *ACS Omega* **2017**, *2*, 9288.
- 192 Crawford, S. E.; Andolina, C. M.; Smith, A. M.; Marbella, L. E.; Johnston, K. A.; Straney, P. J.; Hartmann, M. J.; Millstone, J. E. *J. Am. Chem. Soc.* **2015**, *137*, 14423.
- 193 Lisowski, C. E.; Hutchison, J. E. *Anal. Chem.* **2009**, *81*, 10246.
- 194 Pandya, A.; Joshi, K. V.; Sutariya, P. G.; Menon, S. K. *Anal. Methods* **2012**, *4*, 3102.
- 195 Han, C.; Zhang, L.; Li, H. *Chem. Commun. (Cambridge, U. K.)* **2009**, 3545.
- 196 Kumar, P.; Deep, A.; Kim, K.-H. *Trends Anal. Chem.* **2015**, *73*, 39.
- 197 Li, Q.; Yan, B. *J. Rare Earths* **2019**, *37*, 113.
- 198 Xu, H.; Cao, C.-S.; Kang, X.-M.; Zhao, B. *Dalton Trans.* **2016**, *45*, 18003.
- 199 Zou, D.; Zhang, J.; Cui, Y.; Qian, G. *Dalton Trans.* **2019**, *48*, 6669.
- 200 Yan, B. *Acc. Chem. Res.* **2017**, *50*, 2789.
- 201 Liu, S.; Zhou, Y.; Zheng, J.; Xu, J.; Jiang, R.; Shen, Y.; Jiang, J.; Zhu, F.; Su, C.; Ouyang, G. *Analyst* **2015**, *140*, 4384.
- 202 Chong, X.; Kim, K.-J.; Li, E.; Zhang, Y.; Ohodnicki, P. R.; Chang, C.-H.; Wang, A. X. *Sens. Actuators, B* **2016**, *232*, 43.
- 203 Zhao, S. N.; Song, X. Z.; Zhu, M.; Meng, X.; Wu, L. L.; Feng, J.; Song, S. Y.; Zhang, H. *J. Chem. Eur. J* **2015**, *21*, 9748.
- 204 Sun, N.; Yan, B. *Phys. Chem. Chem. Phys.* **2017**, *19*, 9174.
- 205 Sun, N.-N.; Yan, B. *J. Alloys Compd.* **2018**, *765*, 63.
- 206 Shen, X.; Yan, B. *RSC Adv.* **2016**, *6*, 28165.
- 207 Gao, Y.; Zhang, X.; Sun, W.; Liu, Z. *Dalton Trans.* **2015**, *44*, 1845.
- 208 Wang, J.-M.; Lian, X.; Yan, B. *Inorg. Chem.* **2019**, *58*, 9956.
- 209 Weng, H.; Yan, B. *Anal. Chim. Acta* **2017**, *988*, 89.

- 210 Wu, J.-X.; Yan, B. *Inorg. Chem. Commun.* **2016**, *70*, 189.
- 211 Kim, J.; Baczewski, A. T.; Beaudet, T. D.; Benali, A.; Bennett, M. C.; Berrill, M. A.; Blunt, N. S.; Josue, E.; Borda, L.; Casula, M.; Ceperley, D. M.; Chiesa, S.; Clark, B. K.; Clay, R. C.; Delaney, K. T.; Dewing, M.; Esler, K. P.; Hao, H. X.; Heinonen, O.; Kent, P. R. C.; Krogel, J. T.; Kylanpaa, I.; Li, Y. W.; Lopez, M. G.; Luo, Y.; Malone, F. D.; Martin, R. M.; Mathuriya, A.; McMinis, J.; Melton, C. A.; Mitas, L.; Morales, M. A.; Neuscammen, E.; Parker, W. D.; Flores, S. D. P.; Romero, N. A.; Rubenstein, B. M.; Shea, J. A. R.; Shin, H.; Shulenburg, L.; Tillack, A. F.; Townsend, J. P.; Tubman, N. M.; Van der Goetz, B.; Vincent, J. E.; Yang, D. C.; Yang, Y. B.; Zhang, S.; Zhao, L. N. *Journal of Physics-Condensed Matter* **2018**, *30*.
- 212 Zhang, Y.; Li, B.; Ma, H.; Zhang, L.; Zheng, Y. *Biosens. Bioelectron.* **2016**, *85*, 287.
- 213 Shen, X.; Yan, B. *J. Colloid Interface Sci.* **2016**, *468*, 220.
- 214 Zhang, D.; Zhou, Y.; Cuan, J.; Gan, N. *CrystEngComm* **2018**, *20*, 1264.
- 215 An, J.; Farha, O. K.; Hupp, J. T.; Pohl, E.; Yeh, J. I.; Rosi, N. L. *Nat. Commun.* **2012**, *3*, 604.
- 216 Li, L.; Shen, S.; Ai, W.; Song, S.; Bai, Y.; Liu, H. *Sens. Actuators, B* **2018**, *267*, 542.
- 217 Hao, J.-N.; Yan, B. *Chem. Commun. (Cambridge, U. K.)* **2015**, *51*, 7737.
- 218 Zhao, X.; Liu, D.; Huang, H.; Zhong, C. *Microporous Mesoporous Mater.* **2016**, *224*, 149.
- 219 Zheng, H.-Y.; Lian, X.; Qin, S.-J.; Yan, B. *Acs Omega* **2018**, *3*, 12513.
- 220 Xiaoxiong, Z.; Wenjun, Z.; Cuiliu, L.; Xiaohong, Q.; Chengyu, Z. *Inorg. Chem.* **2019**, *58*, 3910.
- 221 Hua, W.; Zhang, T.; Wang, M.; Zhu, Y.; Wang, X. *Chem. Eng. J. (Lausanne)* **2019**, *370*, 729.
- 222 Zhang, X.; Jiang, K.; He, H.; Yue, D.; Zhao, D.; Cui, Y.; Yang, Y.; Qian, G. *Sens. Actuators, B* **2018**, *254*, 1069.
- 223 Zhou, Y.; Yan, B. *Inorg. Chem.* **2014**, *53*, 3456.
- 224 Qin, S.-J.; Yan, B. *Sens. Actuators, B* **2018**, *272*, 510.
- 225 Dou, Z.; Yu, J.; Xu, H.; Cui, Y.; Yang, Y.; Qian, G. *Microporous Mesoporous Mater.* **2013**, *179*, 198.
- 226 Lian, X.; Yan, B. *ACS Appl. Mater. Interfaces* **2018**, *10*, 14869.
- 227 Hao, J.-N.; Yan, B. *New J. Chem.* **2016**, *40*, 4654.
- 228 Xu, X.-Y.; Yan, B. *ACS Appl. Mater. Interfaces* **2014**, *7*, 721.
- 229 Qin, S.-J.; Hao, J.-N.; Xu, X.-Y.; Lian, X.; Yan, B. *Sens. Actuators, B* **2017**, *253*, 852.
- 230 Lian, X.; Yan, B. *Inorg. Chem.* **2016**, *55*, 11831.
- 231 Luo, J.; Liu, B.-S.; Zhang, X.-R.; Liu, R.-T. *J. Mol. Struct.* **2019**, *127347*.
- 232 Wang, Z.; Wang, X.; Li, J.; Li, W.; Li, G. *J. Inorg. Organomet. Polym. Mater.* **2019**, *1*.
- 233 Zhang, J.; Yue, D.; Xia, T.; Cui, Y.; Yang, Y.; Qian, G. *Microporous Mesoporous Mater.* **2017**, *253*, 146.
- 234 Hao, J.-N.; Yan, B. *J. Mater. Chem. A* **2014**, *2*, 18018.
- 235 Li, Y.-A.; Ren, S.-K.; Liu, Q.-K.; Ma, J.-P.; Chen, X.; Zhu, H.; Dong, Y.-B. *Inorg. Chem.* **2012**, *51*, 9629.
- 236 Liu, L.; Zhang, X.-N.; Han, Z.-B.; Gao, M.-L.; Cao, X.-M.; Wang, S.-M. *J. Mater. Chem. A* **2015**, *3*, 14157.
- 237 Zheng, X.; Fan, R.; Song, Y.; Wang, A.; Xing, K.; Du, X.; Wang, P.; Yang, Y. *J. Mater. Chem. C* **2017**, *5*, 9943.
- 238 Fan, T.-T.; Li, J.-J.; Qu, X.-L.; Han, H.-L.; Li, X. *CrystEngComm* **2015**, *17*, 9443.
- 239 Luo, F.; Batten, S. R. *Dalton Trans.* **2010**, *39*, 4485.
- 240 Jia, J.; Xu, J.; Wang, S.; Wang, P.; Gao, L.; Chai, J.; Shen, L.; Chen, X.; Fan, Y.; Wang, L. *CrystEngComm* **2016**, *18*, 7126.
- 241 Qu, X.-L.; Zheng, X.-L.; Li, X. *RSC Adv.* **2016**, *6*, 69007.
- 242 Huang, W.; Pan, F.; Liu, Y.; Huang, S.; Li, Y.; Yong, J.; Li, Y.; Kirillov, A. M.; Wu, D. *Inorg. Chem.* **2017**, *56*, 6362.
- 243 Guo, M.; Liu, S.; Guo, H.; Sun, Y.; Guo, X.; Deng, R. *Dalton Trans.* **2017**, *46*, 14988.
- 244 Zhou, Z.; Xing, X.; Tian, C.; Wei, W.; Li, D.; Hu, F.; Du, S. *Sci. Rep.* **2018**, *8*, 3117.
- 245 He, H.; Zhang, L.; Deng, M.; Chen, Z.; Ling, Y.; Chen, J.; Zhou, Y. *CrystEngComm* **2015**, *17*, 2294.
- 246 Ma, B.; Xu, J.; Qi, H.; Sun, J.; Chai, J.; Jia, J.; Jing, S.; Fan, Y.; Wang, L. *Solid State Chem.* **2018**, *258*, 42.
- 247 Guo, X.; Wang, P.; Xu, J.; Shen, L.; Sun, J.; Tao, Y.; Chen, X.; Jing, S.; Wang, L.; Fan, Y. *Inorg. Chim. Acta* **2018**, *479*, 213.
- 248 Zou, J.-Y.; Li, L.; You, S.-Y.; Cui, H.-M.; Liu, Y.-W.; Chen, K.-H.; Chen, Y.-H.; Cui, J.-Z.; Zhang, S.-W. *Dyes Pigm.* **2018**, *159*, 429.
- 249 Gao, X.; Chang, S.; Liu, H.; Liu, Z. *Eur. J. Inorg. Chem.* **2016**, *2016*, 2837.
- 250 Chen, C.-X.; Liu, Q.-K.; Ma, J.-P.; Dong, Y.-B. *J. Mater. Chem.* **2012**, *22*, 9027.
- 251 Jia, G.; Yan, B. *New J. Chem.* **2017**, *41*, 12795.
- 252 Li, H.; Li, Q.; Xu, Z. *J. Mater. Chem. C* **2019**, *7*, 2880.
- 253 Qin, J. S.; Zhang, S. R.; Du, D. Y.; Shen, P.; Bao, S. J.; Lan, Y. Q.; Su, Z. M. *Chem. Eur. J* **2014**, *20*, 5625.
- 254 Qin, J. S.; Bao, S. J.; Li, P.; Xie, W.; Du, D. Y.; Zhao, L.; Lan, Y. Q.; Su, Z. M. *Chem. Asian J.* **2014**, *9*, 749.
- 255 Abdelhameed, R. M.; Carlos, L. D.; Silva, A. M.; Rocha, J. *Chem. Commun. (Cambridge, U. K.)* **2013**, *49*, 5019.
- 256 Abdelhameed, R. M.; Carlos, L. D.; Rabu, P.; Santos, S. M.; Silva, A. M.; Rocha, J. *Eur. J. Inorg. Chem.* **2014**, *2014*, 5285.
- 257 He, R.; Wang, Y.-L.; Ma, H.-F.; Yin, S.-G.; Liu, Q.-Y. *Dyes Pigm.* **2018**, *151*, 342.
- 258 Dou, Z.; Yu, J.; Cui, Y.; Yang, Y.; Wang, Z.; Yang, D.; Qian, G. *J. Am. Chem. Soc.* **2014**, *136*, 5527.
- 259 Zhou, Y.; Yan, B. *J. Mater. Chem. C* **2015**, *3*, 8413.
- 260 Hao, J.-N.; Yan, B. *J. Mater. Chem. A* **2015**, *3*, 4788.
- 261 Sun, N.; Yan, B. *Sens. Actuators, B* **2018**, *261*, 153.
- 262 Zhang, Y.; Yan, B. *ACS Appl. Mater. Interfaces* **2019**.
- 263 Zhang, J.; Peh, S. B.; Wang, J.; Du, Y.; Xi, S.; Dong, J.; Karmakar, A.; Ying, Y.; Wang, Y.; Zhao, D. *Chem. Commun. (Cambridge, U. K.)* **2019**, *55*, 4727.
- 264 Qu, X.-L.; Yan, B. *Inorg. Chem.* **2018**, *57*, 7815.
- 265 Xie, W.; Zhang, S.-R.; Du, D.-Y.; Qin, J.-S.; Bao, S.-J.; Li, J.; Su, Z.-M.; He, W.-W.; Fu, Q.; Lan, Y.-Q. *Inorg. Chem.* **2015**, *54*, 3290.
- 266 Chen, X.-B.; Qi, C.-X.; Li, H.; Ding, J.-Y.; Yan, S.; Lei, H.; Xu, L.; Liu, B. *J. Solid State Chem.* **2020**, *281*, 121030.
- 267 Lei, H.; Qi, C.-X.; Chen, X.-B.; Zhang, T.; Xu, L.; Liu, B. *New J. Chem.* **2019**, *43*, 18259.
- 268 Jiang, Y. Y.; Ren, S. K.; Ma, J. P.; Liu, Q. K.; Dong, Y. B. *Chem. Eur. J* **2009**, *15*, 10742.
- 269 Lian, X.; Miao, T.; Xu, X.; Zhang, C.; Yan, B. *Biosens. Bioelectron.* **2017**, *97*, 299.
- 270 Hao, J.-N.; Xu, X.-Y.; Lian, X.; Zhang, C.; Yan, B. *Inorg. Chem.* **2017**, *56*, 11176.
- 271 Hao, J.-N.; Yan, B. *Nanoscale* **2016**, *8*, 12047.
- 272 Pan, H.; Xu, S.; Ni, Y. *Sens. Actuators, B* **2019**, *283*, 731.
- 273 Margariti, A.; Pournara, A. D.; Manos, M. J.; Lazarides, T.; Papaefstathiou, G. S. *Polyhedron* **2018**, *153*, 24.
- 274 Qin, B.-W.; Zhang, X.-Y.; Zhang, J.-P. *New J. Chem.* **2019**, *43*, 13794.
- 275 Song, B.-Q.; Wang, X.-L.; Yang, G.-S.; Wang, H.-N.; Liang, J.; Shao, K.-Z.; Su, Z.-M. *CrystEngComm* **2014**, *16*, 6882.
- 276 Bhattacharyya, S.; Chakraborty, A.; Jayaramulu, K.; Hazra, A.; Maji, T. K. *Chem. Commun. (Cambridge, U. K.)* **2014**, *50*, 13567.
- 277 Gaft, M.; Panczer, G.; Uspensky, E.; Reisfeld, R. *Mineral. Mag.* **1999**, *63*, 199.
- 278 Matsubara, Y.; Ito, A. *J. Chem. Educ.* **2019**, *97*, 300.
- 279 Drew, S. M.; Gross, D. S.; Hollingsworth, W. E.; Baraniak, T.; Zall, C. M.; Mann, K. R. *J. Chem. Educ.* **2019**, *96*, 1046.
- 280 Ivanov, A. S.; Bryantsev, V. S. *Eur. J. Inorg. Chem.* **2016**, *2016*, 3474.

- 281 Lim, S.; Franklin, S. J. *Protein Sci.* **2006**, *15*, 2159.
- 282 Comba, P.; Gloe, K.; Inoue, K.; Krüger, T.; Stephan, H.; Yoshizuka, K. *Inorg. Chem.* **1998**, *37*, 3310.
- 283 Jin, C.; Liu, H.; Kong, X.; Yan, H.; Lei, X. *Dalton Trans.* **2018**, *47*, 3093.
- 284 Dash, S.; Mohanty, S. *Chem. Eng. Technol.* **2018**, *41*, 1697.
- 285 Vo, M. N.; Bryantsev, V. S.; Johnson, J. K.; Keith, J. A. *Int. J. Quantum Chem.* **2018**, *118*, e25516.
- 286 Zhao, W.; Bhushan, A.; Santamaria, A. D.; Simon, M. G.; Davis, C. E. *Algorithms* **2008**, *1*, 130.
- 287 Mutlu, A. Y.; Kiliç, V.; Özdemir, G. K.; Bayram, A.; Horzum, N.; Solmaz, M. E. *Analyst* **2017**, *142*, 2434.



A range of materials are evaluated for their ability to detect and quantify rare earth elements via luminescence techniques.